

# Identification of Coherent Generators Using Linear Trajectory

by

Mir, Mujahid Ali

A Thesis Presented to the

FACULTY OF THE COLLEGE OF GRADUATE STUDIES

KING FAHD UNIVERSITY OF PETROLEUM & MINERALS

DHAHRAN, SAUDI ARABIA

In Partial Fulfillment of the  
Requirements for the Degree of

**MASTER OF SCIENCE**

In

**ELECTRICAL ENGINEERING**

April, 1993

## **INFORMATION TO USERS**

**This manuscript has been reproduced from the microfilm master. UMI films the text directly from the original or copy submitted. Thus, some thesis and dissertation copies are in typewriter face, while others may be from any type of computer printer.**

**The quality of this reproduction is dependent upon the quality of the copy submitted. Broken or indistinct print, colored or poor quality illustrations and photographs, print bleedthrough, substandard margins, and improper alignment can adversely affect reproduction.**

**In the unlikely event that the author did not send UMI a complete manuscript and there are missing pages, these will be noted. Also, if unauthorized copyright material had to be removed, a note will indicate the deletion.**

**Oversize materials (e.g., maps, drawings, charts) are reproduced by sectioning the original, beginning at the upper left-hand corner and continuing from left to right in equal sections with small overlaps. Each original is also photographed in one exposure and is included in reduced form at the back of the book.**

**Photographs included in the original manuscript have been reproduced xerographically in this copy. Higher quality 6" x 9" black and white photographic prints are available for any photographs or illustrations appearing in this copy for an additional charge. Contact UMI directly to order.**

# **U·M·I**

University Microfilms International  
A Bell & Howell Information Company  
300 North Zeeb Road, Ann Arbor, MI 48106-1346 USA  
313/761-4700 800/521-0600

**0001**

**Order Number 1354068**

**Identification of coherent generators using linear trajectory**

**Ali, Mir Mujahid, M.S.**

**King Fahd University of Petroleum and Minerals (Saudi Arabia), 1993**



**IDENTIFICATION OF COHERENT GENERATORS  
USING LINEAR TRAJECTORY**

**BY**

**MIR MUJAHID ALI**

**A Thesis Presented to the  
FACULTY OF THE COLLEGE OF GRADUATE STUDIES  
KING FAHD UNIVERSITY OF PETROLEUM & MINERALS  
DHAHRAN, SAUDI ARABIA**

**In Partial Fulfillment of the  
Requirements for the Degree of**

**MASTER OF SCIENCE  
In  
ELECTRICAL ENGINEERING**

**APRIL, 1993**

**KING FAHD UNIVERSITY OF PETROLEUM AND MINERALS**

**DHAHRAN 31261 , SAUDI ARABIA**

**COLLEGE OF GRADUATE STUDIES**

This thesis written by **Mir Mujahid Ali** under the direction of his Thesis Advisor and approved by his thesis committee. has been presented to and accepted by the Dean of Graduate Studies. in partial fulfillment of the requirements for the degree of MASTER OF SCIENCE.

**Thesis Committee**

M. H. Ali

(Thesis Advisor)

S. A. Al-Barbari

(Member)

A. I. Shihri

(Member)

D. H. W.

(Member)

A. I. Shihri AM

Department Chairman

Dean

Dean, College of Graduate Studies



**DEDICATED TO MY PARENTS**



## **ACKNOWLEDGEMENT**

**Acknowledgement is due to King Fahd University of Petroleum and Minerals for support of this research.**

**The author is greatly indebted to his committee chairman Dr. Mohammed Hamidul Haque for his constant and consistent guidance and encouragement.**

**Thanks are due to my committee members Dr. A.M. Al-Shehri, Dr. S.A.Baiyat and Dr. I.El-Amin for their unstinted support.**

**Finally I wish to thank my parents, brother, sister and my fellow research assistants who have encouraged me wholeheartedly in my endeavours.**

# **TABLE OF CONTENTS**

	<b>Page</b>
<b>List of Tables</b>	<b>ix</b>
<b>List of Figures</b>	<b>xi</b>
<b>Abstract (Arabic)</b>	<b>xiv</b>
<b>Abstract (English)</b>	<b>xv</b>
 <b>I INTRODUCTION</b>	
 1.1 Dynamic Equivalencing of a Power System	1
1.2 Definition of Coherency	3
1.3 Thesis Objective	5
1.4 Scope of the Thesis	6
 <b>II LITERATURE REVIEW</b>	
 2.1 Introduction	8
2.2 Identification of Coherent Generators	9
2.2.1 Methods based on the linearized swing equation	9
2.2.2 Methods based on the actual swing equation	13
2.3 Dynamic Aggregation	18

### **III MATHEMATICAL MODEL**

<b>3.1</b>	<b>Introduction</b>	<b>24</b>
<b>3.2</b>	<b>Generator Model</b>	<b>25</b>
<b>3.2.1</b>	<b>Machine dynamics in the COA frame</b>	<b>28</b>
<b>3.3</b>	<b>Calculation of the Parameters of the Equivalent Model</b>	<b>33</b>
<b>3.3.1</b>	<b>Non-coherent generators</b>	<b>36</b>
<b>3.3.2</b>	<b>Coherent Generators</b>	<b>37</b>
<b>3.3.3</b>	<b>Algorithm</b>	<b>40</b>

### **IV COMPUTATION OF CRITICAL CLEARING TIME USING INDIVIDUAL MACHINE ENERGY**

<b>4.1</b>	<b>Introduction</b>	<b>41</b>
<b>4.2</b>	<b>Individual Machine Energy</b>	<b>42</b>
<b>4.3</b>	<b>The Individual Machine Energy Function</b>	<b>43</b>
<b>4.3.1</b>	<b>Complexities of the energy function</b>	<b>45</b>
<b>4.3.2</b>	<b>Determination of critical energy</b>	<b>48</b>
<b>4.3.3</b>	<b>Method of false position</b>	<b>52</b>
<b>4.3.4</b>	<b>Estimation of system states by the Taylor series expansion</b>	<b>56</b>
<b>4.4</b>	<b>Algorithm for Computing Critical Clearing Time</b>	<b>59</b>
<b>4.5</b>	<b>Simulation Results</b>	<b>60</b>

## **V DETERMINATION OF COHERENT GENERATORS**

5.1	Introduction	64
5.2	Identification of the Study and External System	65
5.3	Identification of Coherent Generators	66
5.3.1	Coherency of the generators during the faulted period	68
5.3.2	Coherency of generators during the early part of the post fault period	69
5.3.3	Coherency of generators during the later part of the post fault period	80
5.4	Algorithm in Brief	81

## **VI SIMULATION RESULTS**

6.1	Introduction	83
6.2	The Test Systems	87
6.2.1	The IEEE system	87
6.2.2	The New England system	125
6.3	Comparison of CPU Time	129

## **VII CONCLUSION**

7.1	Conclusions	133
7.2	Recommendation for Future Work	135

<b>References</b>	<b>137</b>
<b>Appendix A</b>	<b>142</b>
<b>Appendix B</b>	<b>151</b>

## LIST OF TABLES

Table No.	Title	Page
4.1	Selection of initial values of $t$ for a fault on bus # 25 of the IEEE system	53
4.2	Convergence rate of the method of false position in solving eqn. (4.12)	55
4.3	Simulation results of the CCT (secs) for various faults on the IEEE system	62
4.4	Simulation results of the CCT (secs) for various faults on the New England system	63
5.1	Generator angles at $t_{cr}$ and $t_p$	74
5.2	Generator angles obtained by different methods at the end of the early part of the post fault period	79
6.1	Faulted accelerations of generators	89
6.2	Generator angles at $t=0$ and at $t=t_{cr}$	91
6.3	Generator angles at $t_{cr}$ and $(t_{cr} + 0.20)$	94
6.4	Slopes of the generator trajectories during the early part of the post fault period	95
6.5	Admittance distance ratios	98
6.6	Final Coherent groups	101
6.7	Number of generators obtained in different equivalents	109
6.8	Coherent generator groups for various faults on the IEEE system	112
6.9	Coherent generator groups for various faults on the New England system	126

<b>6.10</b>	<b>CPU time (secs) for dynamic equivalencing</b>	<b>131</b>
<b>6.11</b>	<b>Comparison of CPU time in seconds for direct simulation</b>	<b>132</b>

## LIST OF FIGURES

<b>Fig. No.</b>	<b>Title</b>	<b>Page</b>
2.1	Hypothetical 5-machine network	19
2.2	Reduced 3-machine network	20
4.1	Variation of PE, KE and total energy 'V' of gen#4 for a 3-ph fault on bus 25 of the IEEE system	49
4.2	Variation of $\dot{V}_{pei}$ of gen # 4 for a 3-ph fault on bus 25 of the IEEE system	54
4.3	Variation of system RKE for a 3-ph fault on bus 25 of the IEEE system cleared after 0.27 secs	61
5.1	Swing curves of gen # 9 for a 3-ph fault on bus 29 of the New England system cleared after 0.13 secs	67
5.2	Plot of rotor angles during the early part of the post fault period for a 3-ph fault on bus 29 of the New England system (CCT=0.13 secs)	71
5.3	Plot of rotor angles during the early part of the post fault period for a 3-ph fault on bus 10 of the IEEE system (CCT= 0.18 secs)	72
6.1	Single line diagram of 20-machine IEEE system	84
6.2	Single line diagram of 10-machine New England system	85
6.3	Swing curves of generators 10-16 for a 3-ph fault on bus 25 of the IEEE system (CCT=0.27 secs)	102
6.4	Swing curves of generators 17-20 for a 3-ph fault on on bus 25 of the IEEE system (CCT=0.27 secs)	103
6.5	Swing curves of generators 1,3,8,9 for a 3-ph fault on bus 25 of IEEE system (CCT=0.27 secs)	104



6.6	Swing curves of gen. # 4 for a critically stable and unstable case for a 3-ph fault on bus 25 of the IEEE system	107
6.7	Swing curves of gen. # 7 for a critically stable and unstable case for a 3-ph fault on bus 25 of the IEEE system	108
6.8	Swing curves of generators 4-9 for a 3-ph fault on bus 10 of the IEEE system (CCT=0.18 secs)	113
6.9	Swing curves of generators 10-16 for a 3-ph fault on bus 10 of the IEEE system (CCT=0.18 secs)	114
6.10	Swing curves of generators 17-20 for a 3-ph fault on bus 10 of the IEEE system (CCT=0.18 secs)	115
6.11	Swing curves of gen. # 2 for a critically stable and unstable case for a 3-ph fault on bus 10 of the IEEE system	116
6.12	Swing curves of generators 4-9 for a 3-ph fault on bus 12 of the IEEE system (CCT=0.47 secs)	117
6.13	Swing curves of generators 10-15 for a 3-ph fault on bus 12 of the IEEE system (CCT=0.47 secs)	118
6.14	Swing curves of generators 16-20 for a 3-ph fault on bus 12 of the IEEE system (CCT=0.47 secs)	119
6.15	Swing curves of gen. # 3 for a critically stable and unstable case for a 3-ph fault on bus 12 of the IEEE system	120
6.16	Swing curves of generators 1-7 for a 3-ph fault on bus 59 of the IEEE system (CCT=0.39 secs)	121
6.17	Swing curves of generators 8,9,13,14 for a 3-ph fault on bus 59 of the IEEE system (CCT=0.39 secs)	122
6.18	Swing curves of generators 17-19 for a 3-ph fault on bus 59 of the IEEE system (CCT=0.39 secs)	123
6.19	Swing curves of gen. # 11 for a critically stable and unstable case for a 3-ph fault on bus 59 of the IEEE system	124
6.20	Swing curves of generators 1-4 and 6-9 for a 3-ph fault on bus 20 of the New England system (CCT=0.20 secs)	127

6.21	Swing curves of generators 2,3,4,6,7 for a 3-ph fault on bus 29 of the New England system (CCT=0.13 secs)
------	--

128
-----

## موجز رسالة البحث

الاسم : مير مجاهد علي  
عنوان البحث : تحديد المولدات المتوافقة باستخدام المسار الخطي  
التخصص : هندسة كهربائية  
تاريخ الدرجة : ابريل ١٩٩٣م

يعرض هذا البحث طريقة لتحديد المولدات المتوافقة في شبكة القدرة الكهربائية ووضعت معايير تحديد التوافق بافتراض أسوأ الظروف أي باعتبار أن وقت ازاله العطب يقارب الوقت الحرج ، وتم تحديد الوقت الحرج في البداية باستخدام مفهوم طاقة الماكينة الواحد .

تم اختبار توافق المولدات على مدى ثلاث فترات ، وتم تحديد التوافق اثناء فترة العطل بفحص الانحراف النسبي لزاوية الدوران . كما تم تحديد التوافق في الجزء الأول من الفترة التالية للعطل بدراسة منحنيات مسار المولد ثم تم تحديد التوافق في الجزء الاخير من فترة مابعد العطل بفحص مسافات الدخول بين المولدات . كما تم الحصول على نموذج النظام المختصر باستبدال مجموعة من المولدات المتوافقة بمولد مكافئ للمجموعة . أما المدخلات لنموذج النظام المختصر فقد وجدت من خلال الاستفاده بمبدأ ثبات القدرة الحقيقية بين النموذج الاصلي والنموذج المختصر .

وتم اختبار الطريقة المقترحة لتحديد المولدات المتوافقة على مختلفة الاعطال في شبكتين من شبكات القدرة . ثم قورنت النتائج التي تم الحصول عليها مع النتائج المستخلصة ملاحظة المنحنيات المتأرجحة التي تولدت من عملية المحاكاه . وفي النهاية تم اجراء مقارنة بين الوقت CPU المطلوب لحل مجال الوقت في النماذج الاصلية والنماذج ذات النظام المختصر .

درجة الماجستير في العلوم  
جامعة الملك فهد للبترول والمعادن  
الظهران - المملكة العربية السعودية

## **THESIS ABSTRACT**

**Name of student:** Mir Mujahid Ali  
**Title of study :** Identification of Coherent Generators  
using Linear Trajectory  
**Major Field :** Electrical Engineering  
**Date of Degree :** April, 1993

This thesis presents a method of finding the groups of coherent generators of a power system. The coherency identification criteria are developed for the most severe condition i.e. by considering the fault clearing time to be very close to the critical clearing time (CCT). The CCT is first determined using the concept of individual machine energy.

Coherency of generators is checked in three periods. Coherency during the faulted period is determined by checking the relative rotor angle deviations. Coherency during the early part of the post fault period is determined by checking the slopes of the generator trajectories. Coherency during the later part of the post fault period is determined by checking the admittance distances between the generators. The reduced order model is obtained by replacing a group of coherent generators by an equivalent generator. The parameters of the reduced order model are obtained using the real power invariance principle between the original and the reduced models.

The proposed method of determining the coherent generators has been tested for various faults on two power networks. Results obtained are compared with those found by observing the swing curves generated by simulation. Finally a comparison of the CPU time required for the time domain solutions in the original and the reduced order models is given.

**MASTER OF SCIENCE DEGREE**

**KING FAHD UNIVERSITY OF PETROLEUM AND MINERALS**

**Dhahran, Saudi Arabia.**

## **CHAPTER I**

### **INTRODUCTION**

#### **1.1 DYNAMIC EQUIVALENCING OF A POWER SYSTEM**

Determination of transient stability is one of the major items of power system operation and planning. Transient stability is the ability of a system to remain in synchronism following major disturbances such as sudden changes in load or generation powers, or in transmission system configuration due to faults and line switching. Conventionally the transient stability is determined by observing the swing curves. These swing curves are generated by solving the generator swing equations in the time domain. The time domain solution approach can be used with any degree of modelling sophistication. However, this is a very time consuming and cumbersome process. For large interconnected power systems, it is very difficult to generate the swing curves of all generators for all conceivable contingencies even with the help of the most modern computers.

Alternatively, the transient stability and hence the Critical Clearing Time (CCT) can be determined by the Transient Energy Function (TEF) method without explicitly solving the swing equations. The TEF method is based on the Lyapunov's second ( or direct ) method. Recent results of the TEF method indicate that it can determine the critical clearing time efficiently and accurately, only for the classical model of a power system.

In both methods, the computational time can be significantly reduced if the transient stability is determined in a reduced order equivalent model of the original system. The reduced order model which can faithfully represent the same dynamic behavior of the original system is called the dynamic equivalent.

The dynamic equivalent is used to efficiently analyse the transient stability of a large interconnected power system. Dynamic equivalents are also used for stabilizer design and investigation of electric power transfer limits among areas [1].

In the dynamic equivalencing process, the original system is divided into two systems or areas called the "study system" and the "external system". The "study system" includes the disturbance and a small number of generators of great concern. These generators are severely disturbed and are in general responsible for the system instability. The system states like voltage, current, angle and speed of these generators are very important for

control and protection purposes. The rest of the generators are considered in the "external system". The generator in the "external system" do not contribute significantly to the system instability. Thus the dynamic equivalencing technique/methodology is applied to these generators only. Several methods of dynamic equivalencing have been reported in the literature. These can be broadly classified into three categories :

- i) Modal approach.
- ii) Coherency approach.
- iii) Estimation approach.

Of these the coherency based approach has received much attention in recent years because of its simplicity and reliability. In this work the coherency based approach is used to obtain the dynamic equivalent of a power system.

## **1.2 DEFINITION OF COHERENCY**

A group of generators is considered to be coherent if they move or swing together during the transient period. Mathematically a generator pair (i,j) is said to be coherent if they satisfy

$$\theta_{ij}(t) = x_{ij} \pm \epsilon \quad (1.1)$$

where

$\theta_{ij}(t)$  is the relative angle between the  $i^{th}$  and the  $j^{th}$  generators.

$x_{ij}$  is a constant.

$\epsilon$  is a small positive number.

A generator pair (i,j) is said to be perfectly coherent if  $\epsilon = 0$  in eqn. (1.1). In this case, the generator angles are not independent. By knowing the angle of one generator and the constant  $x_{ij}$ , it is possible to find the angle of the other generator. Thus the system is reducible and it is not necessary to represent both generators in the dynamic analysis of a power system. In a real power system, it is very unlikely to get a perfectly coherent generator pair. However, it is well known that, in a large power system, many generators tend to swing together or be coherent (within a certain tolerance) under the influence of a remote disturbance. The dynamic equivalent of a power system is obtained by replacing each group of coherent generators by an equivalent generator. It is worth mentioning here that the accuracy of the dynamic equivalent model depends on the degree of coherency of the generators ( $\epsilon$  in eqn. (1.1)) in each group.



### **1.3 THESIS OBJECTIVE**

A group of coherent generators should remain coherent for the entire transient period. The transient period can be divided into three regions namely.

- i) Faulted period.
- ii) Early part of the post fault period.
- iii) Later part of the post fault period.

In this work the final groups of coherent generators will be determined by finding the pairs of coherent generators in the above three periods for the most severe case i.e by considering that the fault clearing time is very close to the CCT. A method of determining the CCT will also be presented.

Determination of generator coherency during the faulted period is very simple because the faulted period is relatively short and the faulted generator accelerations are more or less constant. Generator coherency during this period will be determined by checking the relative angles between generators. The generator angles will be estimated through the Taylor series expansion.

Determination of coherency in the early part of the post fault period is of prime interest to us. It is assumed that the early part of the post fault period

is the time period which starts at the fault clearing time and extends till the time at which the rotor angle of the severely disturbed generator reaches its peak, for a stable condition. Coherency during this period will be checked using a combination of the second step Taylor series expansion and linear trajectory.

The time period after the rotor angle of the severely disturbed generator has passed its peak may be considered as the later part of the post fault period. Coherency of the generators in this period will be determined by checking the admittance distances between the generators.

Once the groups of coherent generators are determined the reduced order dynamic equivalent model can be obtained by replacing each group of coherent generators by an equivalent generator.

#### 1.4 SCOPE OF THE THESIS

This thesis presents a method of determining the groups of coherent generators for a severe disturbance like a three phase fault. It is considered that the fault is cleared around CCT. The CCT is computed using the concept of individual machine energy. Generator coherency is determined using a combination of Taylor series expansion, linear trajectory of the generators and the admittance distances between the generators. A method of obtaining

a reduced order equivalent model by replacing all coherent generator groups by their equivalents is also presented.

The thesis is presented in the following sequence :

- i) A brief literature survey on coherency determination and dynamic equivalencing is first presented in CHAPTER II.
- ii) The mathematical model of a power system in the Center of Angle (COA) frame and the determination of the reduced order equivalent model is then presented in CHAPTER III.
- iii) Determination of CCT using individual machine energy function is presented in CHAPTER IV.
- iv) A method of determining the coherent generator pairs in the three regions namely faulted, early part of the post fault and later part of the post fault is presented in CHAPTER V.
- v) Results of the proposed method of identifying the coherent generators for a number of fault cases on two power networks are presented in CHAPTER VI.
- vi) Conclusions and recommendations for future work in this field are finally presented in CHAPTER VII.

## **CHAPTER II**

### **LITERATURE REVIEW**

#### **2.1 INTRODUCTION**

The dynamic equivalencing process of a power system, based on coherency, consists of two parts namely :

- i) Identification of coherent generators
- ii) Dynamic aggregation

The most accurate method of identifying the coherent generators is by solving the swing equation and observing the relative angles between the generators. However, this is a very time consuming and computationally prohibitive process especially in the case of large power systems. In order to reduce computational time many methods have been reported in the literature to determine the coherent generators. While some of them used

special integration techniques, others used the linearized swing equations. Some authors proposed the direct method of determining coherency without solving the swing equations.

Dynamic aggregation involves replacing each group of coherent generators by an equivalent generator and obtaining the parameters of the reduced order equivalent model. The methods of identifying the coherent generators and dynamic aggregation reported in the literature are reviewed in the following sections.

## **2.2 IDENTIFICATION OF COHERENT GENERATORS**

The various methods proposed for the identification of coherent generators can be discussed under two broad categories namely, the methods based on the linearized swing equation and the actual swing equation.

### **2.2.1 Methods Based on the Linearized Swing Equation**

Most of the coherency identification methods are based on the linearized swing equation. The linearized swing equations are derived by assuming the following [2]:

- i) The groups of coherent generators are independent of the size of the

disturbance.

- ii) The coherent groups are independent of the amount of detail in the generator unit models. Therefore, the classical model of a power system is considered and the effect of dynamics of the excitation and turbine. governor systems is ignored.
- iii) The effect of a fault may be reproduced by considering the unfaulted network and pulsing the mechanical powers to the generator to achieve the same accelerating powers which would have existed in the faulted network for a time equal to the fault clearing time.

Under these assumptions the mechanical equations for the motion of a synchronous generator 'i' in an 'n' generator system can be written as [3].

$$M_i \frac{d^2 \Delta \delta_i}{dt^2} = \Delta P_{mi} - \Delta P_{ei} \quad (2.1)$$

where

$\Delta$ : represents a deviation from a specified steady state operating point.

$\Delta \delta_i$ : rotor angle deviation in radians

$\Delta P_{mi}$ : change in mechanical input power in p.u.

$\Delta P_{ei}$  : change in electrical output power in p.u.

$M_i$  : inertia constant in p.u.

Podmore [3] solved the linearized equations (2.1) using the trapezoidal method to obtain the time domain solution. A clustering algorithm was then used to process the swing curves to determine the generator coherency. In this method of determining the coherent groups, a pair of generator swing curves is compared and the generator pair is identified as coherent if the maximum change in the angular difference falls within a specified tolerance. Though the method gives reasonably accurate results for small perturbations or disturbances, it is very time consuming and computationally prohibitive especially for large power systems.

Lee and Schweppe [4] used the same linearized equation but split the power system into three circles which they defined as the inner, middle and the outer circle. The generators in the inner circle are of utmost importance since they are in the vicinity of the fault. The generators in the middle circle are the ones on which the coherency criteria is applied while the generators in the outer circle are too far away to be affected. Therefore, the generators in the outer circle are replaced by an equivalent generator. They suggested a pattern recognition approach for determining generator coherency. The

pattern recognition approach is based on some criteria that depend on the faulted accelerations, the inertia constants and the admittance distances. The faulted accelerations govern the system dynamics during the faulted period and the generators which appears to be coherent during the faulted period may actually fall apart in the post fault period. Thus resulting in the wrong identification of coherent generator groups.

Wu and Narshimamurthi [5] used the state space representation of the linearized swing equation to determine coherency in terms of generator inertia constants and their equivalent admittance distances to the bus ( or point ) of the disturbance. Gallai and Thomas [6] also used the same state space representation and developed a coherency identification index to identify the coherent generators.

Hiyama [7] used the linearized swing equation to propose a coherency identification criteria in the frequency domain.

Recently Pires de Silva et.al. [8] solved the linearized swing equation using special integration techniques which involved a linear simulation method. The coherent generators were determined by comparing the generator angular speed deviations through a clustering algorithm.

Many of the above methods received very little attention due to their complexities. On the whole it may be emphasised that the linearized model is



valid for small perturbations only and the model may give erroneous results. if the disturbance is severe, as in the case of a three phase fault for a relatively longer duration.

### **2.2.2 Methods Based on the Actual Swing Equation**

Many other methods have been proposed for determining the coherency of generators without linearizing the swing equations. Some of the methods determined the coherency of generators without explicitly solving the swing equations. These methods are briefly discussed hereunder.

Haque and Rahim [9] proposed a method of coherency determination which involved checking the relative rotor angle deviations and the admittance distance between generators. Generator rotor angles during the faulted period and the early part of the of the post fault period were calculated using a two-step Taylor series expansions. The first step is used to find the angles during the faulted period while the second step is used to find the angles in the early part of the post fault period. Since the faulted system accelerations remain more or less constant , this method gives fairly accurate results during the faulted period. However, during the early part of the post fault period the method is accurate for a short period only ( $< 0.2$  secs), beyond which the accuracy of the Taylor series is affected by the truncated part of the series. Coherency of the generators during the later part of the post fault period was determined by checking the admittance distances

between the generators. The authors showed that the groups of coherent generators may depend on the degree of disturbances and hence the fault clearing time. This finding is in contradiction with the previous assumption made in linearizing the swing equation.

In general the Liapunov or energy function and the unstable equilibrium points (UEP) are used to determine the transient stability of a power system. The energy function has two components namely the potential and the kinetic energy. Several methods of identifying the coherent generators based on the energy function and/or UEP are reported in literature.

Ohsawa et. al. [10] determined coherent generators using the Liapunov function. They proposed a criterion based on the fact that the component of the Liapunov function for a group of coherent generators is not significant when compared to the total value of the function for the entire system. Thus the value of the function will not change significantly by aggregating the group of generators. The above concept is based on the fact that if a generator pair is coherent then the difference in the relative angle between them, computed at two different points is small. Thus all the relative angular difference terms of the coherent groups in the Liapunov function tend to zero. The component of the Liapunov function are computed using the faulted system states around the critical clearing time. The main drawback of this method is that it totally ignores the dynamics of the post fault system. The

generators which are coherent during the faulted period may not be so in the post fault period, and so this method may not yield the correct result. The method also requires a prior knowledge of the critical clearing time to compute the groups of coherent generators.

Haque and Rahim [11] considered the effects of the post fault dynamics by evaluating the value of the energy function at different approximate unstable equilibrium points. They proposed that the energy required to pull a pair of non-coherent generators from their stable equilibrium point (SEP) is almost the same as the sum of the energy required to pull the generators independently. On the other hand, the energy required to pull a pair of coherent generators is approximately equal to the maximum energy required to pull either of generators out of step. An index representing the normalized energy required by one generator to pull another generator was used to determine the tentatively coherent pairs of generators in the post fault period. These generator pairs were expected to remain coherent in the post fault period irrespective of the fault location. The final groups of coherent generators for a particular fault location were determined by choosing a study system depending upon the fault location. The generator relative rotor angle deviations were checked during the faulted period among the tentatively coherent pairs in the external system.

Spalding et. al. [12] determined coherent generators through computation

of the system singular point or the unstable equilibrium point (UEP). The method is based on the comparison of the relative rotor angle deviation at two points, the prefault operating point and the postfault UEP, among a group of generators which belong to the same geographical area. However, a group of geographically close generators which satisfy the relative angle deviation criteria at these two points may not necessarily maintain coherency during the excursion from prefault to postfault states, because the system goes through a change in configuration, from prefault, faulted to postfault. This method totally ignores the dynamics of the faulted system. Also the method determines the UEP in the machine angle reference frame at which the difference of the system losses at two equilibrium points is assigned to the reference machine only. They computed the UEP by the Newton-Raphson's method and the computation of UEP by the Newton-Raphson method has some convergence problems [13].

Haque [14] improved the above method by determining coherent generators in the external system through a combination of faulted system dynamics, UEP and the admittance distances between the generators. The faulted generator angles are estimated through a Taylor series expansion. The UEP is computed by the Davidson-Fletcher-Powell (DFP) method in the COA reference frame at which the difference of losses at the two equilibrium points is distributed among all the machines in accordance to their inertia constants. This method gives better results than Spalding's method because

it includes the effects of faulted system dynamics. Also the DFP method is better suited for computing the UEPs since it has less convergence problems.

Rudnick et. al. [15] proposed a method of coherency recognition using the system rate of change of kinetic energy. This is the only reported method that determined generator coherency by considering the fault to be cleared at critical clearing time. In this method the derivative of the kinetic energy component of the Liapunov function called the rate of change of kinetic energy (RKE) of the generators is used to compute the CCT. The CCT was identified as the time at which the RKE of the system reached the minimum. The post fault generator accelerations are computed and compared around CCT to determine the coherency during the post fault period. An admittance distance check was then performed to eliminate generators which are geographically apart from the groups determined. Finally, the angular difference between the load flow solution (prefault angles) and the value at CCT was checked for all coherent generator pairs. The major drawback of this method is that the acceleration of the generators at CCT ( $\ddot{\delta}_{cr}$ ) may not represent the behavior of the generators in the entire post fault period. Thus, this method may fail to identify the correct group of coherent generators. The method of determining the CCT using the system RKE can sometimes give erroneous results. This concept of determining groups of coherent generators around CCT will be used in this thesis.

## 2.3 DYNAMIC AGGREGATION

As mentioned earlier, the dynamic aggregation process involves the replacement of each group of coherent generators by an equivalent or fictitious generator to obtain the reduced order equivalent of the system.

The aggregation procedure can be illustrated with the help of a small hypothetical 5-generator network shown in Fig. 2.1. Let us assume that the generator group (3,4,5) is coherent. This coherent group is to be replaced by an equivalent generator 'e' and the parameters of the reduced order network are to be computed. Since the network has 5 generators the admittance matrix of the original system will be of order (5x5). However, the dimension of the new admittance matrix  $[Y^{new}]$  of the reduced order equivalent will be (3x3) as is evident from Fig. 2.2. Some of the elements of this  $[Y^{new}]$  matrix will remain unchanged (like element  $Y_{12}$ ). Lines 2,3..10 in Fig. 2.1 are to be replaced by two equivalent lines as shown in Fig. 2.2.

Thus in brief, dynamic aggregation requires computation of some of the elements of the new admittance matrix, and the parameters of the equivalent generator. Many methods of dynamic aggregation have been proposed, some of them are discussed below.

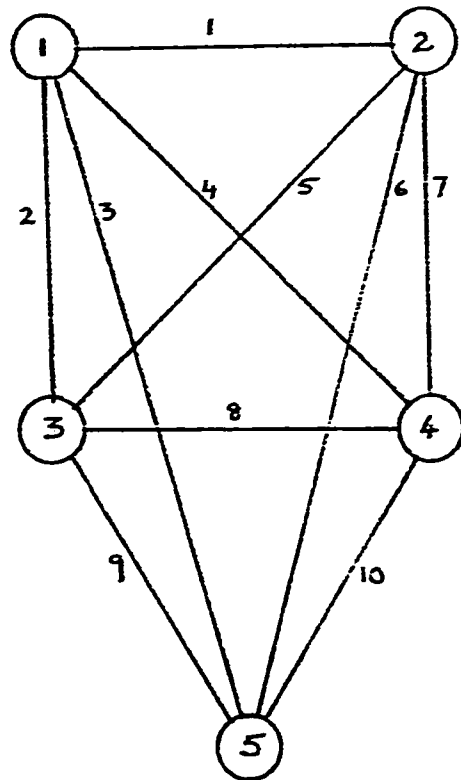


Fig. 2.1 Hypothetical 5-machine network

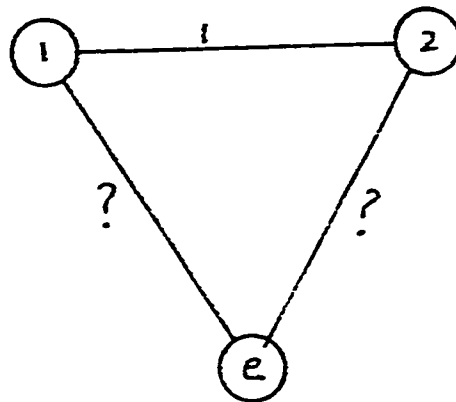


Fig. 2.2 Reduced 3-machine network



Podmore [16] proposed a method of dynamic aggregation by preserving the network structure of the non-coherent part. The equivalent obtained by this method can be used in any standard transient stability program. Generator bus reduction was performed by connecting all the generators in a coherent group to an equivalent bus through an ideal phase shifting transformer. The generation, load and shunt admittances were summed and transferred to the equivalent bus. The original coherent buses were then eliminated by series combination of the original branch and the ideal transformer. The reduction procedure for the generator buses affects only those branches which are connected to the coherent generator buses. The balanced load flow conditions on the original buses is preserved and a balanced load flow condition is created for the equivalent bus. The next step involved the reduction of load buses where the coherent generators are connected. Sparsity oriented reduction techniques were used to reduce load buses. Certain key buses which are special in a topological sense were identified and retained. These key buses tend to be buses which either have a high number of connections or buses which connect sub-areas that have few ties to the rest of the system. The rest of the buses having minimum number of connections were eliminated at each step of reduction. Finally the group of coherent generators on the equivalent bus were replaced by an equivalent generator. The equivalent generator model obtained has the same electrical output response of the entire coherent group. The terminal voltage

of the equivalent generator is the same as the terminal voltage at the equivalent bus to which the coherent group is connected.

Ghafurian and Berg [17] proposed a method of dynamic aggregation using the complex power invariance principle. In this method the equations of one of the generators in a coherent group was preserved. The modified reduced order admittance matrix was obtained by adding the effects of the eliminated generators onto the retained generator in the coherent group. This method retains the terminal busbars of all the remaining generators. Due to this the voltage and generator controls can be included with a desired degree of detail. Preserving the basic physical structure of the original system enables the model to be easily implemented into any conventional transient stability program.

In general, the reactive power has a negligible influence on the generator phase angles and thus it can be neglected in the dynamic aggregation process. Thyagarajan [18] used only the real power invariance principle to determine the parameters of the reduced order equivalent. Like the above approach, this method retained the terminal busbar of the generators, thus preserving the physical structure of the original system

Rahim and Haque [19] proposed a method of computing the reduced order equivalent based on coherency. The parameters of the reduced order model were obtained using the real power invariance principle. This method will be used in chapter III to determine the reduced order equivalents.

## **CHAPTER III**

### **MATHEMATICAL MODEL**

#### **3.1 INTRODUCTION**

The initiation and removal of a fault in a power system can be seen as a case where the system is going through a change in configuration. There are three stages in this process namely the prefault, faulted and the postfault. The prefault condition is the steady state operating condition obtained from the load flow studies and is outside the scope of this work. However, the dynamics of the system during the faulted and the postfault period are inherently non-linear and their exact representation is very complex.

Transient stability is a very fast phenomenon. It involves the computation of system states for a very short period of time. During this short period, the dynamics of various controls like turbines, governor, prime mover and excitation systems are not so important because of their relatively longer

time constants [20,21].

In this chapter the mathematical model of a power system will be developed. This will be followed by a method of determining the parameters of the reduced order dynamic equivalent model.

### **3.2 GENERATOR MODEL**

The mathematical model of a generator used in this study is commonly known as the classical model [21]. This model is based on the following assumptions:

- i) The mechanical power input to the generator remains constant during the period of transient.
- ii) Damping or asynchronous power is negligible.
- iii) The synchronous generator can be represented by a constant voltage source behind a transient reactance.
- iv) The angle of the synchronous generator rotor coincides with the electrical phase angle of the voltage behind the transient reactance.
- v) Loads are represented by constant impedances based on the prefault voltage condition obtained from the load flow solution.

Consider an n-generator power system. The dynamics of the i-th generator in the classical model of the power system can be written as [21]

$$M_i \frac{d^2 \delta_i}{dt^2} = P_{mi} - P_{ei} \quad (3.1)$$

where

$M_i$  = inertia constant of the i-th generator

$\delta_i$  = rotor angle of the i-th generator in a synchronously rotating reference frame or axis

$P_{mi}$  = input mechanical power to the i-th generator

$P_{ei}$  = electrical output power of the i-th generator

The generator output power is given by

$$P_{ei} = \sum_{j=1}^n (C_{ij} \sin \delta_{ij} + D_{ij} \cos \delta_{ij}) \quad (3.2)$$

where

$$C_{ij} = E_i E_j B_{ij} \quad (3.3)$$

$$D_{ij} = E_i E_j G_{ij} \quad (3.4)$$

$$\delta_{ij} = \delta_i - \delta_j \quad (3.5)$$

$$Y_{ij} = (G_{ij} + jB_{ij}) \quad (3.6)$$

Y is the reduced admittance matrix obtained by eliminating all the load and generator terminal buses and retaining only the generator internal buses.  $E_i$  and  $E_j$  are the magnitudes of the internal voltages of generators i and j respectively [13].

Eqn. (3.2) can be simplified and rewritten as

$$P_{ei} = E_i^2 G_{ii} + \sum_{\substack{j=1 \\ j \neq i}}^n (C_{ij} \sin \delta_{ij} + D_{ij} \cos \delta_{ij}) \quad (3.7)$$

By defining

$$P_i = P_{mi} - E_i^2 G_{ii} \quad (3.8)$$

and

$$P_{ei} = \sum_{\substack{j=1 \\ j \neq i}}^n (C_{ij} \sin \delta_{ij} + D_{ij} \cos \delta_{ij}) \quad (3.9)$$

Eqn. (3.1) can be rewritten as

$$M_i \frac{d^2 \delta_i}{dt^2} = P_i - P_e \quad (3.10)$$

It may be mentioned here that eqn. (3.10) can also be written with respect to the Machine Angle Reference (MAR) frame. In this reference frame the generator with the heaviest inertia is generally chosen as the reference generator and the rotor angles of the other generators are measured with respect to the reference generator. Generally, in this reference frame the system is considered to be unstable if the angle of any generator exceeds 180 degrees in the post fault period. However, results of ref. [22] indicate that in some cases the system was found to be stable even after the angle of some of the generator exceeded 180 degrees in the post fault period. In order to overcome such problems the Center of Angle (COA) reference frame can be used.

### 3.2.1 Machine Dynamics in the COA Frame

Most of the recent direct methods of determining the transient stability are based on the classical model of a power system in the COA or Center of Inertia (COI) reference frame. In this reference frame, a power system is



considered to be unstable as soon as the angle of any generator reaches 180 degrees. The generator angles in this reference frame are measured with respect to the center of inertia of the entire system. This reference frame is time varying and represents the mean motion of a system [13]. The transformation of eqn. (3.10) into the COA reference frame offers physical insight to the transient stability problem formulation in general. The swing equation in the COA frame can be derived as follows :

In the COA frame the motion of each generator is resolved into two components as follows:

- i) The motion of the inertia center which is defined by

$$\delta_o = \frac{1}{M_T} \sum_{i=1}^r M_i \delta_i \quad (3.11)$$

where

$$M_T = \sum_{i=1}^n M_i \quad (3.12)$$

- ii) The relative angle between each generator rotor and the inertia center, also called off-center angle is defined by

$$\theta_i = \delta_i - \delta_o \quad (3.13)$$

differentiating the above equation twice w.r.t. time yields

$$\frac{d^2 \theta_i}{dt^2} = \frac{d^2 \delta_i}{dt^2} - \frac{d^2 \delta_o}{dt^2} \quad (3.14)$$

The off-center angles and their derivatives are not all independent and have the following properties [13]

$$\sum_{i=1}^n M_i \theta_i = 0 \quad (3.15)$$

and

$$\sum_{i=1}^n M_i \theta_i^{(m)} = 0 \quad (3.16)$$

Here  $\theta_i^{(m)}$  is the m-th derivative of  $\theta_i$ . With the above properties we can proceed to derive the expression for the swing equation in the COA frame.

Adding eqn. (3.10) for n generators we get

$$\sum_{i=1}^n \left( M_i \frac{d^2 \delta_i}{dt^2} \right) = \sum_{i=1}^n P_i - \sum_{i=1}^n P_{ei} \quad (3.17)$$

Differentiating eqn. (3.11) twice w.r.t. time and rearranging the terms yields

$$M_T \frac{d^2 \hat{\delta}_o}{dt^2} = \sum_{i=1}^n \left\{ M_i \frac{d^2 \delta_i}{dt^2} \right\} \quad (3.18)$$

Substituting eqn. (3.18) in (3.17) gives us

$$M_T \frac{d^2 \hat{\delta}_o}{dt^2} = \sum_{i=1}^n P_i - \sum_{i=1}^n P_{ei} \quad (3.19)$$

where

$$\sum_{i=1}^n P_{ei} = \sum_{i=1}^n \sum_{\substack{j=1 \\ j \neq i}}^n (C_{ij} \sin \delta_{ij} + D_{ij} \cos \delta_{ij}) \quad (3.20)$$

Since the reduced admittance matrix is symmetric

$$D_{ij} = D_{ji} \text{ and } C_{ij} = C_{ji}$$

Therefore, the expression for  $\sum_{i=1}^n P_{ei}$  can be written as

$$\sum_{i=1}^n P_{ei} = 2 \sum_{i=1}^{n-1} \sum_{j=i+1}^n D_{ij} \cos \delta_{ij} \quad (3.21)$$

Now if we define  $P_{CCA}$  as

$$P_{COA} = \sum_{i=1}^n P_i - 2 \sum_{i=1}^{n-1} \sum_{j=i+1}^n D_{ij} \cos \delta_{ij} \quad (3.22)$$

Eqn. (3.19) will reduce to

$$M_T \frac{d^2 \delta_c}{dt^2} = P_{COA} \quad (3.23)$$

Multiplying eqn. (3.23) by  $M_i$  and rearranging we get

$$M_i \frac{d^2 \delta_c}{dt^2} = \frac{M_i}{M_T} P_{COA} \quad (3.24)$$

The dynamics of the center of angle are governed by the above equation.

The system equations in terms of the off center angle can be obtained by subtracting eqn. (3.24) from (3.10)

$$M_i \left\{ \frac{d^2 \delta_i}{dt^2} - \frac{d^2 \delta_c}{dt^2} \right\} = P_i - P_{ei} - \frac{M_i}{M_T} P_{COA} \quad (3.25)$$

substituting eqn. (3.14) in (3.25) yields

$$M_i \frac{d^2 \theta_i}{dt^2} = P_i - P_{ei} - \frac{M_i}{M_T} P_{COA} \quad (3.26)$$

Eqn. (3.26) represents the swing equation of the i-th generator in the COA reference frame. The second order dynamics given by eqn. (3.26) can be

represented by two first order differential equations by defining a new

variable  $\omega_i = \frac{d\theta_i}{dt} = \dot{\theta}_i$ . Thus eqn. (3.26) can be written as

$$\dot{\theta}_i = \omega_i \quad (3.27)$$

and

$$\dot{\omega}_i = \frac{1}{M_i} \left\{ P_i - P_{ei} - \frac{M_i}{M_T} P_{COA} \right\} \quad (3.28)$$

Eqn. (3.27) and (3.28) will be used to determine the CCT in chapter IV.

### 3.3 CALCULATION OF THE PARAMETERS OF THE EQUIVALENT MODEL [19]

The reduced order model consisting of less number of generators is obtained by replacing each group of coherent generators by an equivalent generator connected to a fictitious bus 'e'. The reduced order model is determined in such a way that the dynamics of the equivalent generator 'e' represents the dynamics of the COA of the coherent group. The parameters of the reduced order model, based on real power invariance principle, between the original and the reduced order system are obtained in the following manner:

The swing equation (3.10) of the  $i$ -th generator is written as

$$M_i \frac{d^2 \delta_i}{dt^2} = P_i - \sum_{\substack{j=1 \\ j \neq i}}^n (C_{ij} \sin \delta_{ij} + D_{ij} \cos \delta_{ij}) \quad (3.29)$$

Let us define

$\Omega$  : Group of coherent generators to be replaced by an equivalent generator

$\delta_e$  : center of angle (COA) of the coherent group

The COA  $\delta_e$  can be written as

$$\delta_e = \frac{1}{M_\Omega} \sum_{k \in \Omega} M_k \delta_k \quad (3.30)$$

where

$$M_\Omega = \sum_{k \in \Omega} M_k \quad (3.31)$$

At this stage if we assume that the generators are perfectly coherent i.e. ( $\alpha = 0$ ) in eqn. (1.1), then angle  $\delta_k$  of any generator in the coherent group ( $k \in \Omega$ ) can be expressed in terms of the angle of any other generator  $p$  ( $p \in \Omega$ ) in that coherent group. thus we can express this relation as

$$\delta_k = \delta_p + R_k \quad (3.32)$$

where  $R_k$  is a constant. Therefore eqn. (3.30) can be rewritten as

$$\delta_e = \delta_p + C \quad (3.33)$$

where

$$C = \frac{1}{M_\Omega} \sum_{k \in \Omega} R_k M_k = \text{constant} \quad (3.34)$$

Define the off-center angle  $\theta_k$  as the relative angle between the generator  $k$  and the COA given by  $\delta_e$

$$\theta_k = \delta_k - \delta_e \quad (3.35)$$

Using eqns. (3.32) and (3.33) in (3.35) we obtain the angle

$$\theta_k = \text{constant} \quad (3.36)$$

This can be directly obtained from the prefault operating angles.

The parameters of the reduced order model can now be obtained by equating the swing equation of various generators in the original and reduced order models.

### 3.3.1 Non-Coherent Generators

Consider the system in which a group of coherent generators  $\Omega$  have already been identified. The swing equation of any non-coherent generator 'i' in an n-generator system can be written as

$$M_i \frac{d^2 \delta_i}{dt^2} = P_i - \sum_{\substack{j=1 \\ j \neq i}}^n (C_{ij} \sin \delta_{ij} + D_{ij} \cos \delta_{ij}) - \sum_{k \in \Omega} (C_{ik} \sin \delta_{ik} + D_{ik} \cos \delta_{ik}) \quad (3.37)$$

Note that

$$\delta_{ie} = \delta_{ie} - \delta_{ke} = \delta_{ie} - \theta_k \quad (3.38)$$

The swing equation of the same generator 'i' in the reduced order system where the entire coherent group has been replaced by an equivalent generator 'e' will be

$$M_i \frac{d^2 \delta_i}{dt^2} = P_i - \sum_{\substack{j=1 \\ j \neq i}}^n (C_{ij} \sin \delta_{ij} + D_{ij} \cos \delta_{ij}) - (C_{ie} \sin \delta_{ie} + D_{ie} \cos \delta_{ie}) \quad (3.39)$$

Since eqns. (3.37) and (3.39) represent the dynamics of the same generator 'i' in the original and the reduced order systems, the power balance of these equations can be equated to get

$$(C_{ie} \sin \delta_{ie} + D_{ie} \cos \delta_{ie}) = \sum_{k \in \Omega} (C_{ik} \sin \delta_{ik} + D_{ik} \cos \delta_{ik}) \quad (3.40)$$



substituting  $\delta_{ik}$  from eqn. (3.38) into eqn. (3.40) and comparing the coefficients of  $\sin\delta_{ie}$  and  $\cos\delta_{ie}$ , we get

$$C_{ie} = \sum_{k \in \Omega} (C_{ik} \cos \theta_k + D_{ik} \sin \theta_k) \quad (3.42)$$

$$D_{ie} = \sum_{k \in \Omega} (D_{ik} \cos \theta_k - C_{ik} \sin \theta_k) \quad (3.42)$$

for all  $i \notin \Omega$

### 3.3.2 Coherent Generators

Similarly the swing equation of the generators in the coherent group ( $k \in \Omega$ ) can be added together to obtain

$$\sum_{k \in \Omega} M_k \frac{d^2 \delta_k}{dt^2} = \sum_{k \in \Omega} P_k - \sum_{k \in \Omega} \sum_{\substack{i=1 \\ i \notin \Omega}}^n (C_{ki} \sin \delta_{ki} + D_{ki} \cos \delta_{ki}) - L \quad (3.43)$$

where

$$L = \sum_{k \in \Omega} \sum_{\substack{j \in \Omega \\ j \neq k}} (C_{kj} \sin \delta_{kj} + D_{kj} \cos \delta_{kj}) \quad (3.44)$$

For any two coherent generators  $k$  and  $j$  the relative angle given by

$$\delta_{ki} = \theta_k - \theta_j = \text{constant} \quad (3.45)$$

Thus the quantity  $L$  given by eqn. (3.44) is a constant. Also for any two coherent generators  $k$  and  $j$

$$\frac{d^2 \delta_k}{dt^2} = \frac{d^2 \delta_j}{dt^2} = \frac{d^2 \delta_e}{dt^2} \text{ (say)} \quad (3.46)$$

Therefore eqn. (3.43) can be rewritten as

$$\left( \sum_{k \in \Omega} M_k \right) \frac{d^2 \delta_e}{dt^2} = \sum_{k \in \Omega} P_k - \sum_{k \in \Omega} \sum_{i=1}^n (C_{ki} \sin \delta_{ki} + D_{ki} \cos \delta_{ki}) - L \quad (3.47)$$

The swing equation of the equivalent generator 'e' representing the coherent group  $\Omega$  in the reduced order model can be written as

$$M_e \frac{d^2 \delta_e}{dt^2} = P_e - \sum_{i=1}^n (C_{ei} \sin \delta_{ei} + D_{ei} \cos \delta_{ei}) \quad (3.48)$$

Since eqn. (3.47) represents the dynamics of the COA of the coherent group and eqn. (3.48) represents the dynamics of the equivalent generator, these two equations can be equated to get

$$P_e = \sum_{k \in \Omega} P_k - L \quad (3.49)$$

$$M_e = \sum_{k \in \Omega} M_k \quad (3.50)$$

$$C_{ei} = \sum_{k \in \Omega} (C_{ki} \cos \theta_k - D_{ki} \sin \theta_k) \quad (3.51)$$

$$D_{ei} = \sum_{k \in \Omega} (C_{ki} \sin \theta_k + D_{ki} \cos \theta_k) \quad (3.52)$$

for all  $i \notin \Omega$

Note that

$$\delta_{ki} = \delta_{ke} - \delta_{ie} = \theta_k + \delta_{ei} \quad (3.53)$$

Also  $P_e$  can be written as

$$P_e = P_{me} - D_{ee} \quad (3.54)$$

Thus rewriting eqn. (3.49) we obtain

$$P_e = \sum_{k \in \Omega} P_{mk} - (\sum_{k \in \Omega} D_{kk} + L) \quad (3.55)$$

Comparing eqns. (3.54) and (3.55) we get

$$P_{me} = \sum_{k \in \Omega} P_{mk} \quad (3.56)$$

and

$$D_{ee} = \sum_{k \in \Omega} D_{kk} + L \quad (3.57)$$

It may be noted here that  $C_{ee}$  is not required in the transient stability studies and therefore has not been determined. However, this quantity could be obtained by using the reactive power invariance principle between the original and the reduced order system.

### 3.3.3 ALGORITHM

The following computational steps are involved in determining the parameters of the reduced order equivalent.

- i) Identify the groups of coherent generators using any suitable method.
- ii) For a particular group of coherent generators compute the reduced order network parameters using the eqns. (3.41), (3.42), (3.50), (3.51), (3.52), (3.56) and (3.57).
- iii) Repeat the above step for all the coherent generator groups.

## **CHAPTER IV**

### **COMPUTATION OF CRITICAL CLEARING TIME USING INDIVIDUAL MACHINE ENERGY**

#### **4.1 INTRODUCTION**

As mentioned earlier that the groups coherent generators may depend on the fault clearing time. Any standard coherency identification method should determine the groups of coherent generators when the fault is cleared around the critical clearing time. In order to achieve this we intend to initially compute the critical clearing time so that a criteria for coherency determination may be developed around that time.

Many versions of direct method exist for determining the critical clearing time. The most popular ones are those using total machine energy and the individual machine energy. We will use the individual machine energy approach because it requires the computation of the energy function of only

the severely disturbed generator and is thus much simpler and faster [23].

## 4.2 INDIVIDUAL MACHINE ENERGY

Lyapunov's second (or direct ) method is generally used to determine the stability of a non linear system. The method is applied to a power system to determine the transient stability or the CCT. The computation of critical clearing time involves finding a Lyapunov function 'V' for the post fault system. For a stable system the function 'V' along the post fault trajectory should be positive definite and its time derivative negative semi-definite at all points except the stable equilibrium point [13].

A power system, at the instant of fault clearing possesses an excess energy that must be absorbed by the network for stability to be maintained. This energy is referred to as the transient energy and can be expressed by the value of a Lyapunov function 'V'.

Studies [23] indicated that not all the transient energy contributes to system separation or instability. Infact, system separation depends on the energy of a certain individual generators or groups of generators called the critical group. These critical group of generators tend to separate from the rest of the generators called the non-critical group. Thus the computation of energy function of the critical group is sufficient to determine the critical

clearing time. In most of the cases the critical group comprises of only one generator.

The critical generator whose energy will be determined is called the severely disturbed generator. The critical generator for a given disturbance is identified by calculating the faulted generator accelerations at  $t=0^+$ . In this study the generator having the largest acceleration is considered as the severely disturbed generator. Only the energy of this generator is required to compute the CCT. However, some faults or disturbances may be found in a multimachine system where more than one generator or a group of generators have significantly large acceleration. In this case the process of determining the CCT may be repeated (by considering only one generator at a time as severely disturbed) and finally the minimum value of these CCTs may be considered as the actual value.

#### 4.3. THE INDIVIDUAL MACHINE ENERGY FUNCTION

Let 'i' be the critical or severely disturbed generator for a given fault. The swing equations of this generator are given by eqn. (3.27) and (3.28). Multiplying eqn. (3.28) by  $\dot{\delta}_i$  and rearranging we get

$$\{M_i \ddot{\delta}_i - P_i + P_{ei} + \frac{M_i}{M_T} P_{COA}\} \dot{\delta}_i = 0 \quad (4.1)$$

Since the function 'V' is required to be evaluated in the post fault region, eqn. (4.1) is integrated with respect to time between the limits  $t=t_s$  and  $t=t_r$ , where  $t_s$  is the time at which the post-fault trajectory reaches the Stable Equilibrium Point (SEP) and  $t_r$  is the fault clearing time or the initial time of the post fault system. The integral of eqn. (4.1) is called the energy function  $V_i$  of the critical generator.

$$V_i = \frac{1}{2} M_i \omega_i^2 - P_i(\theta_i - \theta_i^s) + \sum_{j=1}^n C_{ij} \int_{\theta_i^s}^{\theta_i} \sin \theta_{ij} d\theta_j + \sum_{j=1}^n D_{ij} \int_{\theta_i^s}^{\theta_i} \cos \theta_{ij} d\theta_j \\ + \frac{M_i}{M_T} \int_{\theta_i^s}^{\theta_i} P_{COA} d\theta_i \quad (4.2)$$

where  $\omega(t_s) = 0$ ,  $\theta$  is the angle at  $t_s$ ,  $\theta(t_s) = \theta^s$  is the post fault SEP.

The first term on the right hand side of eqn. (4.2) is a function of  $\omega^2$  and can be considered as the kinetic energy of the generator. The rest of the terms on the right hand side depend on  $\theta$  and can be considered as the potential energy of the severely disturbed generator. Thus we may write eqn. (4.2) as

$$V_i = V_{kei}(\omega) + V_{pei}(\theta) \quad (4.3)$$

During the faulted period the severely disturbed generator accelerates



thus increasing its potential as well as kinetic energy. After the fault is cleared the kinetic energy starts converting into potential energy to maintain the stability of the system. This process continues till a point is reached where the kinetic energy is at its minimum (zero) and the potential energy is maximum  $V_{peimax}$ . This value of potential energy, for the critically stable situation represents the energy absorbing capability of the post fault system and is the critical value of  $V$ , i.e.

$$V_{icr} = V_{peimax} \quad (4.4)$$

Instability of the system occurs if the total energy of the disturbed generator, at the instant of fault clearing exceeds its critical energy.

#### 4.3.1 Complexities of the Energy Function

Eqn. (4.2) cannot be evaluated analytically because it contains path dependant integrals. Also it requires the postfault SEP  $\Omega^*$ . However the equation can be simplified and evaluated under the following assumptions :

- a) The correct path of these integrals is the post fault system trajectory. One way of evaluating these integrals is by determining the system trajectory by simulation and then using the trapezoidal method to evaluate the integrands. However, determination of the system

trajectory by simulation is very time consuming. In order to simplify the computation of  $V$ , a linear trajectory in the angular space [23,24,25] is assumed. This enables the relative angle terms to be expressed in terms of one of the angles with respect to which the integrals are to be evaluated. With this assumption, the integrals of eqn. (4.2) can be evaluated analytically.

- b) For a stable case, if the fault is cleared by tripping a line, the system will settle down to a new stable equilibrium point known as the post fault SEP. The angle at the SEP is  $\theta^*$ . Generally the prefault SEP  $\theta^*$  is very close to the post fault SEP [26]. Therefore, at this stage we can assume  $\theta_i^* \approx \theta_i^0$ , where  $\theta_i^0$  is the prefault SEP obtained from the prefault load flow data. The error involved in this case can be corrected by adding a correction term  $V_{corr}$ , when evaluating the energy function  $V$ , [27].

$$V_{i'cr} = V \Big|_{\theta_i^*}^{\theta_{i'magv}} = V \Big|_{\theta_i^0}^{\theta_{i'magv}} + V \Big|_{\theta_i^*}^{\theta_i^0} \quad (4.5a)$$

and

$$V(t_{cr}) = V \Big|_{\theta_i^*}^{\theta_{i'cr}} = V \Big|_{\theta_i^0}^{\theta_{i'cr}} + V \Big|_{\theta_i^*}^{\theta_i^0} \quad (4.5b)$$

Here  $V \Big|_{\theta_i^*}^{\theta_i^0}$  is the correction term  $V_{corr}$  and represents the potential

energy at the prefault operating point  $\theta^0$  w.r.t. the postfault SEP  $\theta^*$ .

$\theta_{\max}$  is the angle at which  $V_{\max}$  occurs and  $V(t_{cr})$  is the value of the V-function at critical clearing time. But for a critical situation

$$V_{\max} = V(t_{cr}) \quad (4.6)$$

and since  $V_{\max}$  is being added to both equations (4.5a & b) this quantity gets cancelled

Thus eqn. (4.2) can now be written as [25]

$$V_i = \frac{1}{2} M_i \omega_i^2 - P_i^{\text{pr}}(\theta_i - \theta_i^0) - \sum_{j=1}^n C_{ij}^{\text{pr}}(\theta_i - \theta_i^0) x (\cos \theta_{ij} - \cos \theta_{ij}^0) / (\theta_{ij} - \theta_{ij}^0) +$$

$$\sum_{j=1}^n D_{ij}^{\text{pr}}(\theta_i - \theta_i^0) x (\sin \theta_{ij} - \sin \theta_{ij}^0) / (\theta_{ij} - \theta_{ij}^0) + \frac{M_i}{M_T} (\theta_i - \theta_i^0) x \left\{ \sum_{j=1}^n P_j^{\text{pr}} - \right.$$

$$\left. 2 \sum_{j=1}^{n-1} \sum_{k=j+1}^n D_{jk}^{\text{pr}} x (\sin \theta_{jk} - \sin \theta_{jk}^0) / (\theta_{jk} - \theta_{jk}^0) \right\} \quad (4.7)$$

where  $C_{ij}^{\text{pr}}$  and  $D_{ij}^{\text{pr}}$  are the parameters of the reduced post fault admittance matrix. Since eqn. (4.2) contains path dependant integrals the sign definiteness of  $V_i$  cannot be readily determined analytically. However extensive simulations reported in ref. [23] support the argument that  $V_i$  is

positive definite. Likewise it has been reasoned that  $\dot{V}_f$  is negative semi-definite.

#### 4.3.2 Determination of Critical Energy

The maximum potential energy  $V_{pot\_max}$  of the critical generator can be determined by calculating  $V_{pot}$  along the faulted trajectory till a point where it reaches the maximum. This is done under the assumption that the sustained fault trajectory and the critically unstable trajectory do not change significantly within the stability boundary [13].

Fig. 4.1 shows the variation of  $V_{pot}$ ,  $V_{kin}$  and  $V_f$  of the severely disturbed generator # 4 for a sustained fault on bus # 25 of the IEEE system. Values of  $V_{pot}$ ,  $V_{kin}$  and  $V_f$  have been obtained by evaluating eqn. (4.3) along the faulted trajectory. The angle and speed are obtained by using the Taylor series expansion. From the plot it is clear that potential energy of generator # 4 reaches the maximum at  $t_p = 0.38$  secs. This maximum value of potential energy is the critical value  $V_{i_{cr}}$ . The CCT is the time at which the total energy ( $V_{pot} + V_{kin}$ ) equals  $V_{i_{cr}}$  which is approximately 0.27 secs in this case.

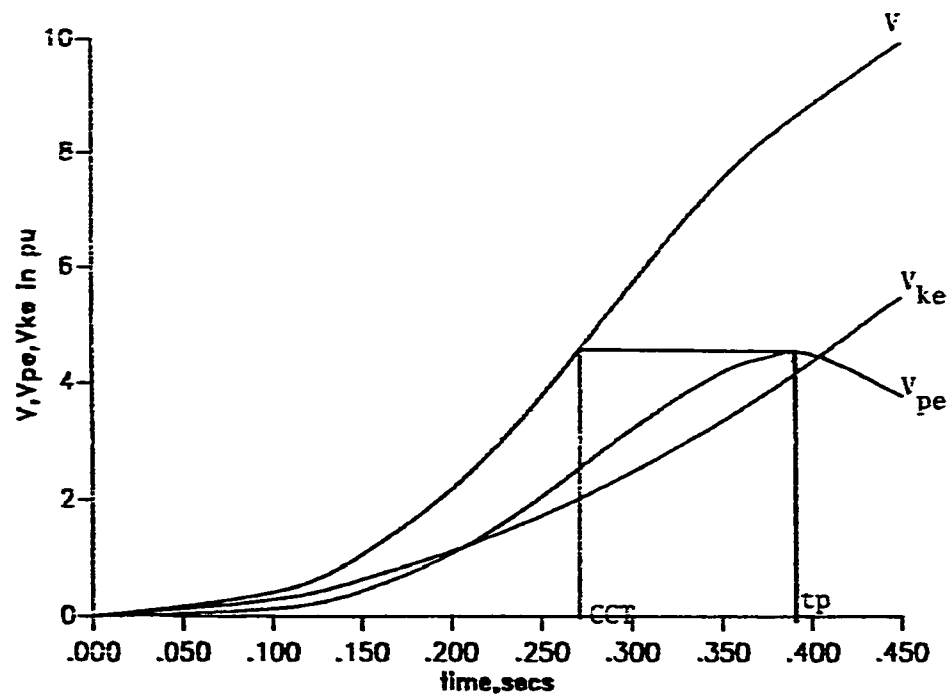


Fig. 4.1 Variation of PE, KE and total energy 'V' of gen#4 for a 3-ph fault on bus 25 of the IEEE system

An easier method would be to differentiate the expression for  $V_{pe}$  and equate it to zero to find the time at which  $V_{pe}$  becomes maximum. This is done by rewriting eqn. (4.2) as

$$V_i = \frac{1}{2} M_i \omega_i^2 + \int_{\theta_i^*}^{\theta_i} \left( -P_i + P_{ei} + \frac{M_i}{M_T} P_{COA} \right) d\theta_i \quad (4.8)$$

The above equation can be split into two parts which can be written as

$$V_{pe,i}(\omega) = \frac{1}{2} M_i \omega_i^2 \quad (4.9)$$

and

$$V_{pe,i}(\theta) = \int_{\theta_i^*}^{\theta_i} \left( -P_i + P_{ei} + \frac{M_i}{M_T} P_{COA} \right) d\theta_i \quad (4.10)$$

Differentiating eqn. (4.10) w.r.t. time we obtain

$$\dot{V}_{pe,i} = \omega_i \left( -P_i + P_{ei} + \frac{M_i}{M_T} P_{COA} \right) = f(t) \quad (4.11)$$

The terms  $P_i$ ,  $P_{ei}$  and  $P_{COA}$  in eqn. (4.11) are all functions of generator angles ( $\theta$ ). The generator angle ( $\theta$ ) and time ( $t$ ) are related by the Taylor series expansion, explained separately in section 4.3.4. Finding the value of  $t_p$  (time at which  $V_{pe}/\max$  occurs) involves the solution of the following equation.

$$f(t) = 0 \quad (4.12)$$

The function  $V_{pei}$  is maximum when its derivative  $\dot{V}_{pei}$  is zero. Ref.[23] determined  $V_{peimax}$  by calculating  $V_{pei}$  along the sustained fault trajectory using a special program which used the trapezoidal method of integration. Ref. [25] used the Newton Raphson's method to solve eqn. (4.12) The Newton Raphson's method requires the second derivative of  $V_{pei}$ .

In this study we will solve eqn. (4.12) by using the method of false position. This method does not require the second derivative of  $V_{pei}$ . The solution of eqn. (4.12) yields quantities  $t_p$  (time at which  $V_{peimax}$  occurs) and  $\theta_{peimax}$  (angle at which  $V_{peimax}$  occurs).  $\theta_{peimax}$  is substituted in the potential energy part of eqn. (4.7) to obtain  $V_{peimax}$  and hence  $V_{ucr}$ . Once  $V_{ucr}$  is known a second set of iterations is required to compute the critical clearing time  $t_{cr}$  and  $\theta_{cr}$  ( angle at  $t_{cr}$ ) by solving the following equation.

$$V_{kei}(\omega) + V_{pei}(\theta) - V_{ucr} = 0 \quad (4.13)$$

The values of  $\theta_{cr}$  of all the generators obtained at the CCT will be used to determine the coherent generator pairs during the faulted period as will be discussed in the next chapter.

### 4.3.3 Method of False Position [28]

Values of  $t_c$  and the critical clearing time can be determined from eqn. (4.12) and (4.13) respectively. These equations can be solved by the method of false position. This method has been used because it is computationally fast and unlike the Newton Raphson method it does not require the second derivative of  $V_{rei}$ .

The method of false position requires selection of two initial values of the function at  $t_1$  and  $t_2$ , which are opposite in sign. These are obtained by computing the value of the function at certain intervals of time till successive values of the function with opposite signs are found. This is illustrated in Table 4.1 which shows the selection of two initial values of the function  $\dot{V}_{rei}$  that are opposite in sign. The values indicated in Table 4.1 are for a fault on bus# 25 of the IEEE system.  $\dot{V}_{rei}$  is being computed for generator # 4 which is considered to be the severely disturbed in this case. A new value of time ( $t_3$ ) is obtained at the end of each iteration by using linear interpolation between  $t_1$  and  $t_2$  as shown in Fig. 4.2. The value of the function (say  $f_3$ ) is computed at  $t_3$ . Depending upon the sign of  $f_3$ , one of the initial values ( $t_1$  or  $t_2$ ) is replaced by  $t_3$ . This iterative procedure is continued till the value of the function ( $f_3$ ) evaluated at the end of an iteration tends to zero. The corresponding value of  $t_3$  is the solution of the equation.



**TABLE 4.1**

Selection of initial values of  $t$   
for a fault at bus #25 in IEEE system

Time (sec)	$V_{res}$
0.10	3.6255
0.20	16.625
0.30	22.008
0.40	-12.471

f1

f2

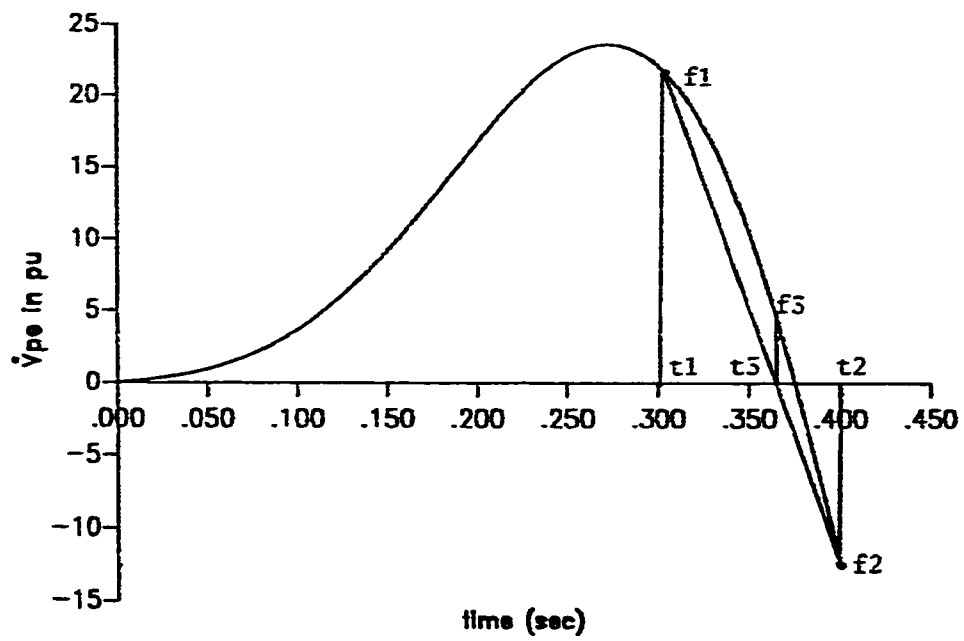


Fig. 4.2 Variation of  $\dot{V}_{pe}$  of gen # 4 for a 3-ph fault on bus 25 of the IEEE system

**TABLE 4.2**

Convergence rate of the method of false position in  
solving eqn. (4.12)

Iter.No.	$t_1$	$t_2$	$f_1$	$f_2$	$t_3$	$f_3$
1	0.3000	0.4000	22.000	-12.471	0.3640	5.079
2	0.3640	0.4000	5.079	-12.471	0.3745	0.505
3	0.3745	0.4000	0.505	-12.471	0.3754	0.004

Table 4.2 indicates the convergence rate of the method of false position in solving eqn. (4.12 ) to find  $t_c$ .

#### 4.3.4 Estimation of System States by the Taylor Series Expansion

The system states ( $\theta$  and  $\omega$ ) are required to compute the function  $V$  and the derivative of  $V_{pci}$ . These states can be obtained by integrating the swing equation. Alternatively the states can be predicted by using the Taylor series expansion [29]. The angle ( $\theta_i$ ) and speed ( $\omega_i$ ) of the  $i$ -th generator at time  $t$  can be expressed by the following TSEs.

$$\theta_i(t) = \theta_i(0) + \theta_i^{(1)}t + \theta_i^{(2)}\frac{t^2}{2!} + \theta_i^{(3)}\frac{t^3}{3!} + \theta_i^{(4)}\frac{t^4}{4!} + \dots \quad (4.14)$$

$$\omega_i(t) = \omega_i^{(1)} + \omega_i^{(2)}t + \omega_i^{(3)}\frac{t^2}{2!} + \omega_i^{(4)}\frac{t^3}{3!} + \dots \quad (4.15)$$

where

$$\theta_i^{(1)} = \omega_i(0)$$

$$\theta_i^{(2)} = \frac{P_{mi}}{M_i} - \sum_{j=1}^{n-1} A_{ij} + d_i$$

$$\eta_i^{(3)} = \sum_{j=1}^n B_{ij} \eta_j^{(1)} + d_2$$

$$\eta_i^{(4)} = \sum_{j=1}^n \{A_{ij} \eta_j^{(1)2} + B_{ij} \eta_j^{(2)}\} + d_3$$

The expressions for  $d_1, d_2, \dots$  are given by

$$d_1 = - \sum_{k=1}^n \frac{P_k}{M_1} + \sum_{k=1}^{n-1} \sum_{j=k+1}^n F_{kj}$$

$$d_2 = - \sum_{k=1}^{n-1} \sum_{j=k+1}^n H_{kj} \eta_{kj}^{(1)}$$

$$d_3 = - \sum_{k=1}^{n-1} \sum_{j=k+1}^n \{F_{kj} \eta_{kj}^{(1)2} + H_{kj} \eta_{kj}^{(2)}\}$$

$$\eta_{ij}^{(m)} = \eta_i^{(m)} - \eta_j^{(m)}$$

$$A_{ij} = (C_{ij} \sin \theta_{ij} + D_{ij} \cos \theta_{ij}) / M_i$$

$$B_{ij} = (-C_{ij} \cos \theta_{ij} + D_{ij} \sin \theta_{ij}) / M_i$$

$$F_{ij} = (2D_{ij} \cos \theta_{ij}) / M_i$$

$$H_{ij} = (2D_{ij} \sin \theta_{ij}) / M_i$$

where  $\theta_i(0)$  is the prefault angle of the  $i$  th generator.  $\theta_i^{(m)}$ :  $m=1,2,3,\dots$  is the  $m$  th derivative of  $\theta_i$  at  $t=0$ . 't' is the time at which the angles are computed. The second and higher order derivatives are obtained from eqn. (2.28) and its successive derivatives. At  $t=0$ ,  $\theta_i^{(1)} = \omega_i = 0$ . This implies that all odd ordered derivatives in eqn. (4.14) and (4.15) are zero. Thus only  $\theta_i^{(2)}$  and  $\theta_i^{(4)}$  are required to be computed. Results of ref.[9] indicate that derivatives upto the fourth order are sufficient to predict the angles fairly accurately. However when the time period is large the error due to the truncated higher order derivatives is large, giving a wrong prediction of the angles. In order to reduce this truncation error a second step Taylor series expansion must be used with updated coefficients. This is given by

$$\theta_i(t') = \theta_i(t_i) + \theta_i^{(1)} t' + \theta_i^{(2)} \frac{t'^2}{2!} + \theta_i^{(3)} \frac{t'^3}{3!} + \theta_i^{(4)} \frac{t'^4}{4!} + \dots \quad (4.16)$$

and

$$\omega_i(t) = \theta_i^{(1)} + \theta_i^{(2)}t + \theta_i^{(3)}\frac{t^2}{2!} + \theta_i^{(4)}\frac{t^3}{3!} + \dots \quad (4.17)$$

Here  $\theta_i^{(m)}$  is the updated m-th derivative of  $\theta_i$  evaluated at  $t = t_c$  and  $t' = t - t_c$ . Note that here the updated odd order derivatives in eqn. (4.16) and (4.17) are not equal to zero.

#### 4.4 ALGORITHM FOR COMPUTING CRITICAL CLEARING TIME

The procedure of finding the CCT by using the individual machine energy can be summarized as follows:

- i) Solve eqn. (4.12) using the method of false position to get  $t_f$  and  $\theta_{\max}$
- ii) Substitute the values of  $\theta_{\max}$  in the potential energy part of the eqn. (4.7) to obtain  $V_{\text{pe}/\max}$  and hence  $V_{\text{ilcr}}$
- iii) Solve eqn. (4.13) using the method of false position to obtain the critical clearing time and  $\theta_{\text{cr}}$ .

## 4.5 SIMULATION RESULTS

In this thesis a criteria for determining the groups of coherent generators will be developed. The groups of coherent generators will be identified for various fault locations on the IEEE and New England system by considering the fault to be cleared around the CCT. These systems have been described in chapter VI. The critical clearing time obtained for some faults using the individual machine energy function are given in Tables 4.3 and 4.4. Results obtained by the Rudnicks method and by simulation are also shown in the tables.

As discussed earlier, Rudnick [15] proposed that CCT is the time at which the rate of change of kinetic energy of the entire system is minimum. This is illustrated in Fig. 4.3 for a fault on bus # 25 of the IEEE system.

Results of Table 4.4 indicate that Rudnick's method gives erroneous results in some systems like the New England system. For example, for a fault on bus # 20 of this system Rudnick's method gave a CCT of 0.29 secs while the actual CCT for this case as found by direct simulation was in between 0.20 and 0.21 secs. The CCT obtained by the individual machine energy method was 0.211 secs.

It is clear from Tables 4.3 and 4.4 that the individual machine energy (IME) method gives a good estimate of the CCT.



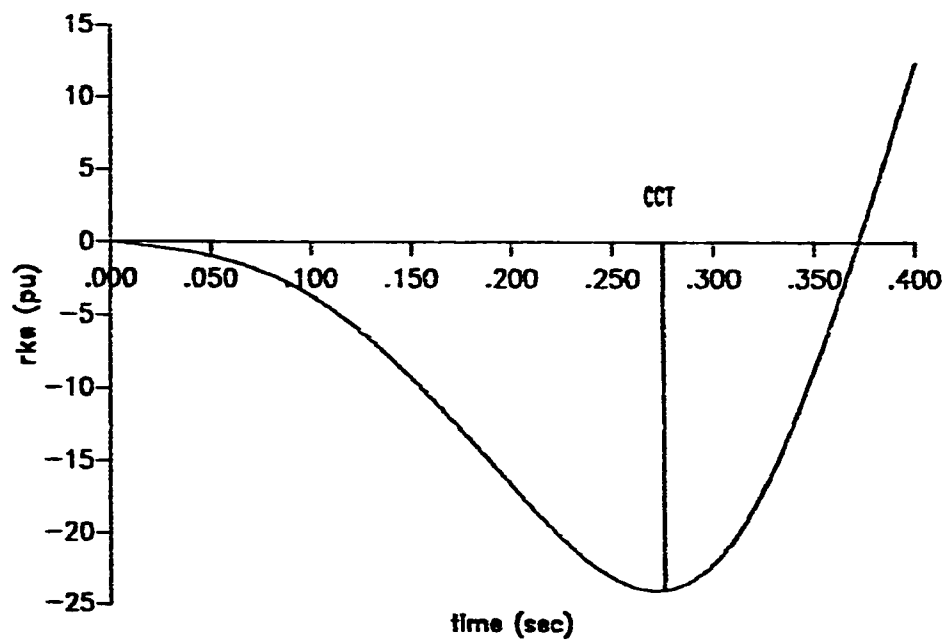


**Fig. 4.3** Variation of system RKE for a 3-ph fault on bus 25 of the IEEE system cleared after 0.27 secs

**TABLE 4.3**

**CCT (secs) obtained for various  
faults on the IEEE system**

<b>Fault at bus #</b>	<b>Line tripped between buses</b>	<b>Using IME method</b>	<b>By direct simulation</b>	<b>By Rudnick's method</b>
10	None	0.171	0.18-0.19	0.18
12	2-12	0.491	0.47-0.48	0.53
25	25-26	0.278	0.27-0.28	0.28
59	63-64	0.393	0.39-0.40	0.39

**TABLE 4.4**

CCT (secs) obtained for various  
faults on the New England system

Fault at bus #	Line tripped between buses	Using IME method	By direct simulation	By Rudnick's method
20	None	0.211	0.20-0.21	0.29
29	9-29	0.136	0.13-0.14	0.22

## **CHAPTER V**

### **DETERMINATION OF COHERENT GENERATORS**

#### **5.1 INTRODUCTION**

As mentioned earlier that a group of coherent generators should remain coherent for the entire transient period i.e. the faulted, early part of the postfault and the later part of the postfault periods. A method of determining the coherent generator groups in the external system using a combination of Taylor series expansion, linear trajectory and admittance distance measurement is presented in this chapter. A technique of identifying the generators in the external system, based on faulted generator accelerations, is also presented.

## 5.2 IDENTIFICATION OF THE "STUDY" AND "EXTERNAL" SYSTEM

In the dynamic equivalencing process the entire system is divided into two areas or subsystems called the "study" and the "external" system. The "study" system includes the generators that are severely affected by the disturbance and the dynamics of these generators are of great concern. The remaining generators are considered in the "external" system. The dynamic equivalencing procedure is applied to these generators only.

The acceleration of a generator depends on the fault location. Generators close to the fault or disturbance have a tendency to accelerate much faster than the generators away from the disturbance. This behavior of the generators is used to identify the the study and external system.

A three phase fault is applied at a generator bus and the faulted generator accelerations are computed at  $t=0$  using eqn. (3.28). An index, based on the ratio of the acceleration of each generator to the largest generator acceleration ( $a_{max}$ ), is proposed in the following, to identify the generators in the external system.

$$\frac{|a_j|}{a_{max}} < \sigma_1 \quad (5.1)$$

where  $a_j$  is the acceleration of generator 'j' in an 'n' generator system and  $\sigma_c$  is a predetermined constant. All generators whose acceleration satisfy eqn. (5.1) are considered in the "external" system on which the coherency criteria is applied.

### 5.3 IDENTIFICATION OF COHERENT GENERATORS

Coherency of generators is required to be checked in three regions namely.

- i) Faulted period.
- ii) Early part of the post fault period.
- iii) Later part of the post fault period.

The faulted period starts from the time a fault is initiated till the time the fault is cleared. It is assumed that the early part of the post fault period is the time period which starts at the fault clearing time and extends till the time at which the rotor angle of the severely disturbed generator reaches its peak. for a stable condition. The time period after the rotor angle of the severely disturbed generator has passed its peak may be considered as the later part of the post fault period. Fig. 5.1 shows these three regions in the swing curve of severely disturbed generator # 9 for a fault on bus # 29 in the New England system. The curve is plotted for the critically stable situation.

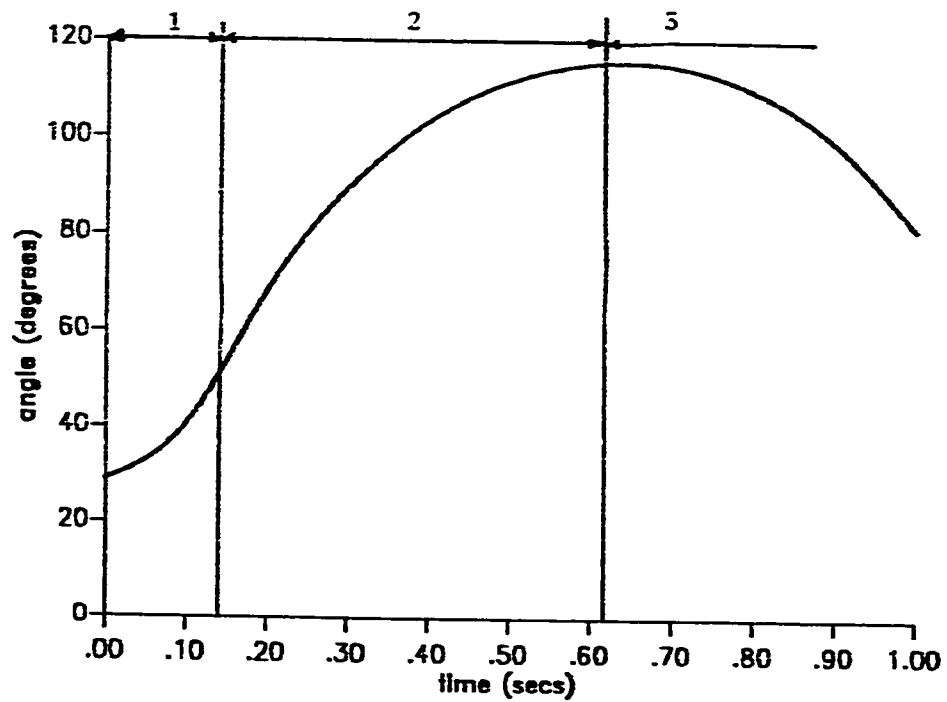


Fig. 5.1 Swing curves of gen # 9 for a 3-ph fault on bus 29 of the New England system cleared after 0.13 secs

1. faulted period
2. early part of the post fault period
3. later part of the post fault period

### 5.3.1 Coherency of the Generators during the Faulted Period

Coherency of generators during this period is determined by considering the fault to be cleared at critical clearing time. The faulted period is relatively short and the generator accelerations are more or less constant. During the faulted period the generator angles are monotonically increasing or decreasing. Coherency during this period can be determined by directly observing the faulted angle deviations between the generators. The generator angles at the time of fault initiation  $\delta_{ij}(0)$  are available from the prefault load flow results and the angles at the CCT,  $\delta_{ij}(t_{cr})$  are available from the solution of eqn. (4.13) as discussed in chapter IV. Therefore coherency during this period can be determined by checking the following criterion.

$$|\delta_{ij}(t_{cr}) - \delta_{ij}(0)| \leq \sigma_2 \quad (5.2)$$

where  $\delta_{ij}(t_{cr})$  and  $\delta_{ij}(0)$  are the relative angles between the generator pair (i,j) at critical clearing time and before the fault ( $t=0$ ), respectively, and  $\sigma_2$  is a predetermined constant.

If it is required to determine the coherency at time  $t$  ( $t < t_{cr}$ ) the truncated Taylor series expansion given by eqn. (4.14) can be used to determine the rotor angles at  $t$  from which the coherency can be determined during the faulted period using the criterion given by eqn. (5.2)



### **5.3.2 Coherency of Generators during the Early Part of the Post Fault Period**

Ref [9] determined the coherent generators in the early part of the post fault period by estimating the generator angles through a second step Taylor series expansion (TSE). The second step TSE can provide fairly accurate results for a short period of time when the fifth and higher order derivatives are neglected. However, if the early part of the post fault period (as shown in Fig. 5.1) is larger than 0.2 secs the second step TSE may give erroneous results. This problem could be overcome in the following manner.

- a) By solving the swing equations using integration techniques as discussed before.
- b) By using multistep Taylor series expansion in the post fault period.
- c) By considering more terms in the second step Taylor series expansion to give better accuracy.
- d) By using correction factors in the truncated Taylor series expansion [30].

All these approaches will definitely yield better results but are time consuming. An easier and quicker method using a combination of second step Taylor series expansion and linear trajectory is discussed hereunder to determine the coherency during this period.

### **Estimation of rotor angles and determination of coherency using linear trajectory**

The generator swing curves (angle vs time) are highly non-linear. However, if the independent variable time ( $t$ ) is eliminated from the swing curves and the generator trajectories (angle vs angle) are plotted, it was observed that the trajectories are more or less linear between two successive peaks of generator angles. When a trajectory is approximated by a straight line it is called a linear trajectory. Note that the linear trajectory does not mean a straight line assumption in time for a generator angle, but it assumes the curved trajectory of all generators are linearly related. The linear trajectory assumption is used in most of the direct methods in evaluating the energy function [23,24,25].

In general, the angle of the severely disturbed generator initially reaches the peak value in the post fault period and the peak for rest of the generators follows the peak of the severely disturbed generator. However, exceptions to this assumption might occur as will be discussed subsequently. Thus the generator angles in the early part of the post fault period can be estimated by considering the linear trajectory assumption.

Simulations have been conducted to verify the linear trajectories of the generators in the early part of the post fault period. The results of two such simulations have been shown in Fig. 5.2 and 5.3.

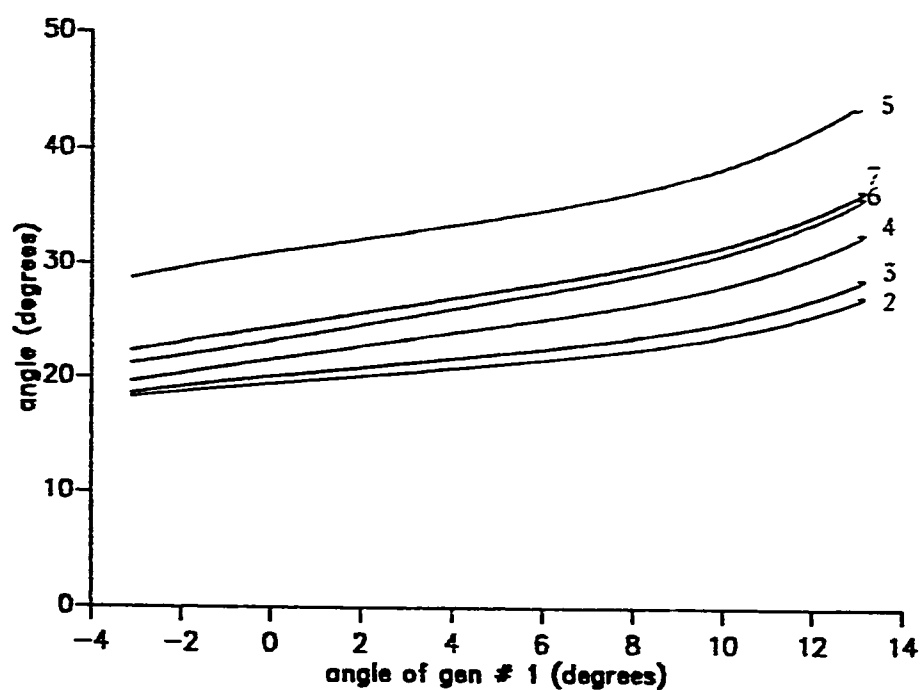


Fig. 5.2 Plot of rotor angles during the early part of the post fault period for a 3-ph fault on bus 29 of the New England system (CCT = 0.13 secs)

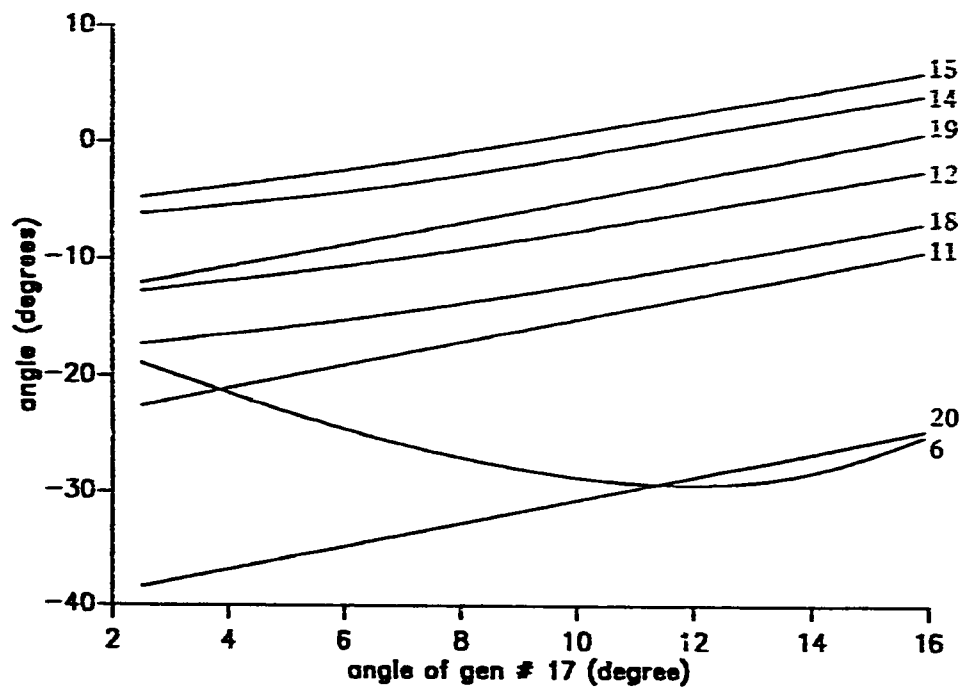


Fig. 5.3 Plot of rotor angles during the early part of the post fault period for a 3-ph fault on bus 10 of the IEEE system (CCT = 0.18 secs)

Fig. 5.2 shows the trajectories of some of the generators in the external system during the early part of the post fault period for a fault on bus # 29 of the New England system. The severely disturbed generator is #9. The generator angles are plotted against the angles of generator # 1. This generator has the largest inertia constant in the external system. Table 5.1 gives the angles of all the generators at critical clearing time ( $t_{cl}=0.13$  secs) and at the end of the early part of the post fault period ( $t_p=0.62$  secs). It is clear from this table that the angle of generator # 1 changes from -2.9 to 13.0 degrees during the early part of the post fault period. This corresponds to a change in angle of the severely disturbed generator (gen # 9) from 48.5 to 115.4 degrees. As seen the trajectories of all the generators are found to be more or less linear during the early part of the post fault period. A slight non-linearity is observed at the end of the early part of the post fault period where the angle of the severely disturbed generator is about to reach the peak. This is the point where the slopes of the trajectories change, indicating the end of the early part of the post fault period. Since this non-linearity is small and restricted to a short region, it does not significantly affect the accuracy of the calculation.

Fig. 5.3 shows the trajectories of some of the generators in the external system during the early part of the post fault period for a fault on bus # 10 of the IEEE system. The severely disturbed generator is # 2. The generator angles have been plotted against the angles of generator # 17 which is the

generator having the largest inertia constant in the external system. In this case the angle of generator # 17 changes from 15.9 degrees (  $t_{cl}=0.18$  secs) to 2.5 degrees (  $t_p=0.57$  secs). This corresponds to the change in the angle of the severely disturbed generator from 48.5 to 115.8 degrees.

**TABLE 5.1**

Generator Angles at  $t_{cr}$  and  $t_p$

GEN #	$\theta_i(t=t_{cr})$	$\theta_i(t=t_p)$	GEN #	$\theta_i(t=t_{cr})$	$\theta_i(t=t_p)$
1	-2.90	13.00	6	18.80	35.90
2	18.00	27.20	7	19.70	36.50
3	18.10	28.80	8	19.30	32.80
4	16.90	32.80	9	48.50	115.40
5	27.90	44.50	10	-11.2	-23.00

The trajectory of all the generators in Fig. 5.3 is found to be more or less linear except generator # 6. This generator is basically operating as a synchronous condenser supplying reactive power. The inertia constants of all the synchronous condensers in this system are relatively small ( $H=8$ ) as compared to most of the other generators in the system ( $H=14-32$ ). When such a generator is in the vicinity of a fault, it accelerates very fast as compared to the other generators because of its less inertia. It is also observed that the angle of this generator reaches the peak much before the severely disturbed generator. The trajectories of this generator changes direction in the early part of the post fault period. However, the non-linearity of this trajectory is not significant till it reaches its peak.

The linear trajectories of the generators enables us to express the angle of any generator in terms of the generator having the largest inertia constant in the external system. If 'k' is the generator having the largest inertia in the external system and 'j' is any other generator, we may express  $\theta_j$  in terms of  $\theta_k$  as

$$\theta_j = m_j \theta_k + c_j \quad (5.3)$$

where  $m_j$  is the slope of the trajectory of generator 'j' and  $c_j$  is the intercept. Thus the relative angle between two generators 'i' and 'j' can be calculated by just subtracting the two linear equations of the generators to obtain

$$\theta_{ij} = m_{ij} \theta_k + c_{ij} \quad (5.4)$$

where

$$\theta_{ij} = \theta_i - \theta_j \quad (5.5)$$

$$m_{ij} = m_i - m_j \quad (5.6)$$

$$c_{ij} = c_i - c_j \quad (5.7)$$

From the plots shown in Fig. 5.2 and 5.3 it is clear that if two generators are coherent or move together then their trajectories will be more or less parallel during the early part of the post fault period. This means that the slopes of their trajectories will be the same within a certain tolerance. Thus, if the slopes of the trajectory of two generators (i,j) are very close the generator pair (i,j) can be considered as coherent during the early part of the post fault period. The second step Taylor series expansion given by eqn. (4.16) can be used to compute the generator angles for a short period of time in the post fault period ( $t_{cr} + 0.20$ ). For such a short period the TSE can give an accurate estimation of the rotor angles. It may be noted here that in eqn. (4.16),  $\theta_i(t_1) = \theta_i(t_{cr})$ ,  $\theta_i^{(m)}$  is the m-th derivative evaluated at  $t = t_{cr}$  using post fault system parameters and  $t' = 0.20$  secs.



The slopes of the trajectories of the generators during the post fault period can now be computed using the relation

$$m_j = \frac{\theta_j(t_2) - \theta_j(t_{cr})}{\theta_k(t_2) - \theta_k(t_{cr})} \quad (5.8)$$

where  $m_j$  is the slope of the trajectory of generator 'j' during the early part of the post fault period  $\theta_j(t_2)$  is the rotor angle at  $t = (t_{cr} \pm 0.20)$  secs obtained by the second step TSE and  $\theta_k(t_{cr})$  and  $\theta_k(t_2)$  are the angles of the generator having the largest inertia at  $t_{cr}$  and  $t_2$  respectively.

The criteria for coherency of a generator pair (i,j) in the early part of the post fault period can therefore be expressed in terms of their slopes as

$$|m_i - m_j| \leq \sigma_3 \quad (5.9)$$

where

$\sigma_3$  is a predetermined constant.

Table 5.2 gives a comparison of the post fault rotor angles obtained by three different methods namely, step by step solution of the swing equation, second step TSE and by prediction of angles through linear trajectory using eqn. (5.3). The results shown are for a 3-phase fault at bus # 10 of the IEEE system. The severely disturbed generator is # 2 and the generator having the

largest inertia constant in the external system which is taken as reference is generator # 17. The fault has been cleared at CCT ( $t=0.18$  secs). At CCT the generator angles considered both in the TSE and linear trajectory are the same. These angles are obtained by the truncated TSE given by eqn. (4.14). The rotor angles shown in the table have been computed at  $t=0.54$  secs. At this instant the angle of generator # 17 is 3.8 degrees. All the other generator angles have been predicted with respect to this angle using eqn. (5.3).

A time of  $t' = 0.36$  secs ( $0.54-0.18$ ) has been considered for computing the rotor angle using the second step TSE (eqn. 4.16).

Table 5.2 clearly shows that the prediction of rotor angles using linear trajectory gives a better estimate of the angles in most of the cases as compared to the second step TSE for longer periods of time. However, in the case of generators 6 and 7 it is observed that the TSE gives a better estimate of the angles. This is because generators 6 and 7 are synchronous condensers having a small moment of inertia ( $H=8$ ). Since these generators are in the vicinity of the fault ( although they are in the external system ) they accelerate very fast and their angles reach a peak before the severely disturbed generator ( Fig. 5.3 ). Once they reach the peak the slope of their trajectories change. As a result of this the linear trajectory may give a slightly larger error for such a case.

**TABLE 5.2**

Generator Angles obtained by different methods at the  
end of the early part of the post fault period.

GEN #	Swing Eqn.	Linear traj.	TSE	Gen #	Swing Eqn.	Linear traj.	TSE
1	13.1	-8.6	-177.8	11	-16.6	-17.0	-18.5
2	115.1	115.2	209.7	12	-12.1	-12.6	-13.9
3	9.4	14.1	3.9	13	-4.9	5.1	-5.9
4	-0.1	-1.2	1.6	14	-5.6	-5.9	-7.4
5	1.1	1.6	2.2	15	-4.0	-4.6	-5.5
6	-21.2	-27.9	-26.0	16	-7.8	-8.1	-9.1
7	-20.6	-34.2	-31.6	17	3.8	3.8	3.2
8	-35.6	-37.4	-48.3	18	-21.2	-21.3	-22.4
9	-38.1	-36.2	-35.4	19	-10.9	-11.1	-12.1
10	-14.8	-15.0	-15.3	20	-37.0	-37.1	-37.9

### 5.3.3 Coherency during the Later Part of the Post Fault Period

Satisfaction of relative rotor angle deviation criteria during the faulted period and the difference in slopes in the early part of the post fault period guarantees that the generator pair (i,j) is coherent until the first swing peak or up to a point where the generators are on the verge of instability. For the stable situation, it is expected that by this time the system must have passed the severely disturbed stage. But satisfaction of the above two criteria does not guarantee that the generator pair will remain coherent for the later part of the post fault period.

Since the system has passed the initial severe thrust of the disturbance, a final check can be made by evaluating the electrical coupling or admittance distance between the pair of generators. Under normal circumstances a pair of generators which are electrically tightly coupled will swing together. The transfer admittance between two generators is a measure of electrical coupling. It may be recalled that transfer admittances are obtained by including the generator transient reactances and eliminating all buses in the system except the generator internal buses. Loads in the system are represented by constant impedances to ground before the load buses are eliminated.

Thus we may consider the generator pair (i,j) to be coherent for the later part of the postfault period if [9].

$$\frac{F_{ij}}{F_i} > \sigma_s \quad (5.10)$$

is satisfied, where

$$F_{ij} = \sqrt{C_{ij}^2 + D_{ij}^2} = |E_i E_j Y_{ij}| \quad (5.11)$$

and

$$F_i = \sum_{j=1}^{n_e} F_{ij} / (n_e - 1) \quad (5.12)$$

Here  $\sigma_s$  is a specified tolerance.  $\varphi$  is the set of generators belonging to the external system and  $n_e$  is the number of generators in the external system.  $F_i$  is the average transfer admittance of the generators in the external system. Thus the ratio  $F_{ij}$  to  $F_i$  indicates the degree of coupling between a generator pair (i,j) in the external system.

#### 5.4 ALGORITHM IN BRIEF

The computational procedure involved in determining the groups of coherent generators is given below.

- i) Assume a three phase fault on a certain generator busbar and select the study system. Generators belonging to the study system are determined by satisfying eqn. (5.1).
- ii) Determine the approximate critical clearing time using the method described chapter IV.
- iii) Determine the pairs of coherent generators during the faulted period by satisfying eqn. (5.2).
- iv) Determine the pairs of coherent generators during the early part of the post fault period by satisfying eqn. (5.9).
- v) Determine the pairs of coherent generators during the later part of the post fault period by satisfying eqn. (5.10).
- vi) Obtain the groups of coherent generators from the coherent pairs found in steps iii, iv and v so that all possible pairs of generators in a group are also coherent.

**Note:** In cases where the disturbance occurs away from a generator bus, the generator having the largest faulted acceleration can be considered as the severely disturbed generator.

## **CHAPTER VI**

### **SIMULATION RESULTS**

#### **6.1 INTRODUCTION**

The method of coherency determination discussed in chapter V has been tested on the following two test power systems.

- i) The 20-machine IEEE system
- ii) The 10-machine New England system

The single line diagrams of these systems are shown in Fig. 6.1 and 6.2. The results obtained by the proposed method has been checked by observing the swing curves produced by numerical integration of the swing equation. It may be noted that in all the cases the group of coherent generators has been obtained by assuming that the fault has been cleared at critical clearing time.

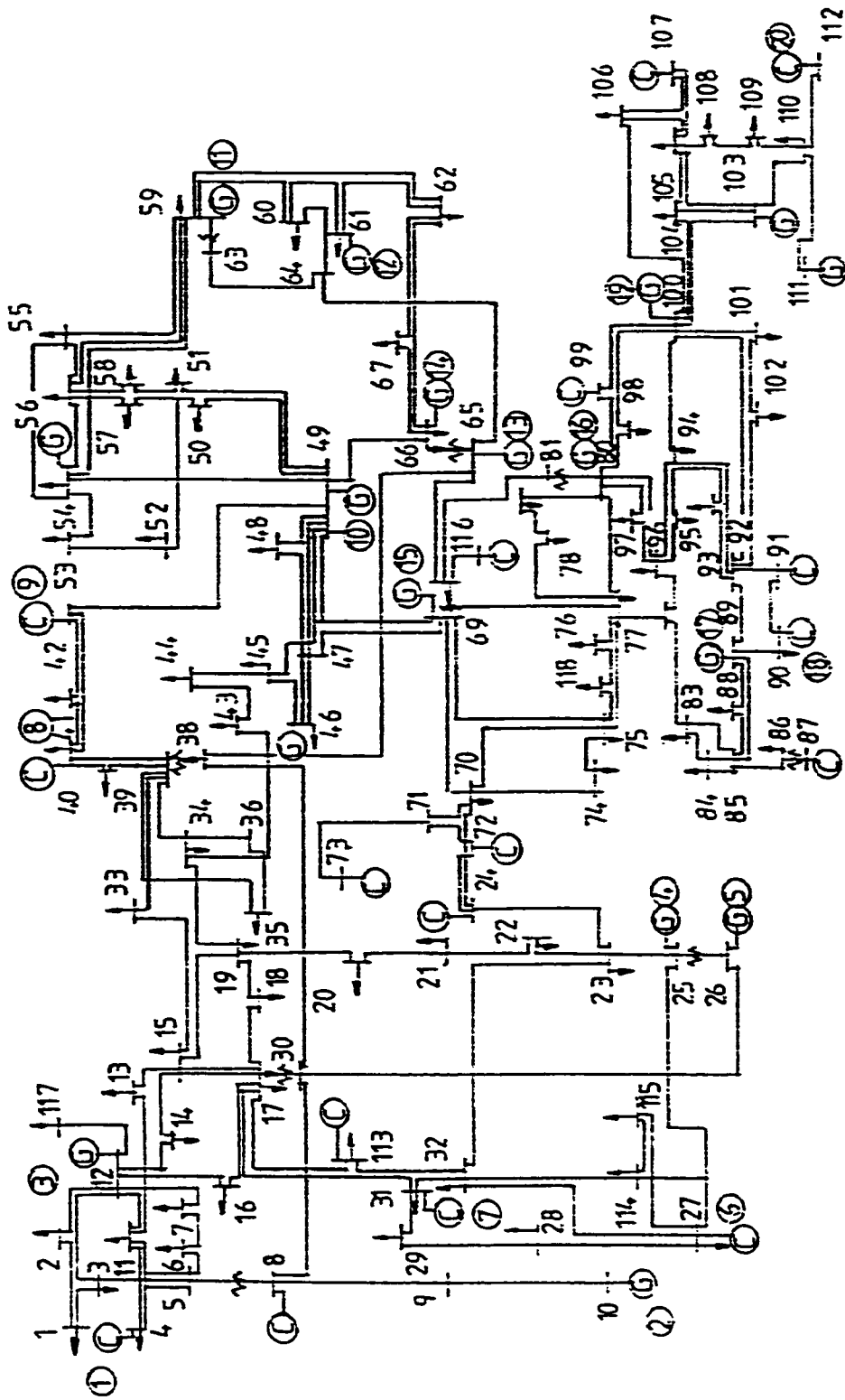


Fig. 6.1 Single line diagram of 20 machine IEEE system



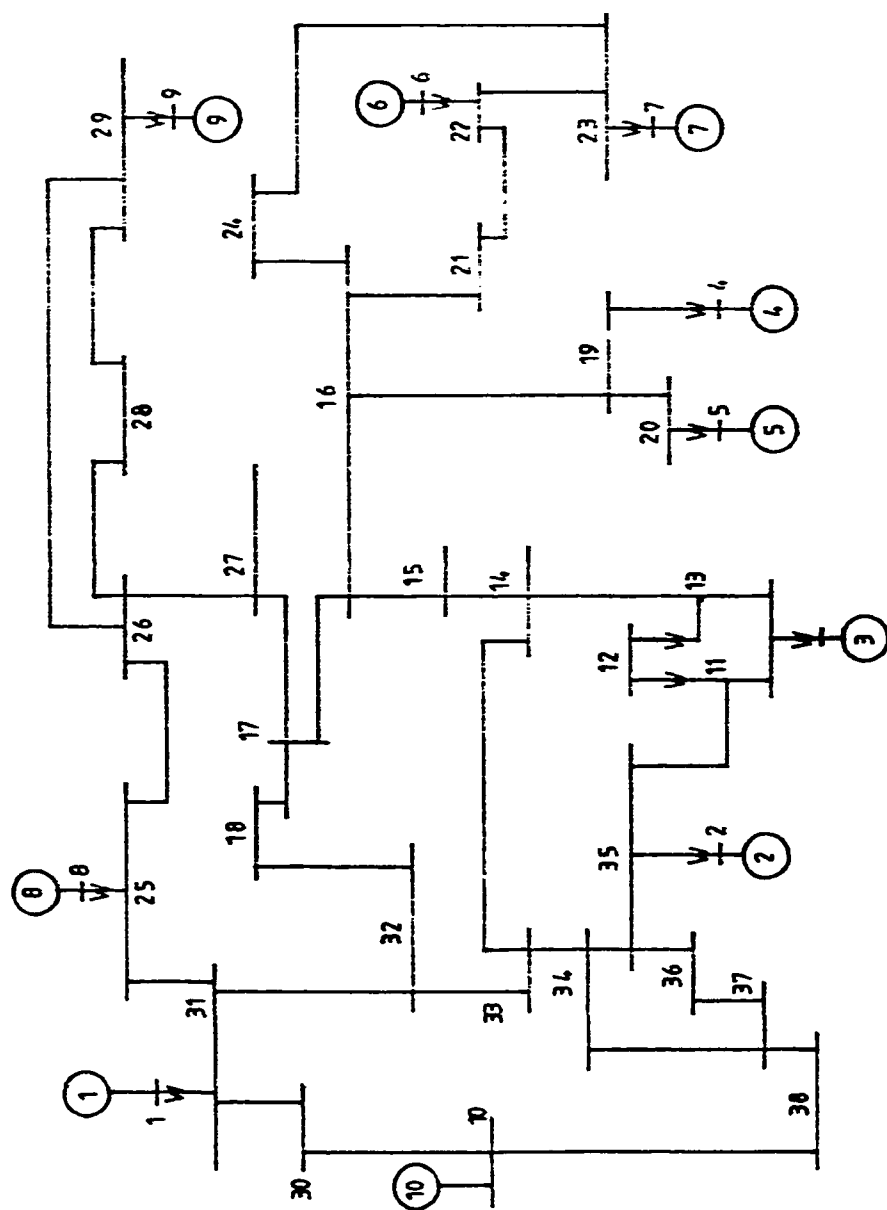


Fig. 6.2 Single line diagram of 10 machine New England system

A reduced order dynamic equivalent model of the system is then obtained by the method described in chapter III. The accuracy of the equivalent model is checked by comparing the swing curves of some of the retained generators, both for the critically stable and unstable situations.

Finally a comparison of CPU time required to solve the system swing equations by the step by step method in the reduced order model and full order model is given.

In determining the groups of coherent generators, the following threshold values are assumed.

- i)  $\sigma_1 = 0.40$
- ii)  $\sigma_2 = 3^\circ$
- iii)  $\sigma_3 = 0.40$
- iv)  $\sigma_4 = 1.0$

These values have been found by trial and error method. The correct selection of these values is essential for determining the final group of coherent generators. Note that the constitution of the coherent groups may depend on the above threshold values.

## **6.2 THE TEST SYSTEMS**

### **6.2.1 The IEEE System :**

The IEEE system consists of 20 generators and 118 buses. The single line diagram of the system is as shown in Fig. 6.1. Generator or unit numbers (encircled) are shown in the diagram. Units not assigned any number have been represented by constant shunt admittances. The system data with initial operating conditions are given in appendix-A. Three phase fault at four different locations has been considered in this system. The fault locations are as follows:

- i) Bus # 10
- ii) Bus # 12
- iii) Bus # 25
- iv) Bus # 59

The critical clearing time for these faults has been calculated in chapter IV and the results are shown in Table 4.3.

To illustrate the proposed method of coherency determination, the results of the fault on bus # 25 have been explained in detail. The critical clearing time for this fault is between 0.27 and 0.28 secs. The fault has been cleared

by tripping the line between buses 25 and 26. The results for the rest of the faults have been summarized in Table 6.8.

### **Determination of generators in 'study' and 'external' system**

As discussed in chapter V, determination of generators in the study system involves investigating the faulted generator accelerations. The faulted accelerations are calculated using eqn. (3.28) at  $t=0$ . The faulted accelerations of all the generators in the system are compared with the generator having the largest acceleration to check whether they satisfy the criteria given by eqn. (5.1). Table 6.1 shows the initial faulted acceleration of all the generators for a three phase fault on bus # 25. It can be observed in the table that gen # 4 has the largest acceleration ( $a_{max}=27.37 \text{ p.u.}$ ). The acceleration ratios given by eqn. (5.1) are also shown in Table 6.1.

**TABLE 6.1**

**Initial faulted accelerations and the acceleration ratios  
of all the generators for a 3-phase fault on bus # 25.**

<b>GEN #</b>	<b>Faulted Accn.</b>	<b>Ratio</b>	<b>GEN #</b>	<b>Faulted Accn.</b>	<b>Ratio</b>
<b>1</b>	<b>-5.04</b>	<b>0.184</b>	<b>11</b>	<b>-1.52</b>	<b>0.055</b>
<b>2</b>	<b>1.89</b>	<b>0.069</b>	<b>12</b>	<b>-1.51</b>	<b>0.055</b>
<b>3</b>	<b>-2.12</b>	<b>0.077</b>	<b>13</b>	<b>-0.64</b>	<b>0.023</b>
<b>4</b>	<b>27.37</b>	<b>1.000</b>	<b>14</b>	<b>-1.11</b>	<b>0.041</b>
<b>5</b>	<b>13.08</b>	<b>0.478</b>	<b>15</b>	<b>-0.46</b>	<b>0.017</b>
<b>6</b>	<b>-23.67</b>	<b>0.864</b>	<b>16</b>	<b>-1.34</b>	<b>0.050</b>
<b>7</b>	<b>-17.54</b>	<b>0.641</b>	<b>17</b>	<b>-1.98</b>	<b>0.073</b>
<b>8</b>	<b>-6.62</b>	<b>0.241</b>	<b>18</b>	<b>-2.27</b>	<b>0.082</b>
<b>9</b>	<b>-4.76</b>	<b>0.173</b>	<b>19</b>	<b>-1.94</b>	<b>0.071</b>
<b>10</b>	<b>-1.47</b>	<b>0.054</b>	<b>20</b>	<b>-2.39</b>	<b>0.087</b>

It can be noticed from the above table that only the acceleration of generator # (1,2,3,8,9,10,11,12,13,14,15,16,17,18,19,20) satisfy the criteria given by eqn. (5.1). Thus these generators can be considered in the external system. Coherency is checked for these generators only. The rest of the generators i.e. # (4,5,6,7) are considered in the study system.

#### **Coherency of generators during the faulted period :**

Coherency during this period is checked by calculating the relative rotor angle deviation between each generator pair at two different instants of time namely at  $t=0$  and at  $t = t_{cr}$  and checking whether their difference satisfies eqn. (5.2). The generator rotor angles at  $t=0$  are obtained from the prefault load flow data and the angles at  $t = t_{cr}$  are obtained from eqn. (4.13). It may be noted here that no additional calculation is required to compute the rotor angles at  $t_{cr}$  because these angles have already been obtained in solving eqn. (4.13) to determine the CCT. Table 6.2 indicates the values of the rotor angles at these two time instants.

TABLE 6.2

Generator Angles at  $t=0$  and at  $t=t_{cr}$ 

GEN #	$\theta_i(t=0)$	$\theta_i(t=t_{cr})$	GEN #	$\theta_i(t=0)$	$\theta_i(t=t_{cr})$
1	-20.693	-25.239	11	-5.357	-8.565
2	14.649	16.153	12	-0.825	-3.958
3	-15.997	-21.999	13	5.401	2.746
4	3.255	60.252	14	5.520	2.595
5	3.406	26.676	15	7.542	5.287
6	-20.571	-58.474	16	4.418	1.300
7	-22.380	-50.939	17	17.764	13.549
8	-30.832	-39.413	18	-7.460	-11.643
9	-30.205	-38.470	19	2.573	-1.420
10	-3.826	-7.493	20	-22.664	-27.515

The following generator pairs satisfy eqn. (5.2) and can thus be considered to be coherent only during the faulted period.

(1.3),(1.10),(1.11),(1.12),(1.13),(1.14),(1.15),(1.16),(1.17). (1.18),(1.19),(1.20).

(3.8),(3.9),(3.10),(3.11),(3.12),(3.16),(1.17). (3.18),(3.19),(3.20).

(8.9)

(10.11),(10.12),(10.13),(10.14),(10.15),(10.16),(10.17). (10.18),(10.19),(10.20).

(11.12),(11.13),(11.14),(11.15),(11.16),(11.17). (11.18),(11.19),(11.20).

(12.13),(12.14),(12.15),(12.16),(12.17). (12.18),(12.19),(12.20).

(13.14),(13.15),(13.16),(13.17),(13.18),(13.19),(13.20).

(14.15),(14.16),(14.17),(14.18),(14.19),(14.20).

(15.16),(15.17),(15.18),(15.19),(15.20).

(16.17),(16.18),(16.19),(16.20).

(17.18),(17.19),(17.20).

(18.19),(18.20).

(19.20).



### **Coherency during the early part of the post fault period :**

The post fault rotor angles of the generators are first computed for a short period of time (0.20 sec) using the second step Taylor series expansion given by eqn. (4.16). The slopes of the generator trajectories are then determined by using eqn. (5.8). It is expected that the slope of the trajectories remains more or less constant in the early part of the post fault period. Coherency during this period is determined by comparing the slopes of the generator pairs and checking whether they satisfy eqn. (5.9).

Table 6.3 shows the generator rotor angles obtained at CCT ( $t_{cr} = 0.27$  secs) and  $t_2$ , where  $t_2 = (t_{cr} + 0.20\text{secs})$ . Table 6.4 shows the slopes of generator trajectories during the early part of the post fault period. It may be noted here that the slope the generator trajectories have been computed with respect to the angles of generator # 17 . This generator has the largest inertia constant in the external system ( $H=32$ ).

**TABLE 6.3**Generator Angles at  $t_{cr}$  and  $(t_{cr} + 0.20)$  secs

GEN #	$\theta_i(t=t_{cr})$	$\theta_i(t=t_2)$	GEN #	$\theta_i(t=t_{cr})$	$\theta_i(t=t_2)$
1	-25.239	-21.706	11	-8.565	-13.851
2	16.153	16.620	12	-3.958	-9.213
3	-21.999	-18.350	13	2.746	-2.216
4	60.252	121.624	14	2.595	-2.874
5	26.676	40.466	15	5.287	-0.079
6	-58.474	-64.081	16	1.300	-4.348
7	-50.939	-53.884	17	13.549	6.636
8	-39.413	-39.992	18	-11.643	-18.569
9	-38.470	-40.071	19	-1.420	-7.937
10	-7.493	-12.623	20	-27.515	-35.041

**TABLE 6.4**

**Slopes of the generator angles during the early part of  
the post fault period**

<b>GEN #</b>	<b>Slope</b>	<b>GEN #</b>	<b>Slope</b>
1	-0.5110	11	0.7639
2	-0.0533	12	0.7591
3	-0.5276	13	0.7200
4	-8.8751	14	0.7920
5	-1.9892	15	0.7783
6	0.7963	16	0.8169
7	0.4158	17	1.0000
8	0.0702	18	0.9994
9	0.2319	19	0.9422
10	0.7437	20	1.0883

The following generator pairs, which have already satisfied the criteria for coherency during the faulted period, satisfy the criteria for coherency during the early part of the post fault period eqn. (5.9)

(1.3),

(8.9),

(10.11),(10.12),(10.13),(10.14),(10.15),(10.16), (10.17),(10.18),(10.19),(10.20)

(11.12),(11.13),(11.14),(11.15),(11.16), (11.17),(11.18),(10.19),(11.20)

(12.13),(12.14),(12.15),(12.16), (12.17),(12.18),(12.19),(12.20)

(13.14),(13.15),(13.16), (13.17),(13.18),(13.19),(13.20)

(14.15),(14.16), (14.17),(14.18),(14.19),(14.20)

(15.16), (15.17),(15.18),(15.19),(15.20)

(16.17),(16.18),(16.19),(16.20)

(17.18),(17.19),(17.20),

(18.19),(18.20),

(19.20),

**Coherency during the later part of the post fault period :**

Generator coherency during this period is determined by first computing  $F_{ij}$  and  $F_i$  using the eqns. (5.11) and (5.12) and then checking whether their ratio satisfies eqn. (5.10). Eqn. (5.10) indicates the degree of electrical coupling between a generator pair. These ratios for the generators in the external system are indicated in Table 6.5.

Notice that the table shows the ratios of only those generators which have been identified as coherent in the earlier two periods. Since  $F_{ij} = F_{ji}$ , only the upper triangle of the admittance distance ratio matrix has been indicated.

**TABLE 6.5**

### Admittance distance ratios

[illegible]

Thus the final coherent generator pairs which have satisfied all criteria given by eqns. (5.2). (5.9) and (5.10) are

(1.3)

(8.9)

(10.11).(10.12).(10.13).(10.14).(10.15).(10.16).

(11.12).(11.13).(11.14).(11.15).(11.16).

(12.13).(12.14).(12.15).(12.16),

(13.14).(13.15).(13.16).

(14.15).(14.16).

(15.16).

(16.17).(16.19),

(17.18).(17.19).(17.20),

(18.19).(18.20).

(19.20).

### **Final coherent groups:**

The final groups of coherent generators are selected very carefully from the final coherent pairs such that each pair of generators in a group is also coherent. Table 6.6 shows the final groups of coherent generators.

Fig. 6.3 shows the swing curves of generators 10.11.12.13.14.15.16. Fig. 6.4 and 6.5 show the swing curves of generators 17.18.19.20 and generators 1.3.8.9 respectively. The swing curves are generated by the step by step method. Close examination of the swing curves clearly indicates that the results obtained by the proposed method are in perfect agreement with those given in Table 6.6 within a tolerance of  $\epsilon = \pm 6^\circ$ .

Results obtained by the proposed method are also compared with those reported in ref. [14]. It may be recalled that ref. [14] determined the coherent generators by considering a fault clearing time of 0.2 secs. In this work the fault clearing time is considered to be the CCT (0.27 secs). For this fault, the results obtained by both the methods are the same. However, some faults may be found [9] where the groups coherent generators may depend on the fault clearing time.



**TABLE 6.6****Final coherent groups**

<b>By Proposed Method</b>	<b>By Direct Simulation</b>	<b>By Method of Ref-14</b>
(1.3)	(1.3)	(1.3)
(8.9)	(8.9)	(8.9)
(10.11.12.13. 14.15.16)	(10.11.12.13. 14.15.16)	(10.11.12.13. 14.15.16)
(17.18.19.20)	(17.18.19.20)	(17.18.19.20)

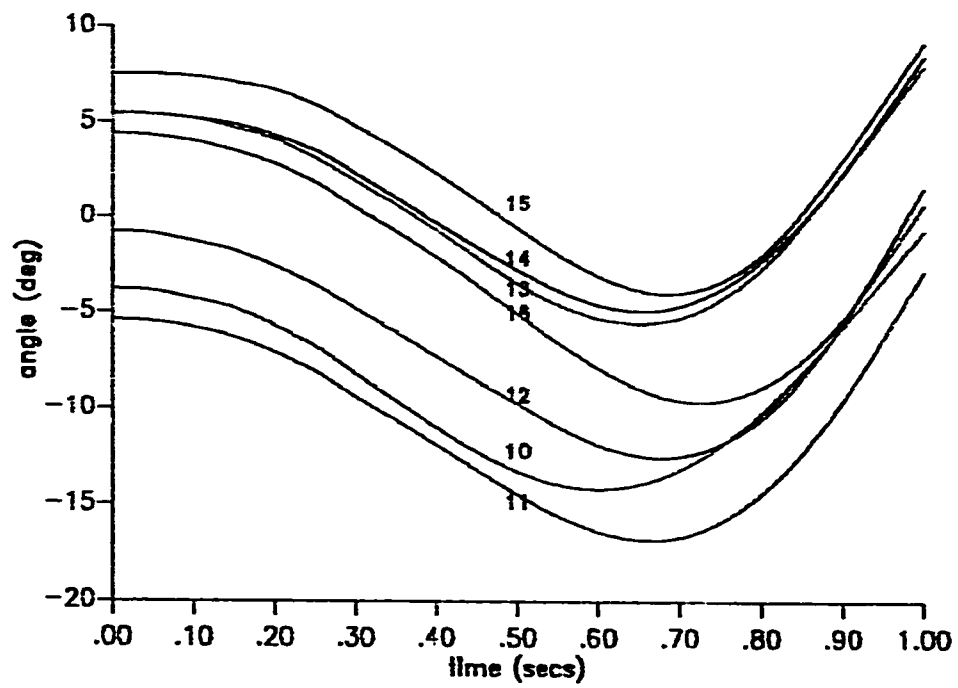


Fig. 6.3 Swing curves of generators 10-16 for a 3-ph fault on bus 25 of the IEEE system (CCT=0.27 secs)

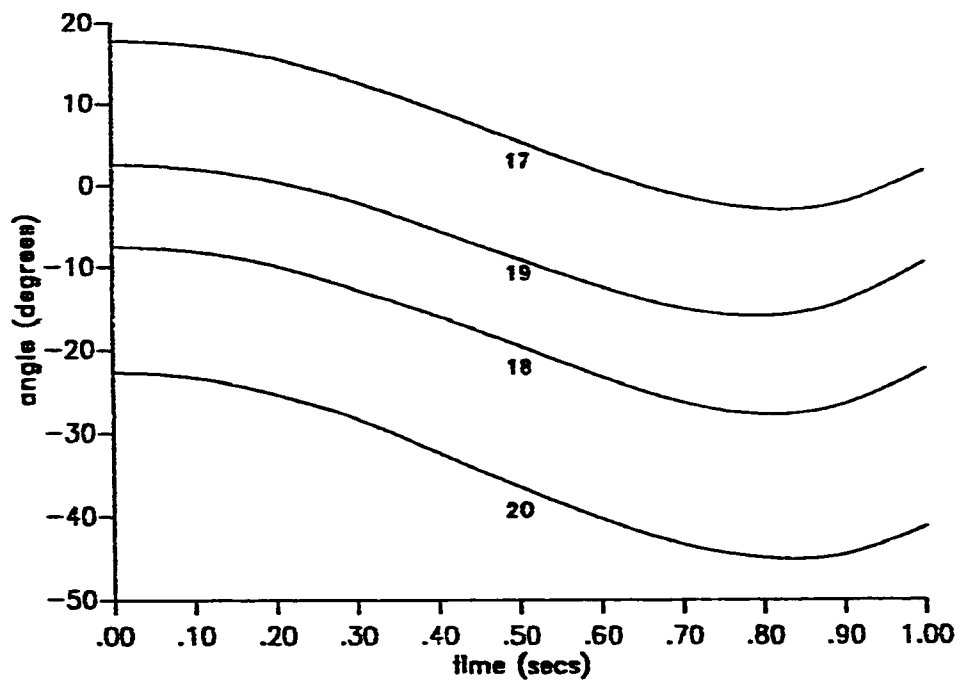


Fig. 6.4 Swing curves of generators 17-20 for a 3-ph fault on  
on bus 25 of the IEEE system (CCT = 0.27 secs)

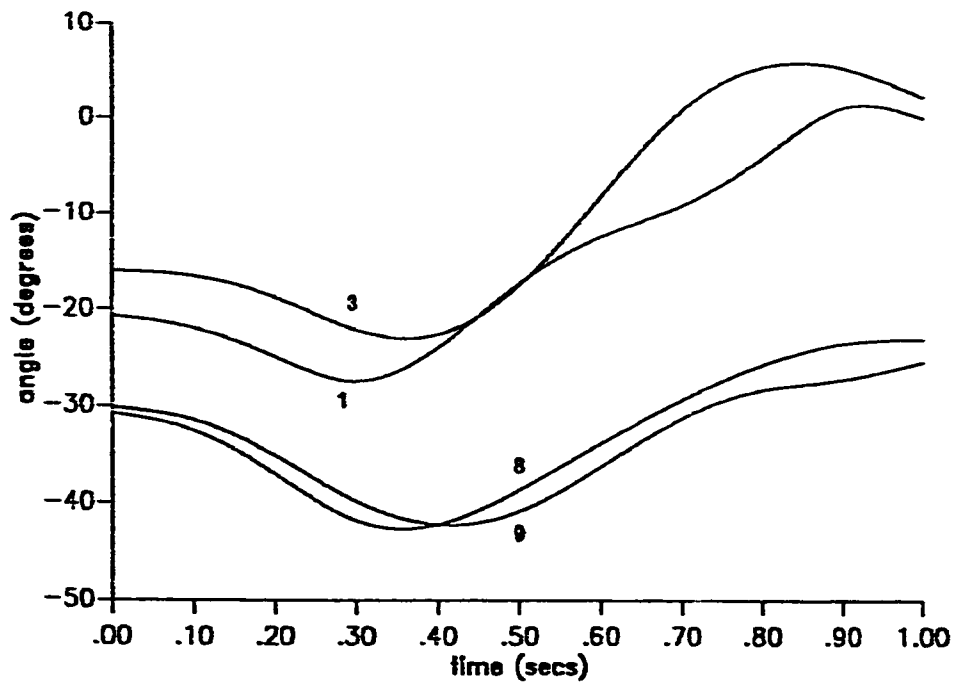


Fig. 6.5 Swing curves of generators 1,3,8,9 for a 3-ph fault on bus 25 of IEEE system (CCT = 0.27 secs)

### **Reduced order dynamic equivalent :**

The parameters of the reduced order model are obtained by replacing each group of coherent generators by their equivalent as described in chapter III. The accuracy of the reduced order model is checked by comparing the swing curves of some of the retained generators both for the critically stable and unstable situations. Fig. 6.6 and 6.7 show the swing curves for generator # 4 and 7 respectively. The fault clearing time considered for the critically stable and unstable cases are 0.27 and 0.28 secs, respectively.

It is observed from the swing curves of the retained generators that the results obtained in the reduced order model are very close to the corresponding actual values found in the original system.

### **Effects of the threshold values ( $\sigma_2, \sigma_3, \sigma_4$ ) on the groups of coherent generators.**

Several dynamic equivalents of the IEEE system were obtained for the three phase fault on bus # 25 using different values of  $\sigma_2$ ,  $\sigma_3$  and  $\sigma_4$ . The results are indicated in Table 6.7. It is clear that the number of generators in the system can be significantly reduced by increasing  $\sigma_2$ ,  $\sigma_3$  and decreasing  $\sigma_4$ . However, the equivalent obtained for these cases may not be very

reliable. On the other hand equivalents obtained by using smaller values of  $\sigma_2$ ,  $\sigma_3$  and larger values of  $\sigma_4$  are quite accurate as is evident from Fig. 6.6 and 6.7. The proper selection of these constant for a particular system is the key to the accurate determination of a dynamic equivalent.

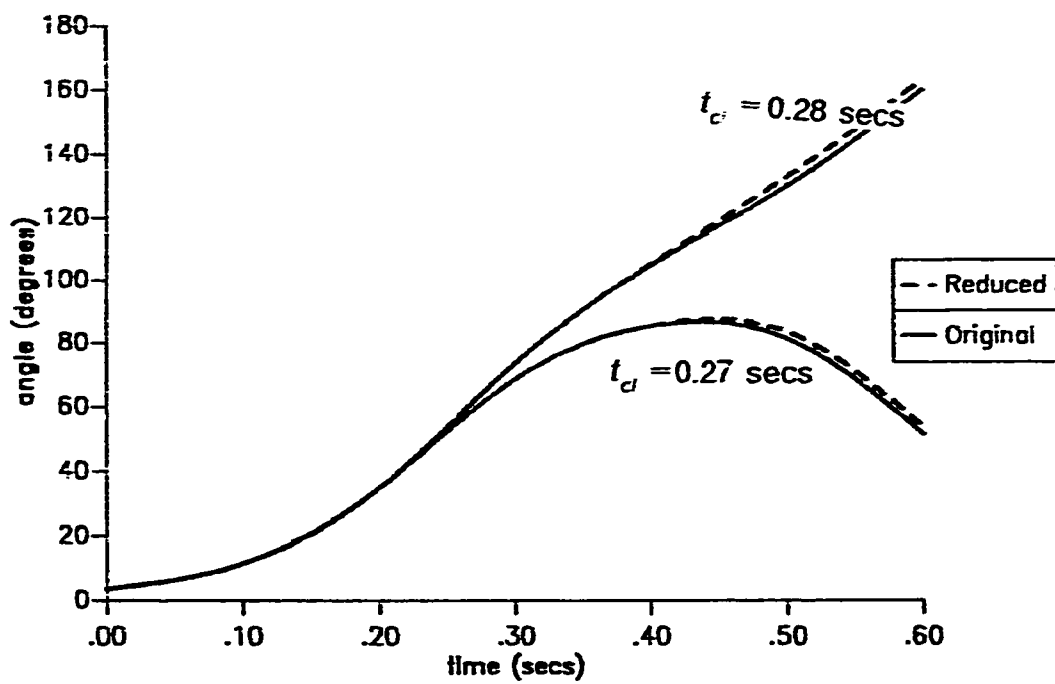


Fig. 6.6 Swing curves of gen. # 4 for a critically stable and unstable case for a 3-ph fault on bus 25 of the IEEE system

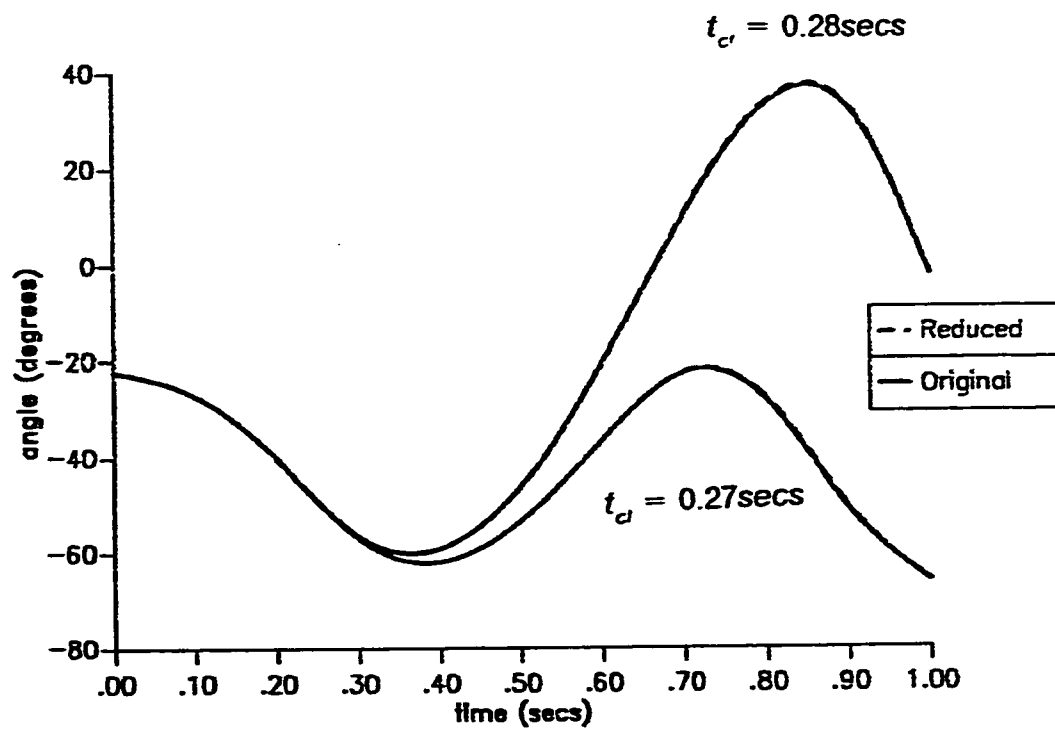


Fig. 6.7 Swing curves of gen. # 7 for a critically stable and unstable case for a 3-ph fault on bus 25 of the IEEE system



**TABLE 6.7**

The number of generators obtained in Different equivalents.

$\sigma_2$ (deg)	$\sigma_3$	$\sigma_4$	Nos of gen.	Coherent groups
1	0.20	1.5	12	I:8.9 II:11.12.13.14.15 III:17.18.19.20
3	0.40	1.0	9	I:1.3 II:8.9 III:10.11.12.13.14.15.16 IV:17.18.19.20
7	0.60	0.6	7	I:1.2.3 II:8.9.10.11.12.13.14.15.16 III:17.18.19.20

### Coherent groups obtained for other faults:

Coherent groups for other fault locations ( on buses 10,12 and 59 ) have been obtained by the same way as discussed in the preceding sections. The summary of the results is given in Table 6.8.

For a fault on bus # 10 the severely disturbed generator is # 2. The generators considered in the study system are 1,2,3. The rest of the generators are considered in the external system. The swing curves of the coherent generator groups (4,5), (6,7) and (8,9) are shown in Fig. 6.8. Fig. 6.9 and 6.10 show the swing curves of coherent generator groups (10,11,12,13,14,15,16) and (17,18,19,20) respectively. The reduced order dynamic equivalent is also obtained and its accuracy checked by observing the swing curves of one of the retained generators (gen#2) in the reduced order model as well in the original system for both the critically stable ( $t_{cr}=0.18\text{sec}$ ) and unstable ( $t_{cr}=0.19\text{sec}$ ) cases. The comparison of swing curves is shown in Fig. 6.11.

Fig. 6.12 shows the swing curves of coherent generator groups (4,5), (6,7) and (8,9) while Fig. 6.13 and 6.14 show the swing curves of coherent generator groups (10,11,12,13,14,15) and (17,18,19,20), respectively for a fault on bus #12. The severely disturbed generator for this fault is gen #3. The

generators considered in the study system are 1,2 and 3. For this fault the accuracy of the reduced order equivalent has been checked by comparing the swing curves of generator # 3 for the critically stable ( $t_{cr}=0.47\text{sec}$ ) and unstable ( $t_{cr}=0.48\text{sec}$ ) situations. These curves are shown in Fig. 6.15.

Similarly for a fault on bus # 59 the severely disturbed generator was identified as generator # 11. The study system for this fault consists of generators 10, 11 and 12. Fig. 6.16 shows the swing curves of the coherent generator group (1,2,3,4,5,6,7). Fig. 6.17 shows the swing curves of coherent generator groups (8,9),(13,14) while Fig. 6.18 shows the swing curves of the coherent generator group comprising of generators (17,18,19). The accuracy of the reduced order equivalent has been checked by comparing the swing curves of generator # 11 in the reduced order model as well as the original system for both the critically stable ( $t_{cr}=0.39\text{sec}$ ) and unstable ( $t_{cr}=0.40\text{sec}$ ) case. These curves are shown separately in Fig. 6.19.

In all the above cases the tolerances used to compare the swing curves generated by the step by step method is  $\tau = \pm 6^\circ$

**TABLE 6.8**

Coherent generator groups for IEEE system for various faults.

Fault at Bus #	Line tripped between buses	Coh. generators by proposed method	By direct simulation	Gen. in reduced system
#10	None	(4,5)(6,7)(8,9) (10,11,12,13, 14,15,16) (17,18,19,20)	(4,5)(6,7)(8,9) (10,11,12,13, 14,15,16) (17,18,19,20)	8
#12	2-12	(4,5)(6,7)(8,9) (10,11,12,13, 14,15) (17,18,19,20)	(4,5)(6,7)(8,9) (10,11,12,13, 14,15) (17,18,19,20)	9
#59	63-64	(1,2,3,4,5,6,7) (8,9) (13,14) (17,18,19)	(1,2,3,4,5,6,7) (8,9) (13,14) (17,18,19)	10

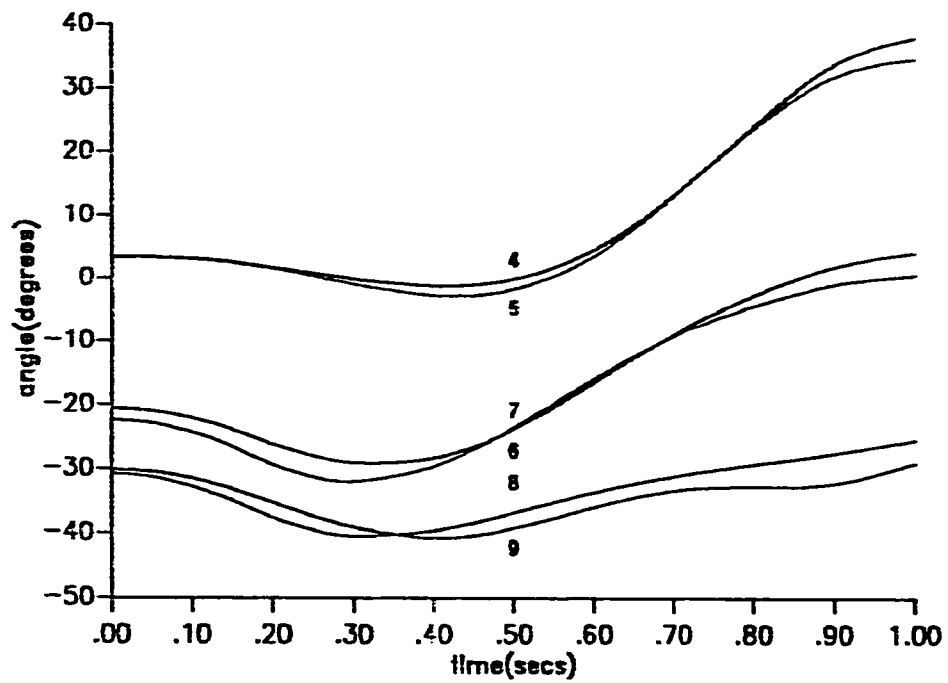


Fig. 6.8 Swing curves of generators 4-9 for a 3-ph fault on bus 10 of the IEEE system (CCT = 0.18 secs)

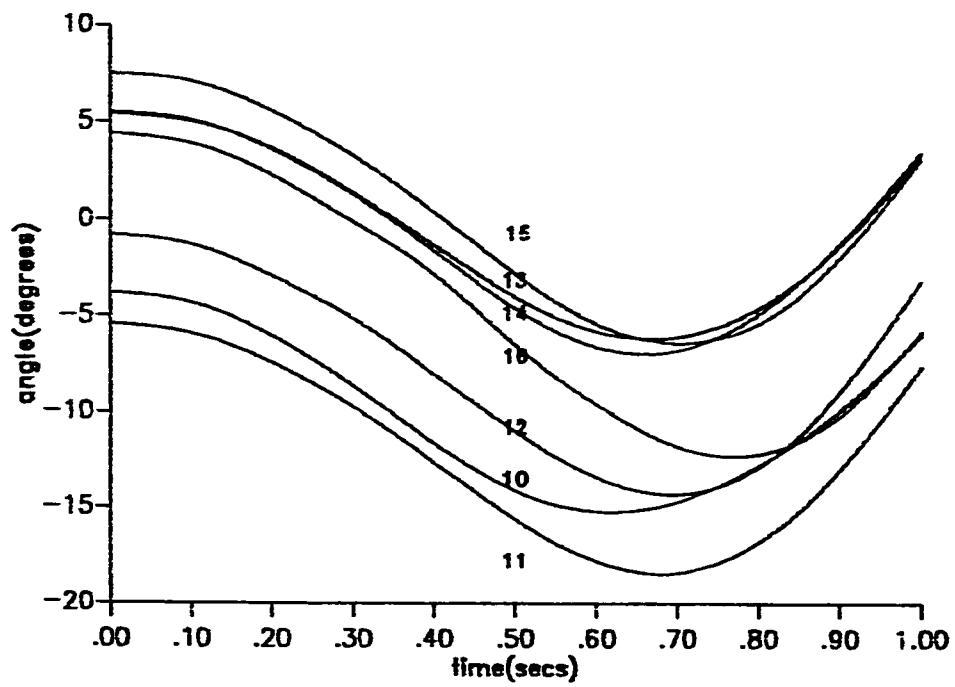


Fig. 6.9 Swing curves of generators 10-16 for a 3-ph fault on bus 10 of the IEEE system (CCT = 0.18 secs)

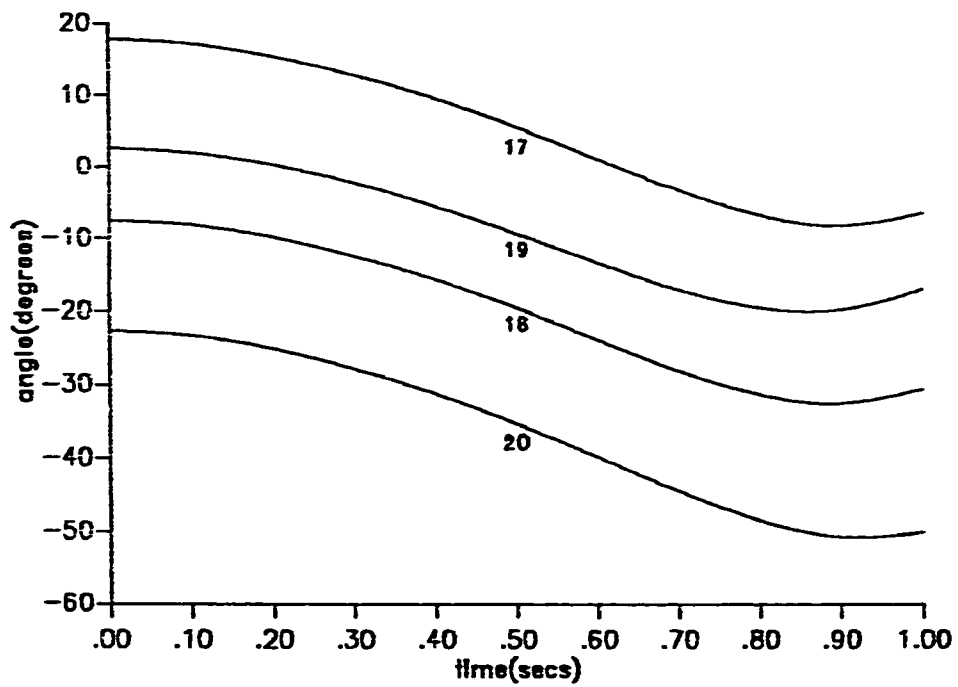


Fig. 6.10 Swing curves of generators 17-20 for a 3-ph fault on bus 10 of the IEEE system (CCT = 0.18 secs)

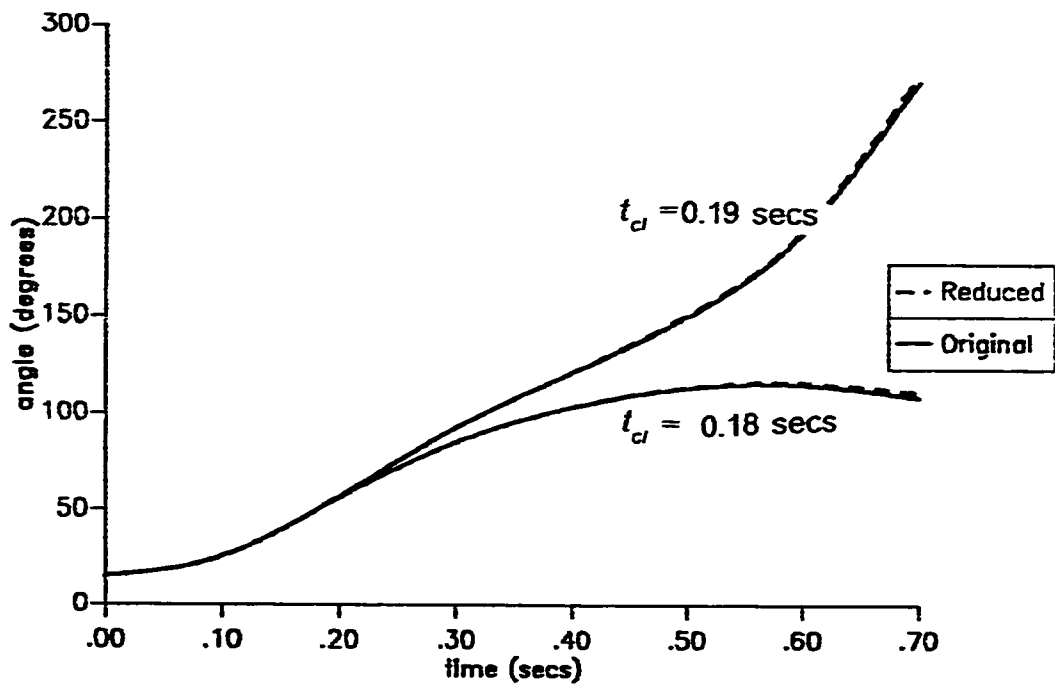


Fig. 6.11 Swing curves of gen. # 2 for a critically stable and unstable case for a 3-ph fault on bus 10 of the IEEE system



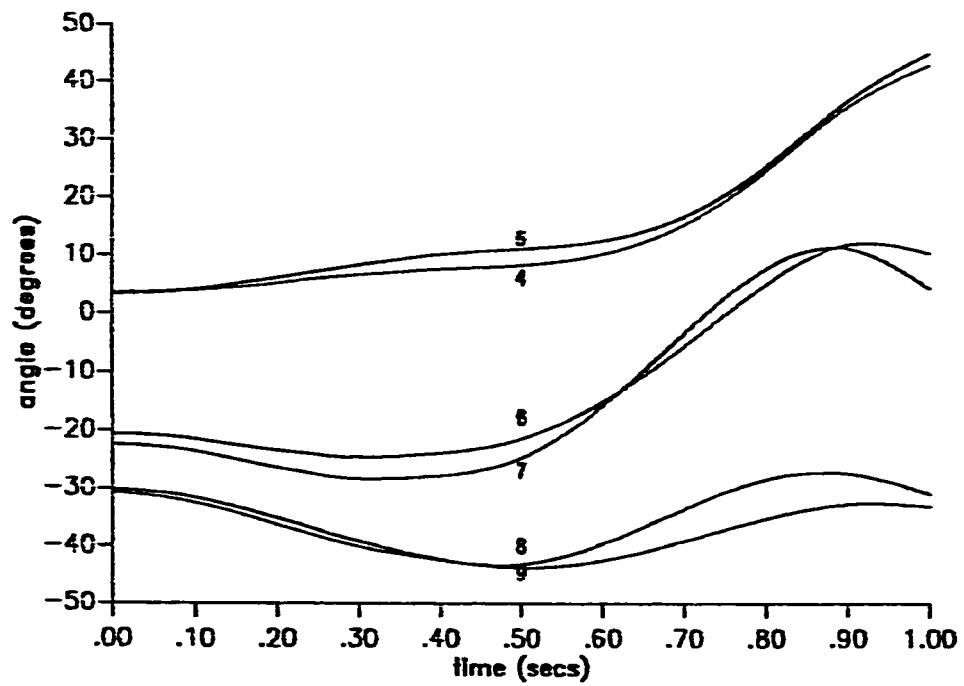


Fig. 6.12 Swing curves of generators 4-9 for a 3-ph fault on bus 12 of the IEEE system (CCT=0.47 secs)

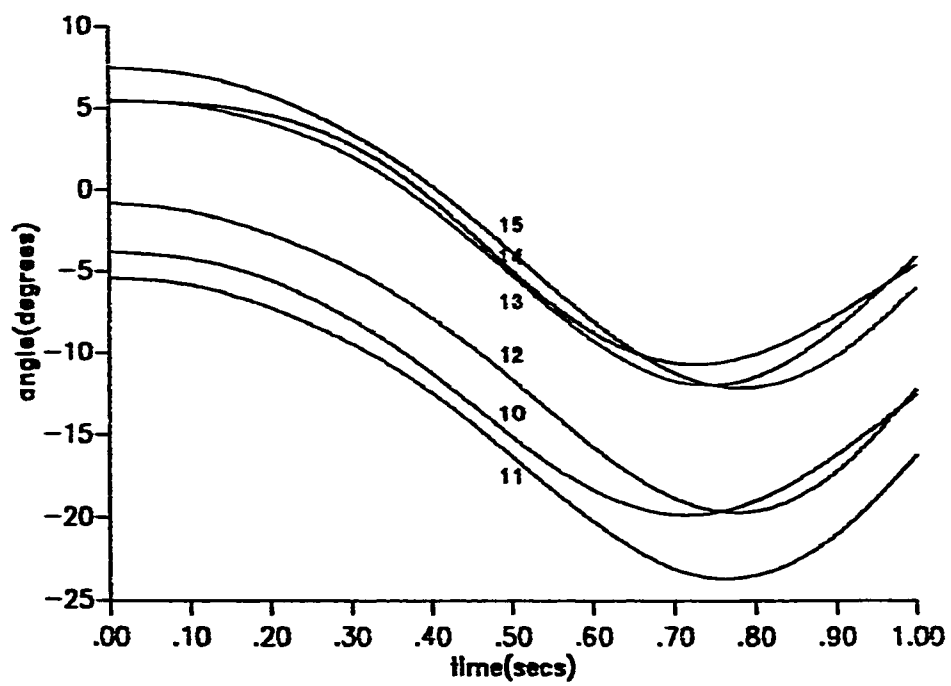


Fig. 6.13 Swing curves of generators 10-15 for a 3-ph fault on bus 12 of the IEEE system (CCT=0.47 secs)

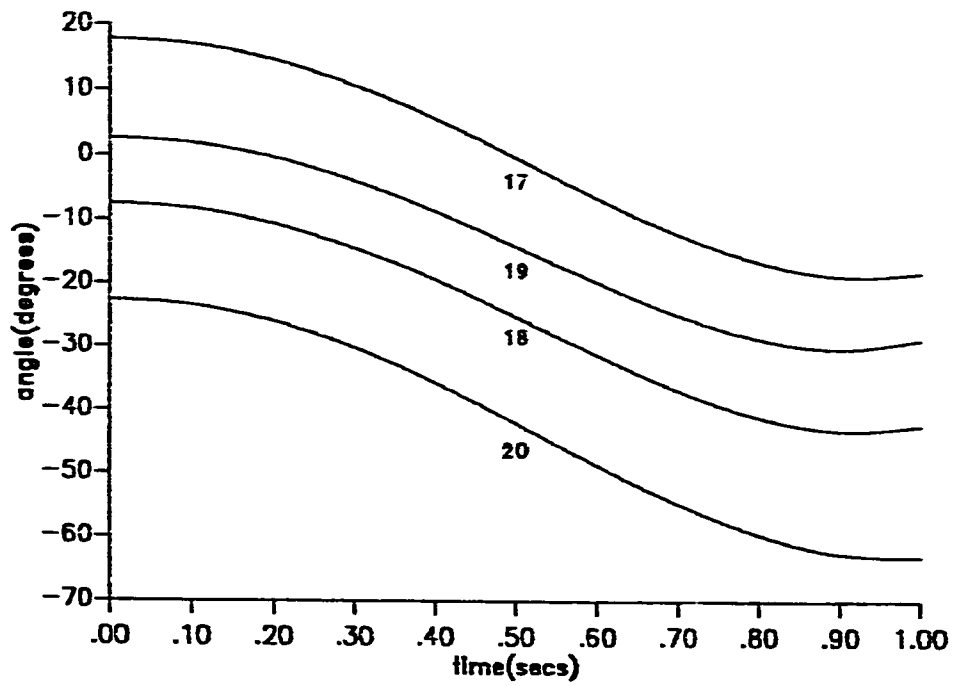


Fig. 6.14 Swing curves of generators 17-20 for a 3-ph fault on bus 12 of the IEEE system (CCT = 0.47 secs)

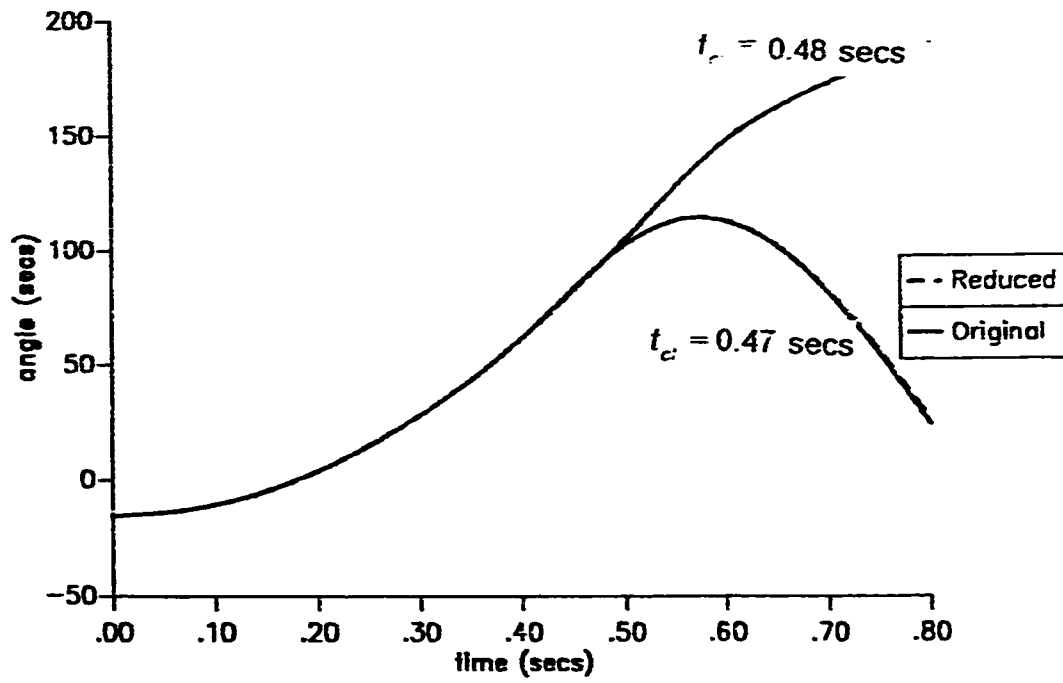


Fig. 6.15 Swing curves of gen. # 3 for a critically stable and unstable case for a 3-ph fault on bus 12 of the IEEE system

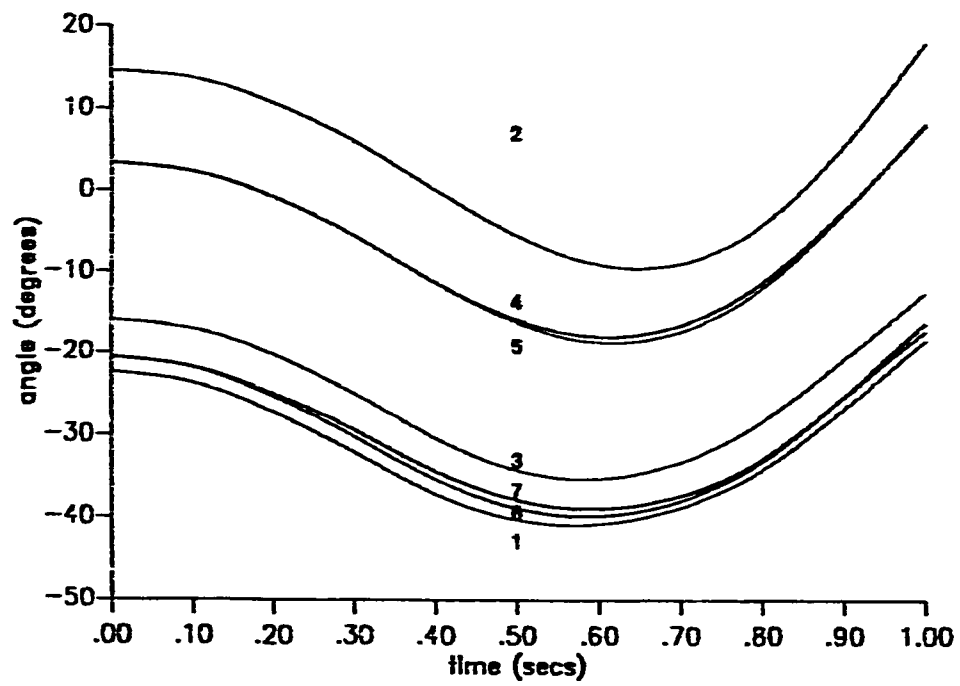


Fig. 6.16 Swing curves of generators 1-7 for a 3-ph fault on bus 59 of the IEEE system (CCT = 0.39 secs)

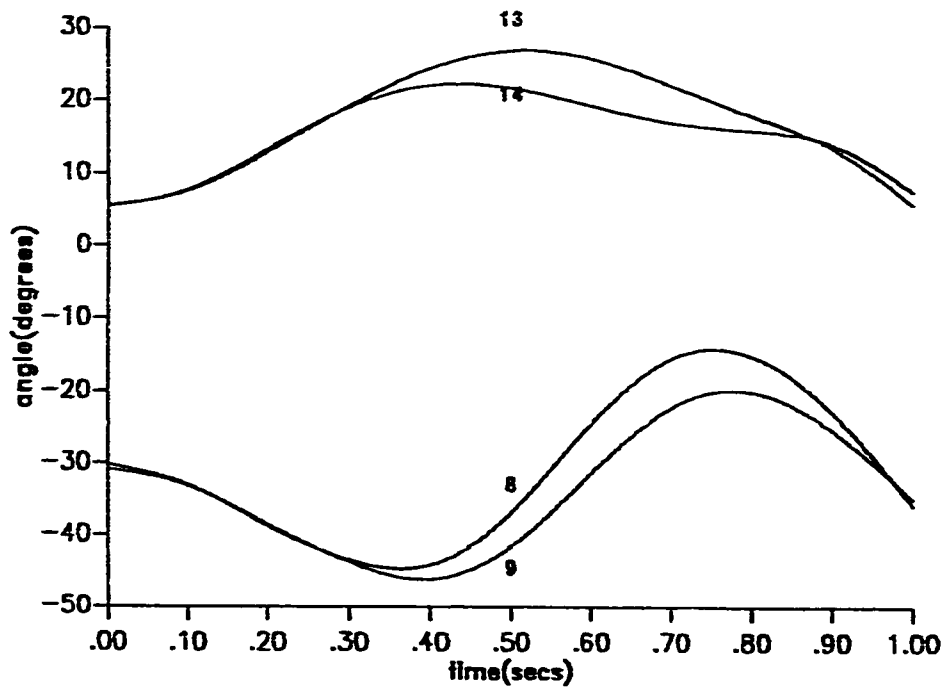


Fig. 6.17 Swing curves of generators 8,9,13,14 for a 3-ph fault on bus 59 of the IEEE system (CCT = 0.39 secs)

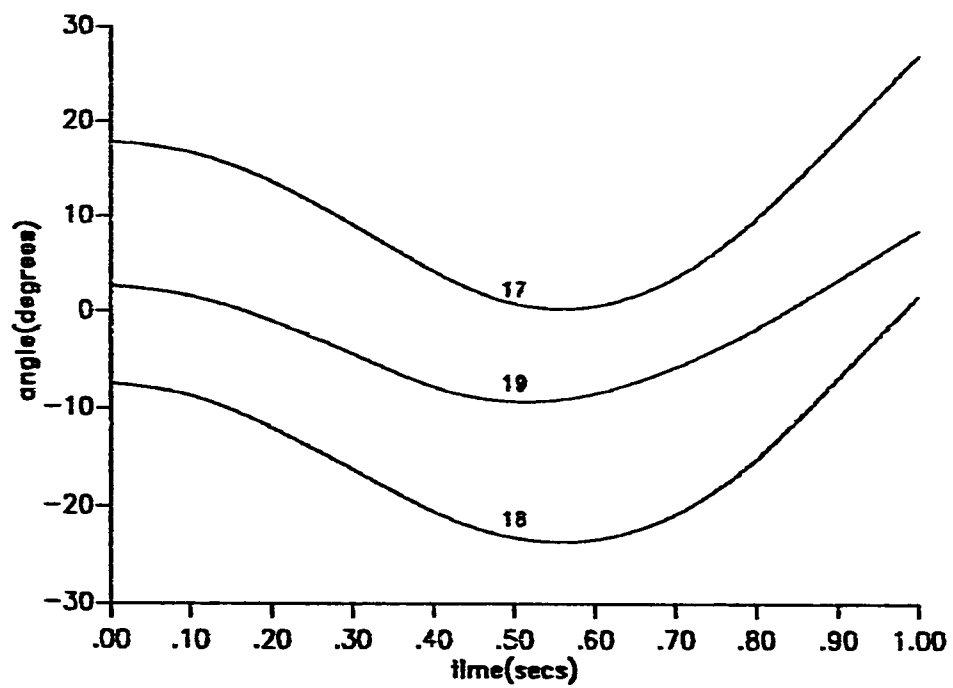


Fig. 6.18 Swing curves of generators 17-19 for a 3-ph fault on bus 59 of the IEEE system (CCT = 0.39 secs)

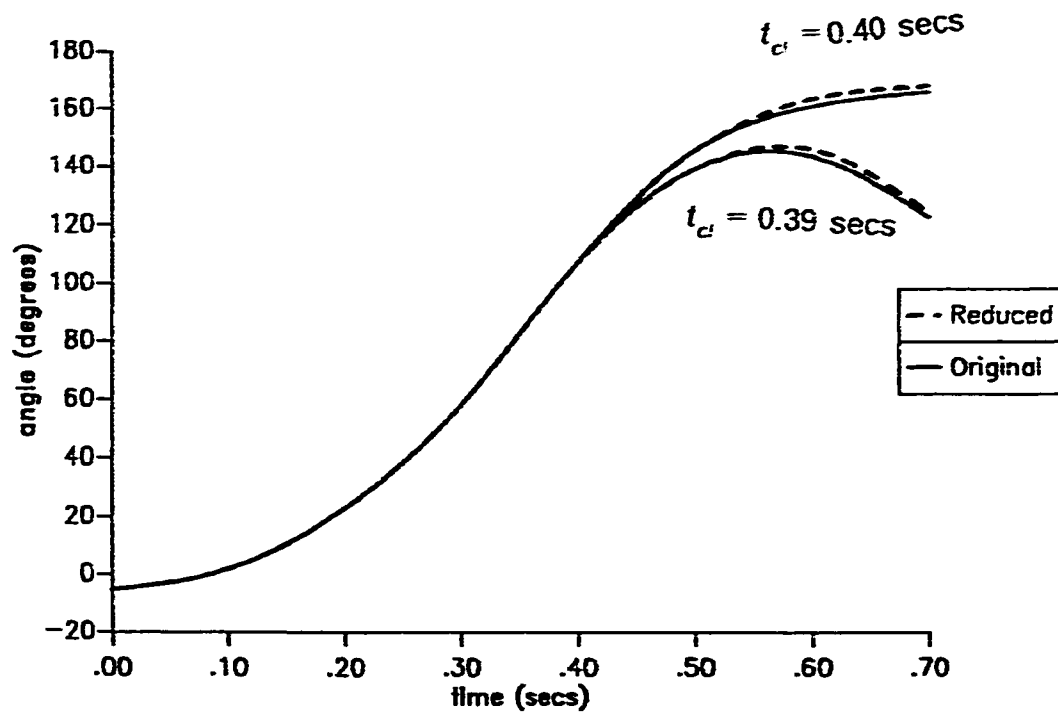


Fig. 6.19 Swing curves of gen. # 11 for a critically stable and unstable case for a 3-ph fault on bus 59 of the IEEE system



### 6.2.2 The New England System :

The New England system consists of 10 generators 39 busbars and 46 lines. The single line diagram is shown in Fig. 6.2. The system data and initial operating conditions are given in appendix-B. This system represents 345 kV bulk transmission networks of New England. Generator 10 is an equivalent power source representing parts of the USA-Canadian interconnection system. It has an inertia constant of  $H = 500$ . The inertia constants ( $H$ ) of rest of the generators in the system are in the range 24.3 to 42 s. Generator 10 has not been considered in the coherency identification process. Three phase fault at two different locations has been considered in this system. The fault locations are as follows

- i) Bus # 20
- ii) Bus # 29

Table 6.9 gives a summary of the various coherent groups obtained for each fault. Fig. 6.20 shows the swing curves of all the generators in the external system for a fault on bus # 20. The generator considered in the study system is generator # 5. It is clear from Fig. 6.20 that the only coherent groups in this case are (1,8),(2,3) and (6,7) . This verifies the fact that the proposed criteria identifies all possible coherent groups falling within the assumed threshold values. Fig. 6.21 shows coherent groups (2,3) and (4,6,7)

for a fault on bus # 29. For this fault the generator in the study system is generator# 9.

**TABLE 6.9**

**Coherent generator groups for New England system for various faults**

<b>Fault at Bus #</b>	<b>Line tripped between buses</b>	<b>Coh. generators by proposed method</b>	<b>By direct simulation</b>	<b>Gen. in reduced system</b>
<b>#20</b>	<b>None</b>	<b>(2.3)(6.7)(1.8)</b>	<b>(2.3)(6.7)(1.8)</b>	<b>7</b>
<b>#29</b>	<b>9-29</b>	<b>(2.3)(4.6.7)</b>	<b>(2.3)(4.6.7)</b>	<b>7</b>

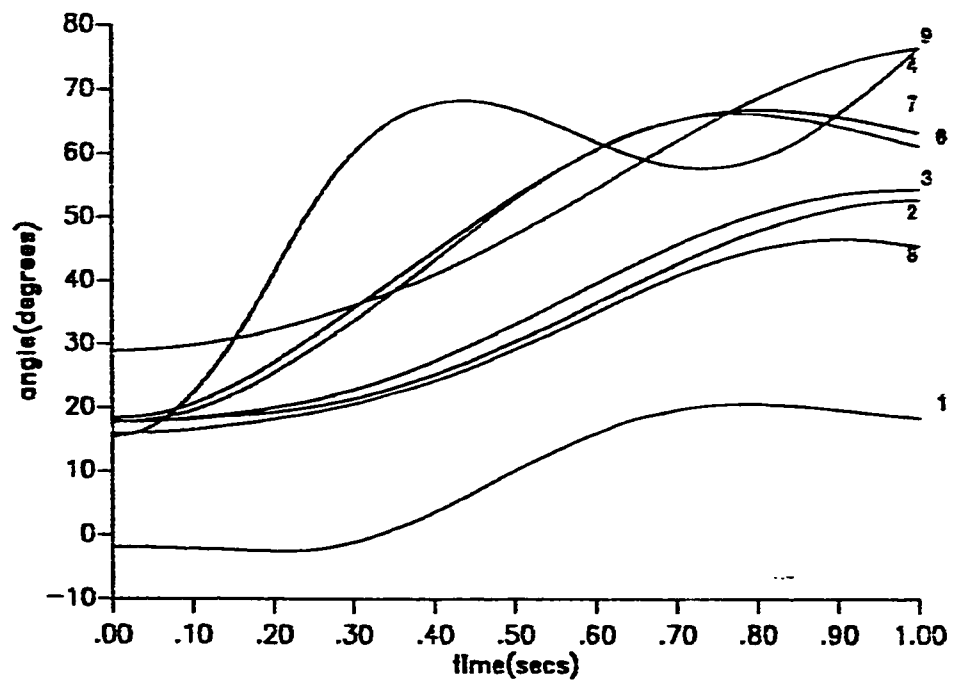


Fig. 6.20 Swing curves of generators 1-4,6-9 for a 3-ph fault on bus 20 of the New England system (CCT = 0.20 secs)

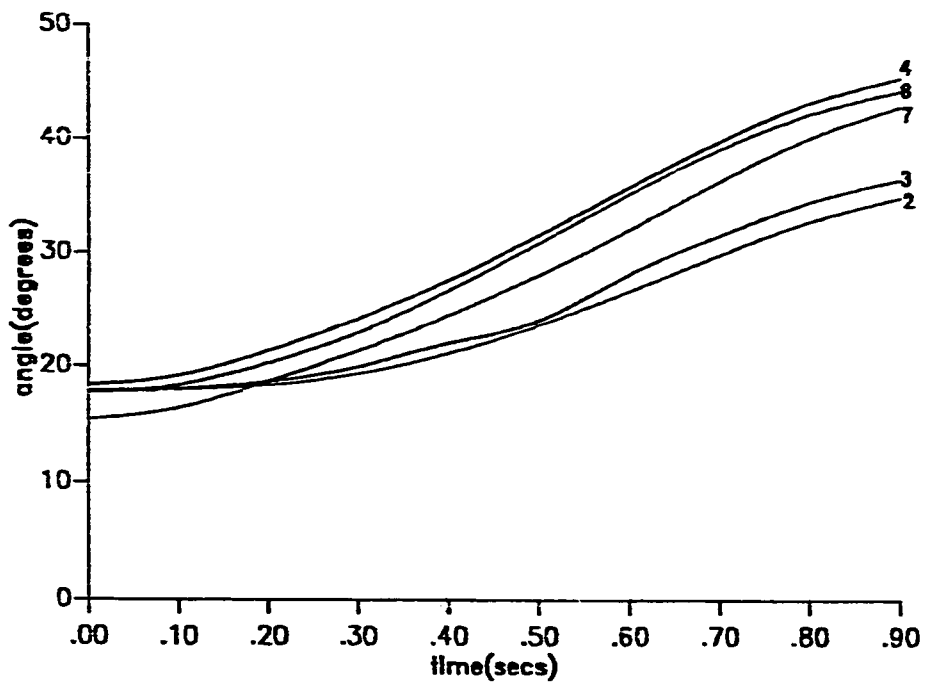


Fig. 6.21 Swing curves of generators 2,3,4,6,7 for a 3-ph fault on bus 29 of the New England system (CCT = 0.13 secs)

### 6.3 COMPARISON OF CPU TIME

The total CPU time required to compute the dynamic equivalent of a power system can be divided into two parts. The first part is the CPU time required to calculate the critical clearing time and the pairs of coherent generators. The second part is the CPU time required to compute parameters of the reduced order equivalent.

Table 6.10 gives the breakup of the CPU time required for each of these computations on the two test systems. The first case shown is the CPU time required to obtain a 7 machine equivalent of the 10-machine New England system for a 3-phase fault on bus # 20. The total CPU time required for this computation is 0.36 secs. The second case shown is the CPU time required to compute the 8-machine equivalent for the 20-machine IEEE system for a 3-phase fault on bus # 10. This computation requires a total CPU time of 1.3 secs.

Table 6.11 gives a comparison of the CPU time required to solve the swing equation by the step by step method for the full order system and reduced order equivalents. The solution of the swing equations has been carried out for a time duration of 1.0 second. The step size used for this computation is 0.01 secs.

It can be seen from Table 6.11 that a CPU time of 0.56 seconds is

required to perform one simulation of the 10-machine New England system whereas only 0.37 secs is required to perform the same simulation on a 7-machine equivalent of the system. The saving in CPU time is 0.19 secs. However, from Table 6.10 we observe that 0.36 sec of CPU time is required to obtain the 7-machine dynamic equivalent. Therefore, the total CPU time required to perform one simulation on the reduced order model is actually  $(0.36 + 0.37) = 0.67$  secs. This is 0.11 sec more than the CPU time required for one simulation of the full order system. However, in actual practice several simulations may be required. In such a case there will be a saving in CPU time because the computation of the dynamic equivalent is required to be done only once. After this the reduced order equivalent can be used to perform any number of simulations.

For the IEEE system, a CPU time of 0.38 secs is required to perform one simulation of the 8-machine equivalent. However, an additional 1.3 secs CPU time is required to obtain the reduced order equivalent from the original system. Therefore the total CPU time required to perform a single simulation in the 8-machine equivalent is  $(1.3 + 0.38) = 1.68$  secs. This indicates a saving of 0.52 secs of CPU time i.e. a saving of 24 % can be achieved.

From the above discussion it is clear that the dynamic equivalencing process may not be advantageous for performing a single simulation on a small system like the New England system. However, for larger systems like

the the IEEE system. there is a substantial saving in CPU time.

**TABLE 6.10**  
CPU time (secs) for Dynamic Equivalencing

Task	New England System	IEEE System
Coherency by the Proposed method	0.21	0.60
Obtaining Reduced order Parameters	0.15	0.70
Total	0.36	1.3

**TABLE 6.11**  
Comparison of CPU time in seconds for  
direct Simulation.

System	Original System	Reduced Equivalent
New England	0.56	0.31
IEEE	2.2	0.38



## **CHAPTER VII**

### **CONCLUSIONS**

#### **7.1 CONCLUSION**

A method of determining the groups of coherent generators has been proposed in this work. The coherency identification criteria has been developed for the most severe case i.e. by considering the fault clearing time is close to the critical clearing time (CCT). The critical clearing time is computed using the concept of individual machine energy. This concept requires much less computation time because it involves the computation of energy function of only the severely disturbed generator. The system states required in this case are estimated by the Taylor series expansion. The method of false position is used to solve the necessary equations iteratively. The above approach of determining the CCT was tested for various faults on the IEEE system and New England system. Results obtained by this method

were found to be very close to the corresponding actual values obtained by the step by step method. It has also been found that the Rudnick's method of computing CCT using the system RKE can sometimes give wrong results.

Coherency of generators, for the critically stable situation, is checked in three periods viz-a-viz the faulted, early part of the post fault and the later part of the post fault periods. Coherency during the faulted period is determined by checking the relative rotor angle deviations between pairs of generators. The generator angles required in this process are estimated through the Taylor series expansion.

Coherency during the early part of the post fault period is determined using a combination of second step Taylor series expansion and linear trajectory. Slopes of generator trajectories are computed and compared to determine the coherency during this period. It has also been found that the linear trajectory may give a better estimation of generator angles compared to the second step TSE for cases where the early part of the post fault period is relatively long ( $>0.2$  secs). Coherency during the later part of the post fault period is determined by checking the admittance distances between generators.

The proposed method of determining the groups of coherent generators was tested on two power networks for various faults. The groups of coherent generators obtained by this method were checked by observing the swing

curves generated by the step by step method and were found to be in agreement.

Finally the reduced order dynamic equivalent model is obtained by replacing each group of coherent generators by an equivalent generator using the power invariance principle between the original and the reduced systems. The accuracy of the reduced order model was checked by comparing the swing curves of some of the retained generators in the original and reduced order models for the critically stable and unstable cases.

An important observation was that the dynamic equivalencing process may not be very advantageous for small systems like the New England system. However, for large systems like the 20-machine IEEE system, the dynamic equivalencing resulted in a saving of approximately 25 % of the CPU time for a single simulation. It is expected that a further saving in CPU time can be achieved by improving programming efficiency.

## 7.2 RECOMMENDATION FOR FUTURE WORK

Most of the previous work on dynamic equivalencing including the present one is based on the classical model of a power system. In this model it is

assumed that the various equipments associated with the generator controls are slow to response. However, modern generator controls particularly excitation systems are extremely fast. Therefore, it becomes necessary to consider the effects of control equipments in the dynamic equivalencing technique. It is possible that a better model could change the dynamic behavior of the system.

The CPU time required to compute the parameters of the reduced order equivalent can be significantly reduced by using parallel processing technique. Parallel processing can be used to simultaneously calculate the parameters of the faulted and post fault reduced admittance matrices.

## REFERENCES

- [1] YAO NAN YU: 'Electric Power System Dynamics'. Academic Press. New York. 1983.
- [2] 'Development of Dynamic Equivalents for Transient Stability'. Final Report on EPRI Project No. 763. May 1977.
- [3] PODMORE. R: 'Identification of Coherent Generators for Dynamic Equivalents'. IEEE Trans., 1978, vol. PAS-97. (4). pp. 1344-1352.
- [4] LEE. S.T and SCHWEPPE. F.C. : 'Distance Measure and Coherency Recognition for Transient Stability Equivalents'. IEEE Trans., 1973. vol. PAS-82. pp. 1550-1557.
- [5] WU, F.F. and NARASIMHAMURTHI. N.: 'Coherency Identification for Power System Dynamic Equivalents'. IEEE Trans., 1983 ,vol. CAS-30. (3), pp. 140-147.
- [6] GALLAI. A.M. and THOMAS. R.J: 'Coherency Identification for Large Electric Power System '. IEEE Trans., 1982. vol. CAS-29. (11). pp. 777-782
- [7] HIYAMA, T: 'Identification of Coherent Generators using Frequency Response'. IEE PROC., 1988, Pt.C, vol. 128. (5), pp. 262-268.

- [8] PIRES DE SOUZA, EJS. and LIETE DE SILVA, A.M.: 'An Efficient Methodology for Coherency based Dynamic Equivalents', IEE PROC., 1992, Pt.C, vol 139, (5), pp. 371-382.
- [9] HAQUE, M.H. and RAHIM, A.H.M.A.: 'An Efficient Method of Identifying Coherent Generators using Taylor Series Expansions', IEEE Trans., 1988, PWRS-3, (3), pp. 1112-1118.
- [10] OHSAWA, Y. and HAYASHI, M.: 'Coherency Recognition for Transient Stability Equivalents Using Lyapunov Function', Proc 6th PCC, Aug. 1978, vol.2, IPC Science and Tech. Press, pp.815-818.
- [11] HAQUE, M.H. and RAHIM, A.H.M.A.: 'Identification of Coherent Generators using Energy Function', IEE PROC., 1990, Pt.C, vol 137, (4), pp.255-260.
- [12] SPALDING, B.D., YEE, H. and GOUDLE, D.B.: 'Coherency Recognition for Transient Stability Studies using Singular Points', IEEE Trans., 1977, PAS-96, (4), pp. 1368-1375
- [13] PAI, M.A.: 'Power System Stability', North Holland Publishing Co., New York, 1981.
- [14] HAQUE, M.H.: 'Identification of Coherent Generators for Power System Dynamic Equivalents using Unstable Equilibrium Point', IEE PROC.,

1991, Pt.C. vol. 138. (6). pp.546-552.

- [15] RUDNICK. H., PATINO. R.I. and BRAMELLER. A.: 'Power System Dynamic Equivalents: Coherency Recognition using Rate of Change of Kinetic Energy'. IEE PROC., 1981, Pt.C. vol. 128. (6). pp.325-333.
- [16] PODMORE. R.: 'A Comprehensive Program for Computing Coherency based Dynamic Equivalents'. IEEE. PICA conference. 1979. pp.298-306
- [17] GHAFURIAN. A. and BERG. G.J.: 'Coherency based Multimachine Study'. IEE PROC., 1982. Pt.C. vol 129. (4). pp.153-160.
- [18] THYAGARAJAN, T.R. and SHANKARANARAYAN. V.: 'Coherency based Dynamic Equivalents for Transient Stability Studies in Multimachine Systems', IE(India) Journal. June 1988. vol. 68. pp. 224-230.
- [19] RAHIM. A.H.M.A. and HAQUE. M.H.: 'A Special Dynamic Equivalencing Procedure for Rapid Computation of Critical Clearing Time for Large Power Systems', Modelling. Simulation and Control, A. AMSE Press. 1989, vol. 29. (4), pp. 17-36.
- [20] HEYDT. G.T.: 'Computer Analysis for Power Systems'. Macmillan Publishing Co.N.Y.,1986.
- [21] ANDERSON. P.M. and FOUAD. A.A.: 'Power System Control and

Stability'. Iowa State University Press, Ames, Iowa, 1977.

- [22] XUE, Y., VAN CUTSEM TH. and RIBBEN PAVELLA, M.: 'A Simple Direct Method of Fast Transient Stability Assessment of Large Power Systems'. IEEE Trans., May 1988, vol. PS-3, (3), pp. 400-412.
- [23] FOUAD, A.A., MICHEL, ANTONY .N. and VIJAY VITTAL: 'Power System Transient Stability using Individual Machine Energy Function'. IEEE Trans., 1983, vol. CAS-30, (5), pp. 266-76.
- [24] ATHAY, T., PODMORE, R. and VIRAMANI, S.: 'A Practical Method for Direct Analysis of Transient Stability'. IEEE Trans., 1979, vol. PAS-98, (5), pp. 573-84.
- [25] DJUKANOVIC, M., SOBAJIC, D.J. and YOH-HAN PAO: 'Neural Net based Unstable Machine Identification using Individual Machine Energy'. Electrical Power and Energy Systems, 1991, vol. 13, (5), pp. 255-262.
- [26] PAI, M.A.: 'Energy Function Analysis for Power System Stability'. Kluwer Academic Publishers, 1989.
- [27] FOUAD, A.A. and STANTON, S.S.: 'Transient Stability of a Multimachine Power System'. Pt. I and II. IEEE Trans., 1981, vol. PAS-100, (7), pp. 3408-3416.



- [28] SOUTHWORTH, R.W.: 'Digital Computation and Numerical Methods'. Mc Graw Hill, N.Y., 1965.
- [29] HAQUE, M.H. and RAHIM, A.H.M.A.: 'Determination of First Swing Stability Limit of Multimachine Power System through Taylor Series Expansion'. IEE PROC., 1989, Pt.C, vol. 136, (6), pp. 373-379.
- [30] XUE, Y., VAN CUTSEM TH. and RIBBEN PAVELLA, M.: 'Extended Equal Area Criterion: Justification, Generalization, Applications'. IEEE Trans., 1989, vol. PS-04, (1), pp. 44-51.

## APPENDIX-A

## IEEE SYSTEM

TABLE A-1

## BUSBAR DATA OF 20-MACHINE IEEE SYSTEM

BUS NO.	VOLTAGE		GENERATION		LOAD	
	MAG P.U.	ANGLE DEG.	ACTIVE MW	REACTIVE MVA	ACTIVE MW	REACT. MVA
1	0.9555	-19.1730	0.000	0.000	51.000	27.00
2	0.9712	-18.6220	0.000	0.000	20.000	9.00
3	0.9675	18.2760	0.000	0.000	39.000	10.00
4	0.9980	-14.5590	-9.000	-12.851	30.000	12.00
5	1.0019	-14.1110	0.000	0.000	0.000	0.00
6	0.9901	-16.8440	0.000	0.000	52.000	5.00
7	0.9893	-17.2890	0.000	0.000	19.000	2.00
8	1.0152	-9.0850	0.000	0.000	28.000	-159.00
9	1.0328	-1.7150	0.000	0.000	0.000	0.00
10	1.0500	5.8950	450.000	15.385	0.000	0.00
11	0.9847	-17.1260	0.000	0.000	70.000	23.00
12	0.9900	-17.6490	85.000	100.978	47.000	10.00
13	0.9570	-18.4930	0.000	0.000	34.000	16.00
14	0.9828	-18.3600	0.000	0.000	14.000	1.00
15	0.9702	-18.6960	0.000	0.000	90.000	9.60
16	0.9822	-17.9320	0.000	0.000	25.000	10.00
17	0.9929	-16.1200	0.000	0.000	11.000	3.00
18	0.9734	-18.3810	0.000	0.000	60.000	-0.24
19	0.9622	-18.8520	0.000	0.000	45.000	33.90
20	0.9539	-17.8860	0.000	0.000	18.000	3.00
21	0.9535	-16.2380	0.000	0.000	14.000	8.00
22	0.9646	-13.6180	0.000	0.000	10.000	5.00
23	0.9974	-8.6330	0.000	0.000	7.000	3.00
24	0.9921	-8.6980	0.000	0.000	13.000	4.00
25	1.0500	-1.7850	220.000	60.081	0.000	0.00
26	1.0150	-0.0250	314.000	44.019	0.000	0.00
27	0.9680	-14.4190	-9.000	10.586	62.000	13.00
28	0.9609	-16.1540	0.000	0.000	17.000	7.00
29	0.9629	-17.1710	0.000	0.000	24.000	4.00
30	0.9767	-11.0540	0.000	0.000	0.000	0.00
31	0.9670	-17.0670	7.000	36.213	43.000	27.00
32	0.9631	-14.9750	0.000	0.000	59.000	31.20
33	0.9686	-19.3270	0.000	0.000	23.000	9.00
34	0.9832	-18.7450	0.000	0.000	59.000	20.00
35	0.9792	-19.1970	0.000	0.000	33.000	9.00
36	0.9792	-19.2020	0.000	0.000	31.000	5.45
37	0.9878	-18.2600	0.000	0.000	0.000	0.00
38	0.9529	-13.0780	0.000	0.000	0.000	0.00
39	0.9685	-21.6820	0.000	0.000	27.000	11.00
40	0.9700	-22.7860	-46.000	36.046	20.000	23.00
41	0.9664	-23.2180	0.000	0.000	37.000	10.00

TABLE A-1 (CONTINUED)

BUS NO.	VOLTAGE		GENERATION		LOAD	
	MAG P.U.	ANGLE DEG.	ACTIVE MW	REACTIVE MVA	ACTIVE MW	REACT. MVA
42	0.9850	-21.6090	-59.000	47.533	37.000	23.00
43	0.9719	-18.7370	0.000	0.000	18.000	7.00
44	0.9792	-16.2300	0.000	0.000	16.000	8.00
45	0.9831	-14.4140	0.000	0.000	53.000	22.00
46	1.0056	-11.6510	0.000	0.000	9.000	8.20
47	1.0170	-9.3720	0.000	0.000	34.000	0.00
48	1.0202	-10.2290	0.000	0.000	20.000	11.00
49	1.0250	-9.2450	204.000	140.020	87.000	30.00
50	1.0000	-11.2670	0.000	0.000	17.000	4.00
51	0.9645	-13.8700	0.000	0.000	17.000	8.00
52	0.9538	-14.8190	0.000	0.000	18.000	5.00
53	0.9436	-15.8150	0.000	0.000	23.000	11.00
54	0.9551	-14.9380	0.000	0.000	65.000	19.80
55	0.9521	-15.2300	0.000	0.000	63.000	15.60
56	0.9541	-15.0400	0.000	0.000	84.000	13.30
57	0.9694	-13.8060	0.000	0.000	12.000	3.00
58	0.9573	-14.6560	0.000	0.000	12.000	3.00
59	0.9850	-10.8880	155.000	89.323	277.000	113.00
60	0.9930	-7.1000	0.000	0.000	78.000	3.00
61	0.9950	-6.2110	160.000	-29.955	0.000	0.00
62	0.9980	-6.8250	0.000	0.000	77.000	8.80
63	0.9668	-7.5100	0.000	0.000	0.000	0.00
64	0.9817	-5.7400	0.000	0.000	0.000	0.00
65	0.0050	-2.6260	391.000	160.685	0.000	0.00
66	0.0500	-2.7580	392.000	2.633	39.000	18.00
67	1.0189	-5.3940	0.000	0.000	28.000	7.00
68	1.0012	-2.7870	0.000	0.000	0.000	0.00
69	1.0350	0.0000	524.414	-61.097	0.000	0.00
70	0.9841	-6.6460	0.000	0.000	66.000	3.60
71	0.9867	-7.1000	0.000	0.000	0.000	0.00
72	0.9802	-8.4440	0.000	0.000	12.000	8.60
73	0.9912	-7.3160	0.000	0.000	6.000	-10.60
74	0.9581	-7.0880	0.000	0.000	68.000	30.30
75	0.9669	-5.6580	0.000	0.000	47.000	11.00
76	0.9428	-3.3290	0.000	0.000	68.000	95.00
77	1.0061	-4.2580	0.000	0.000	61.000	-64.00
78	1.0035	-4.5240	0.000	0.000	71.000	26.00
79	1.0091	-4.1540	0.000	0.000	39.000	32.00
80	1.0400	-1.7170	477.000	118.006	130.000	26.00
81	0.9946	-2.0880	0.000	0.000	0.000	0.00
82	0.9856	-3.6370	0.000	0.000	54.000	27.00

TABLE A-1(CONTINUED)

BUS NO.	VOLTAGE		GENERATION		LOAD	
	MAG P.U.	ANGLE DEG.	ACTIVE MW	REACTIVE MVA	ACTIVE MW	REACT. MVA
83	0.9818	-2.4890	0.000	0.000	20.000	10.00
84	0.9786	-0.0450	0.000	0.000	11.000	7.00
85	0.9852	1.4450	0.000	0.000	24.000	10.80
86	0.9850	-0.2110	0.000	0.000	21.000	10.00
87	1.0153	-0.4510	0.000	0.000	0.000	-13.70
88	0.9870	4.6530	0.000	0.000	48.000	10.00
89	1.0050	8.7520	607.000	4.495	0.000	0.00
90	0.9850	2.3680	-85.000	62.070	78.000	42.00
91	0.9801	2.4020	0.000	0.000	10.000	11.70
92	0.9901	2.9660	0.000	0.000	65.000	14.40
93	0.9840	-0.0140	0.000	0.000	12.000	7.00
94	0.9877	-2.1540	0.000	0.000	30.000	16.00
95	0.9777	-3.1200	0.000	0.000	42.000	31.00
96	0.9894	-3.2800	0.000	0.000	38.000	15.00
97	1.0091	-2.8430	0.000	0.000	15.000	9.00
98	1.0222	-3.3100	0.000	0.000	34.000	8.00
99	1.0100	-3.7390	0.000	0.000	42.000	15.50
100	1.0170	-2.7860	252.000	110.240	37.000	18.00
101	0.9901	-1.2120	0.000	0.000	22.000	15.00
102	0.9883	1.4760	0.000	0.000	5.000	3.00
104	0.9711	-9.1000	0.000	0.000	38.000	20.00
103	1.0100	-6.5280	0.000	0.000	-17.000	-64.00
105	0.9651	-10.2050	0.000	0.000	31.000	38.66
106	0.9602	-10.4500	0.000	0.000	43.000	16.00
107	0.9521	-13.2690	0.000	0.000	50.000	2.70
108	0.9658	-11.3940	0.000	0.000	2.000	1.00
109	0.9666	-11.8460	0.000	0.000	8.000	3.00
110	0.9729	-12.7020	0.000	0.000	39.000	25.50
111	0.9799	-11.0570	0.000	0.000	-36.000	1.36
112	0.9750	-15.8030	-43.000	43.090	25.000	13.00
113	0.9937	-16.1570	0.000	0.000	6.000	-17.80
114	0.9598	-15.3000	0.000	0.000	8.000	3.00
115	0.9598	-15.3070	0.000	0.000	22.000	7.00
116	1.0045	-3.2230	0.000	0.000	184.000	-91.76
117	0.9726	-19.1760	0.000	0.000	20.000	8.00
118	0.9488	-5.0420	0.000	0.000	33.000	15.00

TABLE A-2

-----  
 LINE DATA OF 20-MACHINE IEEE SYSTEM  
 -----

BETWEEN BUSES		-IMPEDANCE - R(P.U) X(P.U)		SHUNT ADMIT	TAP %
-----		-----		-----	---
1	3	0.0129	0.0424	0.0054	0.0
1	2	0.0303	0.0999	0.0127	0.0
2	12	0.0187	0.0616	0.0078	0.0
3	5	0.0241	0.1080	0.0142	0.0
3	12	0.0480	0.1600	0.0203	0.0
4	5	0.0018	0.0080	0.0010	0.0
4	11	0.0209	0.0688	0.0087	0.0
5	5	0.0000	2.5000	0.0000	0.0
5	6	0.0119	0.0540	0.0071	0.0
5	8	0.0000	0.0267	0.0000	-1.5
6	7	0.0045	0.0208	0.0027	0.0
7	12	0.0086	0.0340	0.0043	0.0
8	9	0.0024	0.0305	0.5810	0.0
8	32	0.0043	0.0504	0.2570	0.0
9	10	0.0026	0.0322	0.6150	0.0
11	12	0.0059	0.0196	0.0025	0.0
11	13	0.0222	0.0731	0.0094	0.0
11	26	0.0203	0.0682	0.0087	0.0
12	14	0.0215	0.0707	0.0091	0.0
12	16	0.0212	0.0834	0.0107	0.0
12	117	0.0329	0.1400	0.0179	0.0
13	15	0.0744	0.2444	0.0313	0.0
14	15	0.0595	0.1950	0.0251	0.0
15	17	0.0132	0.0437	0.0222	0.0
15	19	0.0120	0.0394	0.0050	0.0
15	33	0.0380	0.1244	0.0160	0.0
16	17	0.0454	0.1801	0.0233	0.0
17	18	0.0123	0.0505	0.0064	0.0
17	30	0.0000	0.0388	0.0000	-4.0
17	31	0.0474	0.1563	0.0274	0.0
17	113	0.0091	0.0301	0.0038	0.0
18	19	0.0111	0.0493	0.0057	0.0
19	20	0.0252	0.1170	0.0149	0.0
19	34	0.0752	0.2470	0.0316	0.0
20	21	0.0183	0.0849	0.0108	0.0
21	22	0.0209	0.0970	0.0123	0.0
22	23	0.0342	0.1590	0.0202	0.0
23	24	0.0135	0.0492	0.0249	0.0
23	25	0.0156	0.0800	0.0432	0.0
23	32	0.0317	0.1157	0.0586	0.0

TABLE A-2(CONTINUED)

BETWEEN BUSES		-IMPEDANCE - R(P.U) X(P.U)		SHUNT ADMIT	TAP %
24	70	0.1022	0.4115	0.0510	0.0
24	72	0.0488	0.1950	0.0244	0.0
25	26	0.0000	0.0382	0.0000	-4.0
25	27	0.0318	0.1630	0.0882	0.0
26	30	0.0079	0.0850	0.4540	0.0
27	28	0.0191	0.0855	0.0108	0.0
27	32	0.0229	0.0755	0.0096	0.0
27	115	0.0164	0.0741	0.0099	0.0
28	29	0.0237	0.0943	0.0119	0.0
29	31	0.0108	0.0331	0.0041	0.0
30	38	0.0046	0.0540	0.2110	0.0
31	32	0.0298	0.0985	0.0125	0.0
32	113	0.0615	0.2030	0.0259	0.0
32	114	0.0135	0.0612	0.0081	0.0
33	37	0.0415	0.1420	0.0183	0.0
34	34	0.0000	-7.1428	0.0000	0.0
34	36	0.0087	0.0268	0.0028	0.0
34	37	0.0026	0.0094	0.0049	0.0
34	43	0.0413	0.1681	0.0211	0.0
35	36	0.0022	0.0102	0.0013	0.0
35	37	0.0110	0.0497	0.0066	0.0
37	37	0.0000	4.0000	0.0000	0.0
37	38	0.0000	0.0375	0.0000	-6.2
37	39	0.0321	0.1050	0.0135	0.0
37	41	0.0593	0.1680	0.0210	0.0
38	65	0.0090	0.0986	0.5230	0.0
39	40	0.0184	0.0605	0.0077	0.0
40	41	0.0145	0.0487	0.0061	0.0
40	42	0.0555	0.1830	0.0233	0.0
41	42	0.0410	0.1350	0.0172	0.0
42	49	0.0358	0.1610	0.0860	0.0
43	44	0.0608	0.2454	0.0303	0.0
44	44	0.0000	-10.0000	0.0000	0.0
44	45	0.0224	0.0901	0.0112	0.0
45	45	0.0000	-10.0000	0.0000	0.0
45	46	0.0400	0.1356	0.0166	0.0
46	46	0.0000	-10.0000	0.0000	0.0
46	47	0.0380	0.1270	0.0158	0.0
46	48	0.0601	0.1890	0.0236	0.0
47	49	0.0179	0.0505	0.0063	0.0
47	69	0.0844	0.2778	0.0355	0.0
48	48	0.0000	-6.6666	0.0000	0.0

TABLE A-2 (CONTINUED)

BETWEEN BUSES		- IMPEDANCE - R(P.U) X(P.U)		SHUNT ADMIT	TAP %
49	45	0.0684	0.1860	0.0222	0.0
49	48	0.0179	0.0505	0.0063	0.0
49	50	0.0267	0.0752	0.0093	0.0
49	54	0.0398	0.1450	0.0734	0.0
49	51	0.0486	0.1370	0.0171	0.0
49	66	0.0090	0.0459	0.0248	0.0
50	57	0.0474	0.1340	0.0166	0.0
51	52	0.0203	0.0588	0.0070	0.0
51	58	0.0255	0.0719	0.0089	0.0
52	53	0.0405	0.1635	0.0202	0.0
53	54	0.0263	0.1220	0.0155	0.0
54	56	0.0027	0.0095	0.0036	0.0
54	55	0.0169	0.0707	0.0101	0.0
54	59	0.0503	0.2293	0.0299	0.0
55	56	0.0048	0.0151	0.0019	0.0
55	59	0.0473	0.2158	0.0282	0.0
56	57	0.0343	0.0966	0.0121	0.0
56	58	0.0343	0.0966	0.0121	0.0
56	59	0.0407	0.1200	0.0552	0.0
59	60	0.0317	0.1450	0.0188	0.0
59	61	0.0328	0.1500	0.0194	0.0
59	63	0.0000	0.0386	0.0000	-4.0
60	61	0.0026	0.0135	0.0073	0.0
60	62	0.0123	0.0561	0.0073	0.0
61	62	0.0082	0.0376	0.0049	0.0
61	64	0.0000	0.0268	0.0000	-1.5
62	66	0.0482	0.2180	0.0289	0.0
62	67	0.0258	0.1170	0.0155	0.0
63	64	0.0017	0.0200	0.1080	0.0
64	65	0.0027	0.0302	0.1900	0.0
65	66	0.0000	0.0370	0.0000	-6.5
66	67	0.0224	0.1015	0.0134	0.0
68	65	0.0014	0.0160	0.3190	0.0
68	69	0.0000	0.0370	0.0000	-6.5
68	81	0.0170	0.0202	0.4040	0.0
68	116	0.0003	0.0040	0.0820	0.0
69	49	0.0985	0.3240	0.0414	0.0
69	70	0.0300	0.1270	0.0610	0.0
69	75	0.0405	0.1220	0.0620	0.0
69	77	0.0309	0.1010	0.0519	0.0
70	71	0.0088	0.0355	0.0043	0.0
70	74	0.0401	0.1323	0.0168	0.0
70	75	0.0428	0.1410	0.0180	0.0

TABLE A-2 (CONTINUED)

BETWEEN BUSES		- IMPEDANCE - R(P.U) X(P.U)		SHUNT ADMIT	TAP %
-----		-----		-----	---
71	72	0.0446	0.1800	0.0222	0.0
71	73	0.0087	0.0454	0.0059	0.0
74	74	0.0000	-8.3333	0.0000	0.0
74	75	0.0123	0.0406	0.0051	0.0
75	77	0.0601	0.1999	0.0249	0.0
75	118	0.0145	0.0481	0.0059	0.0
76	77	0.0444	0.0148	0.0184	0.0
76	118	0.0164	0.0544	0.0068	0.0
77	78	0.0037	0.0124	0.0063	0.0
77	80	0.0108	0.0331	0.0350	0.0
77	82	0.0298	0.0853	0.0409	0.0
78	79	0.0054	0.0244	0.0032	0.0
79	79	0.0000	-5.0000	0.0000	0.0
79	80	0.0156	0.0704	0.0093	0.0
80	81	0.0000	0.0370	0.0000	-5.5
80	96	0.0356	0.1820	0.0247	0.0
80	97	0.0183	0.0934	0.0127	0.0
80	98	0.0238	0.1080	0.0143	0.0
80	99	0.0454	0.2060	0.0273	0.0
82	82	0.0000	-5.0000	0.0000	0.0
82	83	0.0112	0.0366	0.0190	0.0
82	96	0.0162	0.0530	0.0272	0.0
83	83	0.0000	-10.0000	0.0000	0.0
83	84	0.0625	0.1320	0.0129	0.0
83	85	0.0430	0.1480	0.0174	0.0
84	85	0.0302	0.0641	0.0061	0.0
85	86	0.0350	0.1230	0.0138	0.0
85	88	0.0200	0.1020	0.0138	0.0
85	89	0.0239	0.1730	0.0235	0.0
86	87	0.0282	0.2074	0.0222	0.0
88	89	0.0139	0.0712	0.0096	0.0
89	90	0.0158	0.0653	0.0794	0.0
90	91	0.0254	0.0836	0.0107	0.0
91	92	0.0387	0.1272	0.0163	0.0
92	93	0.0258	0.0848	0.0109	0.0
92	94	0.0481	0.1580	0.0203	0.0
92	99	0.0079	0.0380	0.0481	0.0
92	100	0.0648	0.2950	0.0386	0.0
92	102	0.0123	0.0559	0.0073	0.0
93	94	0.0223	0.0732	0.0094	0.0
94	95	0.0132	0.0434	0.0055	0.0
94	96	0.0269	0.0869	0.0115	0.0



TABLE A-2 (CONTINUED)

BETWEEN BUSES		-IMPEDANCE - R(P.U) X(P.U)		SHUNT ADMIT	TAP %
94	100	0.0178	0.0580	0.0302	0.0
95	96	0.0171	0.0547	0.0074	0.0
96	97	0.0173	0.0885	0.0120	0.0
98	100	0.0397	0.1790	0.0238	0.0
99	100	0.0180	0.0813	0.0108	0.0
100	101	0.0277	0.1262	0.0164	0.0
100	103	0.0160	0.0525	0.0268	0.0
100	104	0.0451	0.2040	0.0270	0.0
100	106	0.0605	0.2290	0.0310	0.0
101	102	0.0246	0.1120	0.0147	0.0
103	104	0.0466	0.1584	0.0203	0.0
103	105	0.0535	0.1625	0.0204	0.0
103	110	0.0391	0.1813	0.0230	0.0
104	105	0.0099	0.0378	0.0049	0.0
105	105	0.0000	-5.0000	0.0000	0.0
105	107	0.0530	0.1830	0.0236	0.0
105	106	0.0140	0.0547	0.0072	0.0
106	107	0.0530	0.1830	0.0236	0.0
107	107	0.0000	-16.6666	0.0000	0.0
108	105	0.0261	0.0703	0.0092	0.0
108	109	0.0105	0.0288	0.0038	0.0
109	110	0.0278	0.0762	0.0101	0.0
110	110	0.0000	-17.6599	0.0000	0.0
110	111	0.0220	0.0755	0.0100	0.0
110	112	0.0247	0.0640	0.0310	0.0
114	115	0.0023	0.0104	0.0014	0.0

TABLE A-3  
 -----  
 GENERATOR DATA OF 20-MACHINE IEEE SYSTEM  
 -----

GEN NO.	INERTIA CONST. (H)	TRANS. REACT. (P.U)
---	-----	-----
1	8.00	0.0875
2	22.00	0.0636
3	8.00	0.1750
4	14.00	0.1000
5	26.00	0.0538
6	8.00	0.0875
7	8.00	0.0875
8	8.00	0.0875
9	8.00	0.0875
10	12.00	0.1167
11	10.00	0.1400
12	12.00	0.1167
13	20.00	0.0700
14	20.00	0.0700
15	30.00	0.0467
16	28.00	0.0500
17	32.00	0.0437
18	8.00	0.0875
19	16.00	0.0875
20	15.00	0.0467

## APPENDIX-B

NEW ENGLAND SYSTEM  
-----TABLE B-1  
-----EUSEAR DATA OF 10-MACHINE NEW ENGLAND SYSTEM  
-----

BUS NO.	VOLTAGE		GENERATION		LOAD	
	MAG P.U.	ANGLE DEG.	ACTIVE MW	REACTIVE MVA	ACTIVE MW	REACT. MVA
1	1.0475	6.7000	250.400	145.351	0.000	0.00
2	0.9820	10.8820	563.299	205.408	9.200	4.00
3	0.9831	12.6670	650.000	205.780	0.000	0.00
4	0.9972	13.1780	632.000	108.974	0.000	0.00
5	1.0123	11.7390	508.000	167.003	0.000	0.00
6	1.0493	15.1500	650.000	211.152	0.000	0.00
7	1.0635	17.8430	560.000	100.461	0.000	0.00
8	1.0278	12.3180	540.000	0.928	0.000	0.00
9	1.0265	17.5830	830.000	22.778	0.000	0.00
10	1.0300	0.0000	999.551	88.037	1104.000	250.00
11	1.0125	3.8500	0.000	0.000	0.000	0.00
12	0.9998	3.8410	0.000	0.000	8.500	88.00
13	1.0142	3.9610	0.000	0.000	0.000	0.00
14	1.0117	2.3080	0.000	0.000	0.000	0.00
15	1.0158	1.9200	0.000	0.000	320.000	153.00
16	1.0322	3.3370	0.000	0.000	329.400	32.00
17	1.0339	2.3510	0.000	0.000	0.000	0.00
18	1.0313	1.5150	0.000	0.000	158.000	30.00
19	1.0500	7.9610	0.000	0.000	0.000	0.00
20	0.9910	6.5490	0.000	0.000	680.000	103.00
21	1.0321	5.7420	0.000	0.000	274.000	115.00
22	1.0500	10.1890	0.000	0.000	0.000	0.00
23	1.0450	9.9910	0.000	0.000	247.500	84.00
24	1.0377	3.4560	0.000	0.000	308.600	-92.00
25	1.0575	5.5330	0.000	0.000	224.000	47.00
26	1.0521	4.2480	0.000	0.000	139.000	17.00
27	1.0379	2.2240	0.000	0.000	281.000	75.00
28	1.0501	7.7600	0.000	0.000	206.000	27.00
29	1.0500	10.5190	0.000	0.000	283.500	26.00
30	1.0475	1.5690	0.000	0.000	0.000	0.00
31	1.0490	4.1800	0.000	0.000	0.000	0.00
32	1.0304	1.2810	0.000	0.000	322.000	2.00
33	1.0038	0.4210	0.000	0.000	500.000	184.00
34	1.0051	1.5720	0.000	0.000	0.000	0.00
35	1.0074	2.2650	0.000	0.000	0.000	0.00
36	0.9967	0.0700	0.000	0.000	233.800	84.00
37	0.9958	-0.4330	0.000	0.000	522.000	176.00
38	1.0281	-0.2170	0.000	0.000	0.000	0.00
39	1.0170	4.6700	0.000	0.000	0.000	0.00

TABLE B-2

## LINE DATA OF 10-MACHINE NEW ENGLAND SYSTEM

BETWEEN BUSES		-IMPEDANCE - R(P.U) X(P.U)		SHUNT ADMIT	TAP %
1	31	0.0000	0.0181	0.0000	2.5
2	35	0.0000	0.0250	0.0000	7.0
3	39	0.0000	0.0200	0.0000	7.0
4	19	0.0007	0.0142	0.0000	7.0
5	20	0.0009	0.0180	0.0000	0.9
6	22	0.0000	0.0143	0.0000	2.5
7	23	0.0005	0.0272	0.0000	0.0
8	25	0.0006	0.0232	0.0000	2.5
9	29	0.0008	0.0156	0.0000	2.5
10	38	0.0010	0.0250	1.2000	0.0
10	30	0.0010	0.0250	0.7500	0.0
11	12	0.0016	0.0435	0.0000	0.6
11	35	0.0007	0.0082	0.1389	0.0
11	39	0.0004	0.0043	0.0729	0.0
12	13	0.0016	0.0435	0.0000	0.6
13	14	0.0009	0.0101	0.1723	0.0
13	39	0.0004	0.0043	0.0729	0.0
14	15	0.0018	0.0217	0.3660	0.0
14	33	0.0008	0.0129	0.1382	0.0
15	16	0.0009	0.0094	0.1710	0.0
16	17	0.0007	0.0089	0.1342	0.0
16	19	0.0016	0.0195	0.3040	0.0
16	21	0.0008	0.0135	0.2548	0.0
16	24	0.0003	0.0059	0.0680	0.0
17	18	0.0007	0.0082	0.1319	0.0
17	27	0.0013	0.0173	0.3216	0.0
18	32	0.0011	0.0133	0.2138	0.0
19	20	0.0007	0.0138	0.0000	6.0
21	22	0.0008	0.0140	0.2565	0.0
22	23	0.0006	0.0096	0.1846	0.0
23	24	0.0022	0.0350	0.3610	0.0
25	26	0.0032	0.0323	0.5130	0.0
25	31	0.0070	0.0086	0.1460	0.0
26	28	0.0043	0.0474	0.7802	0.0
26	27	0.0014	0.0147	0.2396	0.0
26	29	0.0057	0.0625	1.0290	0.0
28	29	0.0014	0.0151	0.2490	0.0
30	31	0.0035	0.0411	0.6987	0.0
31	32	0.0013	0.0151	0.2572	0.0
32	33	0.0013	0.0213	0.2214	0.0
33	34	0.0008	0.0128	0.1342	0.0
34	37	0.0008	0.0112	0.1476	0.0
34	35	0.0002	0.0026	0.0434	0.0
35	36	0.0006	0.0092	0.1130	0.0
36	37	0.0004	0.0046	0.0780	0.0
37	38	0.0023	0.0363	0.3804	0.0

TABLE B-3

-----

GENERATOR DATA OF 10-MACHINE NEW ENGLAND SYSTEM

-----

GEN NO.	INERTIA CONST. (H)	TRANS. REACT. (P.U)
1	42.00	0.0310
2	30.30	0.0697
3	35.80	0.0531
4	28.60	0.0436
5	26.00	0.1320
6	34.80	0.0500
7	26.40	0.0490
8	24.30	0.0570
9	34.50	0.0570
10	500.00	0.0060

